OPTIMIZATION OF AMIFOSTINE ADMINISTRATION FOR RADIOPROTECTION

by

Zheng Lu

A dissertation submitted in partial fulfillment
of the requirements for the degree of
Doctor of Philosophy
(Pharmaceutical Sciences)
in The Univeristy of Michigan
2007

Doctoral Committee:

Professor David E. Smith, Chair
Professor Gordon L. Amidon
Professor Theodore S. Lawrence
Adjunct Associate Professor Meihua Rose Feng
Research Associate Professor Daniel P. Normolle

DEDICATION

To my grandma Kunhou Tian (田坤厚)
My uncle jicang zhuo （卓济苍）
My wife Yan Cai （蔡燕） and son Victor Lu（卢安博）

For their true love

ACKNOWLEDGEMENTS

I would like to thank my advisor, Dr. David Smith, for his guidance, patience and support during my graduate studies in the Department of Pharmaceutics of the University of Michigan. I appreciate his acceptance of me into his lab as his Ph.D. student when I transferred from University of Minnesota, providing this excellent research opportunity and project for me in the field of pharmaceutical sciences. I have been studying and working in his lab for five years of my life, and I am feeling his lab is my second home, his insightful and instructional advice on my acedemica and my life make me really feel lucky to be a member of his group family.

I am very thankful to Drs. Gordon Amidon, Daniel Normolle, Theodore Lawrence and Rose Feng for serving on my research committee. It was a great pleasure and unique experience to work and interact with these excellent scientists. I must thank Dr. Normolle for his extraordinary effort during my thesis research and his scientific expertises triggered my strong interest in knowing and learning SAS programming and application of it to the field of pharmacokinetics and further advanced statistical study. I appreciate Dr. Rose Feng's guidance, discussion and help during my later phase of my Ph.D. study, she is another great tutor who led me into the world of population pharmacokinetics and NONMEM programming. I also wish to thank Dr. Gordon Amidon for his scientific guidance and advice in my research work and Dr. Theodore Lawrence who is the

principal investigator of the project I have been working for his patience and kindness to offer me this challenging research opportunity to continue my training.

I also acknowledge great help and time from Dr. Thomas Ludden from Globomax, Dr. Jack Cook, Dr. Matt Hutmacher, Dr. Daniele Ouellet, Dr. Sunny Chapel and Bill Frame from Pfizer, they probably won't see this and don't remember their help to me because most help is by emails, however, I will remember their help forever because they are really helpful at that point.

My gratitude extends to the faculty, staff and students at the Department of Pharmaceutical Sciences, University of Michigan, for their friendship, support and help during my stay here, especially our current group members Yongjun, Dilara, Ke, Mohamed, Huidi and Jenney Jie Sheng.

Finally, I am greatly indebted to my parents for their love, patience, support and encouragement. The greatest thanks go to my wife and my uncle for their great help to me, also my grandmother and grandfather living in my heart forever for being the source of inspiration and my spirital support when I face difficulties in my life.

TABLE OF CONTENTS

LIST OF TABLES

Table

LIST OF FIGURES

Figure

LIST OF APPENDICES

Appendix

ABSTRACT

Amifostine has been shown in randomized trials to protect the parotid gland, lung and esophagus from radiation. It is a thiophosphate prodrug that is dephosphorylated to the active free thiol metabolite, WR-1065, by plasma membrane-bound alkaline phosphatase. Selectivity of amifostine may be due to differences between the microenvironment of normal tissues and tumor (e.g., pH and enzymatic activity) and different uptake processes.

We proposed to optimize the use of amifostine as a radiation protector of normal liver, which will permit the safe delivery of higher doses of radiation for patients with both focal and diffuse disease. We carried out nonclinical studies to optimize amifostine selectivity (i.e., the concentration of WR-1065 in liver to tumor) in a rat xenograft model with different dosing routes of drug (systemic vs regional and IV vs SC). The pharmacokinetics of amifostine and WR-1065 were evaluated in a phase I trial of dose-escalating radiation therapy with systemic amifostine for liver cancer patients. Following intravenous dosing of amifostine, the concentrations of WR-1065 in liver and blood were highest at the earliest sampling time and higher doses, while tumor levels were relatively constant with respect to time. Based on our response surface regression model, no significant difference was observed between systemic and regional administrations of amifostine. After subcutaneous dosing of amifostine, optimal selectivity was sustained for a period of 5-20 min. While the liver and tumor concentrations of WR-1065 were initially low and increased steadily over time, blood levels were relatively constant over

time. These findings recommend that the highest intravenous dose of amifostine tolerated be administered, and that radiotherapy begin shortly after dosing for liver cancer patients. A subcutaneous dose, which is an easier administration route, may be a reasonable substitute when dosed 5-20 min before radiotherapy. Clinical pharmacokinetic results indicated that amifostine has a short half-life, a small volume of distribution and a large clearance. WR-1065 has a much longer half-life, and larger volume of distribution and clearance as compared to amifostine. In conclusion, amifostine was converted to WR-1065 rapidly and confined to extracellular fluid in the body. WR-1065 was extensively bound in tissues and converted quickly to disulfides.

CHAPTER 1

RESEARCH OBJECTIVES

The treatment of cancer with radiation therapy and/or chemotherapy has improved in recent years, but precisely targeting malignant tissue has remained a major challenge. While dose escalation may theoretically improve efficacy, toxic effects on nonmalignant tissues and organs continue to be dose limiting. To increase the therapeutic selectivity of chemotherapy and radiation therapy, researchers have tried either to heighten the sensitivity of tumor cells to treatment by three-dimensional radiation, regional drug delivery of chemotherapy and radio- and chemosensitizers, or to protect normal cells with the use of protective agents.[1] The use of protective agents is particularly interesting because of their potential to protect healthy tissue without compromising tumor cell destruction.[2] At present, the Food and Drug Administration (FDA) has approved dexrazoxane, mesna and amifostine, three cytoprotecting agents, for reducing the cytotoxicities associated with chemotherapy and/or radiotherapy of cancer treatment.[3]

Currently, the most potent and broad-spectrum selective chemo- and radioprotective agent known is amifostine.[4,5] Yet, by 2002 its only approved indications are for reducing the renal toxicity associated with cisplatin in patients with advanced ovarian cancer and non-small cell cancer of the lungs, and for reducing xerostomia associated with head and neck cancer radiotherapy.[6]

Amifostine protects almost all normal tissues from the cytotoxic effects of radiation and some chemotherapeutic agents.[7,8] Amifostine is a thiophosphate prodrug that is dephosphorylated to the free thiol active metabolite, WR-1065, by the plasma membrane bound enzyme alkaline phosphatase.[9] A number of studies have attempted to characterize the mechanism of differential protection when amifostine is administered systemically. Amifostine may be actively absorbed by normal tissue cells and only passively absorbed by tumor cells.[10] The selective uptake of WR-1065 may also be due to differences in the tissue microenvironment resulting in the slow entry of the free thiol into tumor masses. Tumors are often relatively hypovascular and have low interstitial pH, resulting in low rates of prodrug activation by alkaline phosphatase. In addition, there is a plentiful distribution of alkaline phosphatase in capillaries and arterioles of normal tissues compared with tumors. Thus, in tumors it is thought that both reduced metabolism of amifostine to the active protector WR-1065 and the low uptake of WR-1065 by the tumor result in a concentration of the free thiol that is much lower than that found in normal organs.[11,12] As a result, healthy tissue is protected from radiotherapy and chemotherapy while tumors with lower levels of the active metabolite are less protected. Transient hypotension, however, is the major dose-limiting adverse effect of amifostine. It is associated with direct relaxation of vascular smooth muscle mediated by free WR-1065.[13] The main metabolic pathway of WR-1065 elimination involves the formation of symmetrical and nonsymmetrical disulfides that might serve as a depot for the active metabolite, free WR-1065.[14]

Compared with intravenous administration, regional chemotherapy may deliver high concentrations of drug to a desired target site while reducing the systemic exposure of

drug. Amifostine is a good candidate for regional drug delivery to the liver because it has a large clearance from the body and is eliminated more extensively by the liver than by the gastrointestinal tract, lungs, or kidneys.[15-18] Approximately 90% of the drug is extracted by the liver (i.e., converted to WR-1065), suggesting that the liver may preferentially take up the active free thiol, WR-1065.[19] We hypothesize that organs with high amifostine clearance and extraction ratio would have a high activation rate of amifostine to WR-1065 and, therefore, would be protected by amifostine. Clinically, a simpler but equally effective mode of administration would make amifostine more convenient for both the patient and the practitioner. Subcutaneous administration of amifostine could potentially reduce the side effects of the drug and be significantly more convenient for both patients and radiation oncologists. To be clinically useful, the SC route would have to be as effective as IV administration.

Radiation therapy has played a minor role in the conventional management of patients with intrahepatic malignancies because the dose of radiation that can be delivered is limited by normal tissue toxicity referred to as radiation-induced liver disease (RILD). For patients with focal intrahepatic cancers, three dimensional treatment planning has permitted the delivery of high doses of radiation, leading to improved local control and, possibly, survival. However, many patients have disease that is too diffuse to be treated with focal techniques. Amifostine has been shown in randomized trials to protect the kidney from cisplatin nephrotoxicity and the parotid gland from radiation due to the greater conversion of the drug to the active metabolite WR-1065 in the normal tissue than in the tumor. Protection appears to result from scavenging oxygen-derived free radicals and hydrogen donation to repair damaged target molecules. Each of these mechanisms

requires that the active metabolite be present at the time of radiation. WR-1065 may also affect the catalytic inactivation of topoisomerase II, which slows cell cycling, thus providing more time for DNA repair.[20] In order to optimize the use of amifostine as a radiation protector of normal liver, which will permit the safe delivery of higher doses of radiation for patients with both focal and diffuse disease, the following specific aims are proposed in this research:

1. **Phase I trial of dose escalating radiation therapy with systemic amifostine for patients with diffuse intrahepatic cancer.**

   We hypothesize that systemic amifostine will permit meaningful selective protection of the normal liver, permitting radiation dose escalation.

2. **Preclinical studies to optimize selectivity and estimate the appropriate dose of regional amifostine.**

   We hypothesize that regional amifostine will be superior to systemic amifostine in producing a higher liver to tumor ratio of WR-1065, causing greater selective protection of normal liver compared to tumor.

3. **Preclinical studies to optimize selectivity and estimate the appropriate dose of subcutaneous amifostine.**

   We hypothesize that subcutaneous administration of amifostine will permit equal protection of normal liver to systemic administration, with equal (or less) systemic toxicity.

References

1. Phillips TL. Sensitizers and protectors in clinical oncology. *Semin Oncol*, 8:65-81, 1981.

2. Links M and Lewis C. Chemoprotectants: a review of their clinical pharmacology and therapeutic efficacy. *Drugs*, 57: 293-308, 1999.

3. Hensley M, Schuchter LM, Lindley C, Meropol NJ, Cohen GI. American Society of Clinical Oncology: Clinical Practice Guidelines for the use of chemotherapy and radiotherapy protectants. *J Clin Oncol*, 17: 3333-3355, 1999.

4. Tannehill SP and Mehta MP. Amifostine and radiation therapy: past, present, and future. *Semin Oncol*, 23: 69-77, 1996.

5. Yuhas JM, Spellman JM and Culo F. The role of WR-2721 in radiotherapy and/or chemotherapy. *Cancer Clin Trials*, 3: 211-216, 1980.

6. PDR (2000) Ethyol, in PHYSICIANS' DESK REFERENCE 54 edition, Medical economics Company, Montvale, NJ.

7. Milas, L., Hunter, N., Reid, B.O., and Thames, J., H.D. Protective effects of S-2-(3-aminopropylamino) ethylphosphorothioic acid against radiation damage of normal tissues and a fibrosarcoma in mice. *Cancer Res*, 42: 18888-1897, 1982.

8. Rasey, J.S., Nelson, N.J., Mahler,P., Anderson, K., Krohn, K.A., and Menard, T. Radioprotection of normal tissues against gamma rays and cyclotron neutrons with WR-2721-LD_{50} studies and ^{35}S-WR-2721 biodistribution. *Radiat Res*, 97: 598-607, 1984.

9. Shaw, L. M., Bonner, H.S., and Brown, D.Q. Metabolic pathways of WR-2721 (ethyol, amifostine) in the BALB/c mouse. *Drug Metab Dispos*, 22: 895-902, 1994.

10. Yuhas, J.M. Active versus passive absorption kinetics as the basis for selective protection of normal tissues by S-2-(3-aminopropylamino) ethylphosphorothioic acid. *Cancer Res*, 40: 1519-1524, 1980.

11. Calabro-Jones, P.M., Aguilera, J.A., Ward, J. F., Smoluk, G.D., and Fahey, R.C. Uptake of WR-2721 derivatives by cell in culture – Identification of the transported form of the drug. *Cancer Res*, 48: 3634-3640, 1988.

12. Rasy, J. S., Grunbaum, A., Krohn, K.A., Menard, T. W., and Spence, A. M. Biodistribution of the radioprotective drug ^{35}S-labeled 3-amino-2-hydroxypropyl phosphorothioate (WR77913). *Radiat Res*, 102: 130-137, 1985.

13. Ryan SV, Carrithers SL, Parkinson SJ, Skurk C, Nuss C, Pooler PM, Owen CS, Lefer AM. Hypotensive mechanisms of amifostine. *J Clin Pharm*, 36: 365-373, 1996.

14. Shaw LM, Bonner HS and Lieberman L. Pharmacokinetic profile of Amifostine. *Semin Oncol*, 23: 18-22, 1996.

15. Symon, Z., Levi, M., Ensminger, W.D., Smith, D.E., and Lawrence, T.S. Selective radioprotection of hepatocytes by systemic and portal vein infusion of amifostine in a rat liver tumor model. *Int J Radiat Oncol Biol Phys*, 50: 473-478, 2001.

16. Shaw, L.M., Bonner, H.S., Turrisi, A., Norfleet, A. L., and Kligerman, M. Measurement of S-2-(3-aminopropylamino) ethanethiol (WR-1065) in blood and tissue. *J Liq Chromatogr*, 9: 845-859, 1986.

17. Burns, J. A., Butler, J. C., Moran, J., and Whitesides, G. M. Selective reduction of disulfides by tris(2-carboxyethyl) phosphine. *J Org Chem*, 56: 2648-2650, 1991.

18. Shaw, L.M., Bonner, H.S., Turrisi, A., Norfleet, A. L., and Glover, D.J. A liquid chromatographic electrochemical assay for S-2-(3-aminopropylamino) ethylphosphorothioate (WR-2721) in human plasma. *J Liq Chromatogr*, 7: 2447-2465, 1984.

19. Levi, M., Knol, J.A., Ensminger, W.D., Deremer, S.J., Dou, C., Lunte, S.M., Bonner, H.S., Shaw, L.M., and Smith, D.E. Regional pharmacokinetics of amifostine in anesthetized dogs: role of the liver, gastrointestinal tract, lungs and kidneys. *Drug Metab Dispos,* 30: 1425-1430, 2002.

20. Snder, R.D. and Grdina, D.J. Further evidence that the radioprotective aminothiol, WR-1065, catalytically inactive mammalian topoisomerase II. Cancer Res, 60: 1186-1188, 2000.

CHAPTER 2

BACKGROUND AND LITERATURE REVIEW

2.1 Problems and solutions of intrahepatic cancer treatment

Approximately 20,000 patients die in the United States from uncontrolled intrahepatic cancer every year, resulting about equally from colorectal cancer metastatic to the liver and from primary hepatobiliary cancer.[1,2] In addition to that, thousands of patients suffer from liver metastases in the context of other systemic cancers (such as breast and lung cancer). However, radiation therapy has played a minor role in the conventional management of these patients. This is because the liver is relatively radiosensitive, with an estimated whole-liver tolerance dose of about 30-33 Gy at 1.5-2 Gy per fraction, and that such doses can (at best) produce only short-term palliation of macroscopic solid tumors. Treatment of the liver with more than this dose can result in radiation-induced liver disease known as RILD (traditionally, but inappropriately, called "radiation hepatitis"). Consequently, during much of the last 30 years, only low doses of radiation have been delivered to patients with intrahepatic cancers, producing few responses and little symptomatic liver toxicity. However, there has been a renewed interest in hepatic irradiation-induced hepatic toxicity because of two advances in the therapy of cancer patients. The first is the development of three-dimensional treatment planning.[3] The application of this powerful new tool enables the safe delivery of high doses of radiation

to focal well-defined volumes while sparing most of the normal liver.[4-7] Although this approach, by permitting the safe delivery of doses in excess of 70 Gy to some liver tumors, appears to improve the outcome of patients with intrahepatic cancer, a number of patients have developed clinical radiation liver injury. The second advance is the introduction of bone marrow transplantation, in which hepatic toxicity, in the form of veno-occlusive disease (VOD), is produced by the combined use of chemotherapy and total body irradiation as part of the preparative regime.

Needless to say, these toxicities can have a significant impact on the quality of life of the patient. Pathologically, it is very similar to the veno-occlusive disease, marked congestion with each lobule, also some necrosis in the affected area, which can result in the liver size decrease. Clinically, patients will feel tired, gain unnecessary weight, develop ascites and so on. Furthermore, these adverse effects may restrict the dose of antineoplastic therapy that can be administered or cause a delay in therapy, perhaps limiting the efficacy of treatment.

In recent years, a number of strategies have been developed to improve the outcome of intrahepatic cancer treatment. Besides the three dimensional treatment planning mentioned above which (combined with hepatic arterial FdUrd) has been successful for patients with fewer than 3-4 lesions, another strategy is the use of cytoprotective drugs to minimize or avert treatment-related toxicities to normal tissue. We hypothesize that the outcome of treatment can be improved further by the application of a radiation protector. Four groups of patients could benefit from this approach:

1) Patients with diffuse gross disease: Although the ability to increase whole liver radiation to 46-52 Gy is unlikely to be curative, it could provide meaningful

palliation for patients with gross disease who are often suffering from significant pain or other tumor related morbidity.

2) Patients with occult intrahepatic disease: Clinical data suggest that an increase in whole liver dose to the 46-52 Gy that would be permitted by the use of a radiation protector could offer the opportunity to cure patients with occult intrahepatic disease. This dose of radiation prevents the recurrence of occult disease in head and neck cancer, lung cancer, gastric cancer, and rectal cancer. It is possible that even lower doses could be effective when administered concurrently with fluoropyrimidines, which are potent radiation sensitizers.

3) Patients with focal liver disease: This is particularly true for patients who can safely receive doses in the range of 45-60 Gy without cytoprotectant. Although these doses can, in combination with hepatic arterial FdUrd, cause tumor regression, they have not produced the long-term survival, which has been experienced by patients who can receive ≥ 70 Gy. In this latter group, a median survival in excess of 16 months has been produced. Thus, the development of a selective radioprotection strategy could permit more patients with focal liver disease to derive the benefit of higher doses that, so far, have relied solely on technical improvements in delivery.

4) Patients who develop VOD after treatment with high dose chemotherapy used in bone marrow transplantation evidence the identical pathologic lesion as those suffering from RILD. Thus, the development of a strategy that protects against RILD could well protect against chemotherapy-induced liver toxicity.

The liver appears to be a particularly promising organ for a radioprotective strategy. If amifostine treatment allowed even a modest increase in the dose of radiation that can be tolerated by the whole liver, tens of thousands of cancer patients a year could benefit. A brief description of the liver anatomy and physiology, pathology of treatment-induced hepatic toxicity, and pharmacodynamics/pharmacokinetics of amifostine is provided below in order to better understand the limitations of chemo- and radiotherapy in the current treatment of hepatic carcinoma.

2.1.1 Anatomy and physiology of the liver[8]

The liver is the largest metabolic organ in the body. It is divided into two lobes – a large right lobe and a smaller left lobe that merges in the middle. The basic functional unit of liver is the liver lobule, which contains specialized epithelial cells called hepatocytes, a network of interconnected plates around a central vein. Large vascular capillaries known as sinusoids form a reservoir of blood, facilitating drug and nutrient removal prior to entering the general circulation. The sinusoids are lined with endothelial cells, or Kupffer cells that engulf worn-out white and red blood cells and foreign substances from the blood.

The liver receives blood from the hepatic artery and the large hepatic portal vein that collects blood from different segments of the GI tract. The arterial blood from the aorta carries oxygen to the liver and accounts for about 25% of liver blood flow. The venous blood containing newly absorbed nutrients from the GI tract accounts for about 75% of liver blood flow. Within the liver, the terminal branches of the hepatic artery and portal vein mix with sinusoids. Blood leaves the liver via the hepatic veins, which join the inferior vena cave. In humans, the average liver blood flow is about 1350 ml/minute.

2.1.2 Liver pathophysiology with radiotherapy

Radiation-induced liver disease (RILD), often called radiation hepatitis, is a syndrome characterized by the development of anicteric ascites approximately 2 weeks to 4 months after hepatic irradiation.[9] RILD resulting from liver radiation can usually be distinguished clinically from that resulting from the preparative regime associated with bone marrow transplantation. However, both syndromes demonstrate the same pathological lesion: veno-occlusive disease (VOD). Grossly, VOD is characterized by areas of marked congestion, which involve chiefly the central portion of each lobule. Foci of yellow necrosis may appear in the center of the affected areas. Although the pathological mechanism of VOD is still unclear, it appears that irradiation results in the accumulation of extensive deposits of fibrin in the liver central veins and in the afferent sinusoids. The fibrin deposits remain for a prolonged period of time, perhaps because the radiation has impaired the fibrinolytic mechanism. Eventually the long-standing fibrin deposits are invaded by fibroblasts and deposition of collagen occurs. RILD typically occurs 4-8 weeks after the completion of treatment in which patients present with fatigue, rapid weight gain and increased abdominal girth. Physical examination reveals ascites and hepatomegaly although, in mild cases, the signs are detectable only by ultrasound or abdominal CT scan. Serum chemistry shows moderate elevations of aspartate transaminase (AST), alanine transaminase (ALT) and alkaline phosphatase. The chief therapy for RILD is diuretics, although some advocate steroids for severe cases.

2.2 Cytoprotectants against chemo- and radiotherapy induced cytotoxicities

2.2.1 Cytoprotectants

Dose-limiting toxicity secondary to antineoplastic chemotherapy and/or radiotherapy is due to the inability of cytotoxic drugs to differentiate between normal and malignant cells. The consequences of this may include impairment of patient quality of life because of toxicity, and reduced tumor control because of the inability to deliver adequate dose-intensive therapy against the cancer. Specific examples of toxicity against normal tissues include cisplatin-related neurotoxicity and nephrotoxicity, myelotoxicity secondary to treatment with alkylating agents and carboplatin, oxazaphosphorine-induced haemorrhagic cystitis, and cumulative dose-related cardiac toxicity secondary to anthracycline treatment.

The concept of site-specific inactivation of chemotherapy drugs and/or highly reactive electrophilic intermediates induced by radiation with cytoprotective agents has been extensively explored in both preclinical and clinical studies. The aim of cytoprotective agents is to improve the therapeutic ratio of the cytotoxic drug by reducing potential dose-limiting toxicity to normal tissue. By definition, cytoprotectants must not compromise the antitumor efficacy of the chemotherapy agent and radiation therapy, and they should not be associated with additional toxicity that might otherwise interfere with the delivery of adequate chemo- and radiotherapy. Consequently, the "ideal" chemo-/radioprotector should have the following properties:[10]

- Act selectively in normal tissues as opposed to tumor
- Be nontoxic

- Access normal tissues in adequate concentrations to elicit radiation modification or chemotherapy protection
- Make a radiation/chemotherapy dose less effective to normal tissues by:
    1. Decreasing radiation-induced damage
    2. Scavenging free radicals
    3. Chemically "repairing" radicals induced by radiation/chemotherapy
    4. Enhancing enzymatic repair pathways
    5. Other mechanisms
- Take into account the appropriate timing of drug delivery and radiation/chemotherapy treatment for maximal protection

In principal, the ideal protector allows for a larger anticancer dose to be delivered to the tumor. It is important to remember that in many tumors, response to radiation or chemotherapy is dose-dependent; therefore, increasing the dose delivered to the tumor will increase the likelihood of tumor cure.

The first cytoprotectant to be used was folinic acid (calcium folinate; leucovorin), designed to overcome methotrexate-induced toxicity. Since that, several cytoprotective compounds have been extensively investigated, including dexrazoxane, glutathione, ORG 2766, mesna and amifostine.[11] Among these compounds, the most noteworthy are dexrazoxane, mesna and amifostine because they have not only been approved by the FDA, but have also been routinely used, worldwide, in a clinical setting.

The anthracycline antibiotics, including doxorubicin (adriamycin), daunorubicin and epirubicin, are among the most active anticancer agents against a wide range of solid and haemopoietic malignancies. However, anthracycline-induced cardiac toxicity, which

appears to be associated with the generation of reactive oxygen species involving the formation of an anthracycline-iron complex, can limit effective clinical use of the above compounds. With this recognition, two promising metal-chelating agents have demonstrated a cardioprotective effect during acute and chronic treatment with doxorubicin and daunorubicin. One of them is razoxane (ICRF-159). Dexrazoxane (ICRF-187) is the more water soluble (+)-enantiomer of razoxane, which can be administered parenterally. The current FDA approval for dexrazoxane use is restricted to women with breast cancer who have already received 6 cycles of doxorubicin-based chemotherapy.

The oxazaphosphorine-based alkylating agents, including ifosfamide and cyclophosphamide, undergo metabolic activation by the hepatic microsomal enzyme system to form phosphoramide mustard and acrolein. Acrolein and other urotoxic metabolites are subsequently excreted intact into the urinary bladder to produce haemorrhagic cystitis. In the absence of a chemoprotective agent, ifosfamide and cyclophosphamide are associated with dose-limiting urothelial toxicity. Mesna (sodium-2-mercapto-ethane sulfonate) has been developed as a specific chemoprotective compound against acrolein-induced bladder toxicity.

Dexrazoxane and mesna have a relatively limited spectra of toxicity protection (i.e., cardiac and urothelial, respectively), whereas amifostine appears to be a broad-spectrum selective cytoprotective agent that has a broader potential tissue-protection spectrum. A broad-spectrum selective cytoprotective agent can be defined as one that protects multiple normal organs from the toxicity of cytotoxic antineoplastic therapies without protecting the tumor. Amifostine was originally developed during the height of the cold

war by the Walter Reed Army Institute of Research (WRAIR) as part of a United States Army classified research project to identify an agent that could be used to protect military personnel and the population against atomic radiation in the event of nuclear warfare. Of 4400 chemicals screened for this purpose, amifostine was selected as having the most effective radioprotective properties and a relative safety profile.[12] Further laboratory and clinical studies have shown that amifostine can protect a broad range of normal tissues and organs (e.g., bone marrow, peripheral nerve, heart, kidney, salivary gland and others with the exception of central nervous system) against the cytotoxic effects of alkylating agents, platinum compounds, anthracyclines, taxanes and irradiation without compromising antitumor cytotoxicity. To date, it is the broad-spectrum cytoprotective agent with the largest preclinical and clinical database. Based on both laboratory and clinical evidence, amifostine may be the most promising radioprotector for the liver.[13]

2.2.2 Chemistry of amifostine

Amifostine (Ethiofos, WR-2721) is a low molecular weight (MW 214.2) thiophosphate ester prodrug. Amifostine is highly water soluble, with the solubility of the trihydrate being more than 9 g per 100 ml at room temperature. The compound has four ionizable groups, two of which are associated with the phosphate function and two with the amino function. At physiological pH, the drug exists as a double zwitterion with an isoelectric point of about 6.6. Amifostine is also very polar, with an octanol/water partition coefficient smaller than 0.01, indicating minimal octanol partitioning. Its free thiol active metabolite (WR-1065) has an octanol/water partition coefficient of 0.037.[14] Because passage of drugs through lipid membranes and interaction with macromolecules at receptor sites sometimes correlate well with the octanol/water partition coefficient of the

drug, both amifostine and WR-1065 are orders of magnitude away from the lipoidal partitioning associated with good membrane permeability.

When administered intravenously, amifostine has shown to have good protection against radiation. However, after oral administration of the compound, a significant amount of the radioprotective activity of the compound is quickly lost,[12] perhaps due to an acid-catalyzed hydrolysis of the ester bond in the stomach prior to absorption. The resulting WR-1065 is presumably further metabolized to inactive compounds resulting in a loss of radioprotective activity. Further detailed studies have indicated that amifostine is unstable at the gastric pH. The stomach pH ranges from 1 to 3, and amifostine is hydrolyzed to WR-1065 under acidic conditions. The hydrolysis reaction of amifostine, which appears to be pH- and temperature- dependent but nonenzymatic, proceeds by cleavage of the P-S bond to yield a thiol (WR-1065) and inorganic phosphate[15]

(i.e., $H_2N(CH_2)_3NH(CH_2)_2SPO_3H_2 + H_2O \rightarrow H_2N(CH_2)_3NH(CH_2)_2SH + H_3PO_4$).

The maximal rate of hydrolysis occurs at pH 3.0. However, at neutral pH, no detectable hydrolysis occurs over 4 hours at room temperature. The half-life for hydrolysis of amifostine at the low pH of stomach juice at physiologic temperature is about 30.5 minutes. The hydrolysis reaction is also strongly temperature dependent. Cooling amifostine sample to 0°C minimizes the hydrolysis rate of amifostine to an acceptable rate even in highly acidic conditions. In the 1 M perchloric acid solution (pH<1) that is used to deproteinize blood samples containing amifostine and WR-1065, the rate of conversion is 0.6%/hr at 0°C. However, at room temperature the rate of hydrolysis in the perchloric acid mixture is 74 times greater.

In studies with cells in culture, no detectable drug uptake or radioprotection can be found when cells were exposed to amifostine in medium alone, but when alkaline phosphatase was added to the medium efficient uptake leading to appreciable cellular levels of WR-1065 and radioprotection were observed.[16] Additionally, amifostine dephosphorylation in mouse alkaline phosphatase enzyme preparations was inhibited by vandate, an alkaline phosphatase competitive inhibitor. All these results support the hypothesis that alkaline phosphatase is the catalyst responsible for the hydrolysis of amifostine and subsequent uptake of WR-1065 by cells in vivo. Alkaline phosphatase is located in the plasma membrane surface of cells and is particularly rich in the endothelial cells of arterioles in various tissues, in the epithelial cells of the proximal tubule of the kidney, and in the microvilli of the small intestine. Studies of standard alkaline phosphatase substrate in rat jejunum and colon specimens localize alkaline phosphatase to the rim of the jejunal brush border and show negligible activity in the colon.[17] Human and mouse isoforms of alkaline phosphatase have a pH optimum between 8 and 9 with amifostine as the substrate.

2.2.3 Detection of amifostine and WR-1065

Several serious obstacles have hampered the development of bioanalytical methods for amifostine. The compound is acid-labile, has no convenient chromophore, and has essentially no solubility in organic solvents because it is extremely polar. Lack of solubility in organic solvents precludes its extraction from biological fluids and its polarity places limitations on the types of chromatographic systems that might be used to separate it from endogenous materials. Detection of the free thiol (WR-1065) in

biological matrixes presents a challenge since the thiol can rapidly be oxidized to form either symmetrical or non-symmetrical (with other endogenous thiols) disulfides.

In spite of these difficulties, direct and reliable measurements of amifostine and WR-1065 in biological matrixes have been achieved in several laboratories using electrochemical detection coupled to liquid chromatography.[18,19] An amperometric electrochemical detector equipped with a thin film Hg/Au working electrode was used, and selectivity was enhanced by the use of a low electrode potential +0.15 V versus Ag/AgCl reference electrode.

In liquid chromatography with electrochemical detection (LCEC), analyte eluting from the analytical LC column undergoes electrolysis by passing over a planar electrode held at a fixed potential. If the potential is greater than that required for the electrolysis of the analyte, a measurable charge passes from electrode to analyte (or vice versa). The resulting current is directly proportional to the concentration of solute passing through the electrode. In terms of thiol detection with amalgamated gold electrode, the mechanism is presented by the following electrochemical oxidation reaction: $2RSH + Hg \rightarrow Hg(SR)_2 + 2H^+ + 2e^-$. The symmetrical disulfide (WR-33278) can be detected by using a dual electrode thin-layer cell in a series arrangement. The upstream electrode, held at –1.0 V vs Ag/AgCl, reduces the disulfides to the thiols which are detected downstream at +0.15 V vs Ag/AgCl. Non-symmetrical disulfides are difficult to detect since they are formed by a variety of protein and/or other compounds that are available physiologically (example: cysteine, glutathione). Alternatively, the total amount of WR-1065-related species could be measured by reducing all disulfides bonds and then measuring the levels of WR-1065.

Other published analytical methods for measuring levels of amifostine and WR-1065, especially for amifostine, are not direct and either use fluorescent derivatization (fluorescamine, monobromobimane) with the detection by fluorescence[20] or utilize the coulometric detector[21] which is believed to be more efficient than a traditional amperometric one. Unfortunately, analytical methods that involve conversion of amifostine to WR-1065 prior to analysis are indirect measures of amifostine, resulting in a more complicated validation process and perhaps less accuracy.

2.3 Pharmacodynamic properties of amifostine

2.3.1 Mechanism of action

Radiotherapy and chemotherapy are two main approaches in cancer patient treatment. Clinically, irradiation is derived from gamma (usually a ^{60}Co or ^{137} Cs source), x-ray or neutron emissions in most situations, whereas an electron beam or beta irradiation is used sometimes. The much more energetic gamma rays and x-rays, like ultra-violet rays, can interact directly with the DNA molecule. However, they cause most of their damage by ionizing the molecules, especially water, surrounding the DNA and/or DNA itself. This forms free radicals, i.e., chemical substances with an unpaired electron. These free radicals, especially those containing oxygen, are extremely reactive and immediately attack neighboring molecules. When such a free radical attacks a DNA molecule, it can change a base, but it frequently causes a single- or double-stranded breakage. Single-stranded breaks are ordinarily not serious because they are easily repaired by rejoining the ends of the severed strand. However, double-stranded breaks are very difficult to repair properly, so they frequently cause a lasting mutation. Additionally, chemotherapy drugs such as alkylating agents or platinum agents (cisplatin, carboplatin) can activate the

formation of DNA-DNA interstrand crosslinks or platinum-DNA and platinum-protein adducts.

Amifostine is a prodrug that is dephosphorylated by the membrane-bound enzyme alkaline phosphatase, to form the free thiol metabolite, WR-0165. WR-1065 is the main metabolite responsible for the cytoprotective effects of amifostine and is the metabolite most readily taken up into cells. Once inside cells, WR-1065 provides protection from radiotherapy and/or chemotherapy through several mechanisms. They include the following:

- WR-1065 can lower intracellular oxygen concentrations by competing with oxygen to prevent oxygen interactions with DNA radicals, which can generate potentially harmful hydroperoxides, resulting in fixation of damage and an increase in the risk of cell death.[22]
- The oxygen-independent mechanism appears to involve radical scavenging, such as those derived from radiation therapy or specific drugs (e.g., doxorubicin-derived superoxide anions), and/or hydrogen donation reactions.[23]
- WR-1065 can not only bind directly, and thus detoxify the active species of alkylating agents[24] or platinum agents[25] in normal tissues, but also partially reduce DNA platination by the cytotoxic agent (formation of cispaltin-DNA adducts).
- Some evidence indicates that both WR-1065 and amifostine can form complexes with cisplatin active species and detoxify them.[26]
- WR-1065 exerts cytoprotective effects, in part, via a catalytic inhibition of the enzyme DNA topoisomerase II alpha, leading to the subsequent accumulation of

cells in G2 phase and to prolong the cell cycle, thus providing more time for DNA repair.[27]

- The symmetric disulfide WR-33278, which is a metabolite of WR-1065, has cytoprotective properties as well. Those cytoprotective properties are explained by the structural similarities of the symmetrical disulfide to the polyamine speramine. WR-33278 binds more avidly to DNA than does speramine and enhances the relaxation of supercoiled DNA mediated by topoisomerase I.[28]
- Post-treatment of irradiated cells with WR-1065 has been shown to markedly attenuate radiation-induced apoptosis. WR-1065 has also reduced apoptosis caused by several chemicals.[29]

The protective effects of amifostine are largely limited to normal, and not tumor, tissue. This selective protection is based on the ability of WR-1065 to be taken up in higher concentration in normal organs than in tumor tissues. This preferential uptake is due to a combination of several biological features.

First, drug delivery is significantly impaired in tumor as compared with normal tissue due to the poor vascularisation of most tumors. Furthermore, alkaline phosphatase, the membrane-bound enzyme responsible for the dephosphorylation of amifostine to WR-1065, is largely distributed in capillaries and arterioles of normal tissues; however, solid tumors are poorly vascularised and tend to contain low levels of alkaline phosphatase. In normal human lung cells, alkaline phosphatase activity was found to be 275-fold higher than in non-small cell lung cancer cells. Consequently, less activation of amifostine to the active metabolite WR-1065 happen in tumor tissues because of lower levels of alkaline phosphatase. Thus, a difference in dephosphorylation ability in healthy versus malignant

tissue may explain the selective protection of amifostine against cytotoxic chemotherapy and/or radiotherapy.[30]

Another factor which contributes to the selective protective effects of amifostine is the difference in pH between normal and tumor tissues. The relatively high pH of normal tissues is optimal for WR-1065 formation as well as WR-1065 uptake. Amifostine is not dephosphorylated by acidic phosphatase, so the acidic pH associated with many tumors may restrict both the formation and uptake of WR-1065. It was shown that a decrease of 0.3 units in pH caused a two-fold reduction in the cell uptake rate of WR-1065. This means that even if WR-1065 does become available to tumor tissues it will not be absorbed by the cells at rate comparable to that of normal tissue.[31,32]

Finally, amifostine may be actively absorbed by normal tissue cells and only passively absorbed by tumor cells. As to the regional delivery of amifostine to the liver, which may offer more protection to the liver than systemic administration, it has been documented that the major source of blood flow to macroscopic hepatic cancers is by way of the hepatic artery. In contrast, the delivery of nutrients to normal tissues is primarily a function of the portal circulation. Thus, amifostine selectivity in liver may not only be enhanced by differences between normal tissue and tumor in alkaline phosphatase activity as described above, but also by differences in the drug's regional route of delivery (i.e., portal vein is favored).[33]

2.3.2 Protection against cytotoxic chemotherapy

The protective activity of amifostine against the tissue damaging effects of cytotoxic agents (e.g., carboplatin, carmustine, chlormethine, cisplatin, cyclophosphamide,

fluorouracil, lomustine, melphalan or oxidopamine) has been assessed in animal models and in patients with cancer.

In a preclinical study with mice,[34] amifostine has been shown to reduce cisplatin-induced nephrotoxicity without interfering with the cisplatin antitumor effect. This study suggests that the protection offered by amifostine allowed a 2.2-fold increase in cisplatin dose to 19 mg/kg before the occurrence of nephrotoxicity, which resulted in an increased antitumor effect of cisplatin. Clinical trials[35-38] of amifostine in combination with cisplatin also demonstrated a significant protection from the nephrotoxicity and neurological toxicities associated with the use of cisplatin, without compromising its antitumor efficacy. In conclusion, amifostine may be considered for the prevention of nephrotoxicity in patients receiving cisplatin-based chemotherapy.

Neutropenia, consisting primarily of leukopenia, is the principal dose-limiting toxic effect of cyclophosphamide. An expert panel from the American Society of Clinical Oncology (ASCO) recommends that amifostine be considered for the reduction of neutropenia-associated events in patients who receive alkylating-agent chemotherapy.[39] Carboplatin toxicity differs significantly from that of cisplatin. The usual dose-limiting toxic effect of carboplatin is bone marrow suppression, particularly thrombocytopenia. Pretreatment with amifostine increased carboplatin maximum tolerated dose from 400 to 500 mg/m^2, without compromising its antitumor activity.[40] Pretreatment with amifostine has shown significant protection of bone marrow, immune system and intestinal crypt cells from the toxicity induced by a broad range of antineoplastic agents in a number of studies.[41-44]

Amifostine does not appear to affect tumor response to, or antitumor activities of, chemotherapy. Although amifostine may demonstrate tumor-protective effects under certain experimental conditions in a small number of early preclinical studies, the protection of tumor cells was typically low and variable, being dependent on dose, tumor type and size, and administration time. No evidence of tumor protection has been reported in clinical trials.[45]

Amifostine is generally well tolerated and is associated with transient side effects, including nausea, vomiting, a warm or flushed feeling and occasional allergic reactions. The most clinically significant toxicity is hypotension. Based on the recommendation by the American Society of Clinical Oncology (ASCO), the suggested dose of amifostine with chemotherapy in adults is 910 mg/m^2, and is administered IV over 15 minutes, 30 minutes before chemotherapy.[39]

2.3.3 Protection against radiotherapy

A protective effect of amifostine against radiation has been convincingly demonstrated in mice, dogs and monkeys against x-, γ- and neutron-irradiation. Yuhas[46] demonstrated a dose-modifying factor (DMF; ratio of irradiation doses with and without amifostine required to produce a specific effect in 50% of animals at a given time) of 2.7 against 30-day mortality in mice. Protection of dogs with amifostine was demonstrated at 200 mg/kg, a dose producing one death due to drug, but five other animals survived the toxic effects of irradiation. At 150 mg/kg amifostine, a better tolerated dose, 8 of 16 dogs survived the toxic effects of irradiation. Rhesus monkeys were protected by 250 mg/kg of amifostine administered intravenously 30 minutes before irradiation.[12] While some studies in animal models have shown minimal protection of the tumor, only limited

preclinical data are available regarding intrahepatic cancers. Studies in rats[47,48] have demonstrated that systemic administration of amifostine protects hepatocytes with a dose modification factor of 2, and that the liver is protected from fibrosis with a dose modification factor that is greater than 2. However, these studies did not determine whether the protection of normal liver extends to protection of tumor cells from the cytotoxic effects of radiotherapy.

Symon et al.[49] have recently evaluated whether systemic or portal venous administration of amifostine could protect the normal liver from the effects of ionizing radiation without compromising tumor cell kill in a rat liver tumor model. A micronucleus assay was used in this study and has been shown to be a sensitive measure of hepatocyte radiosensitivity. For instance, Alati et al.[50] have shown that the radiation dose response for the induction of micronuclei in hepatocytes is linear both in air and under hypoxic conditions. Rats implanted with liver tumors were infused with 200 mg/kg amifostine over 15 min via the femoral or portal vein. After a single 6-Gy fraction irradiation, the frequency of hepatocyte micronuclei after administration of saline, systemic amifostine and portal venous amifostine was 18.7 ± 1%, 6.8 ± 1% and 9.9 ± 2%, respectively, corresponding to a radiation equivalent effect of 6 ± 0.5 Gy, 1.8 ± 0.3 Gy, and 2.5 ± 1.3 Gy, respectively. Both amifostine conditions showed considerably less radiation effect than saline-treated control ($p<0.01$); the two amifostine conditions did not differ significantly ($p=0.3$). The surviving fraction of tumor cells was not affected by amifostine treatment and was 0.03 ± 0.02 and 0.05 ± 0.03 for systemic and portal venous delivery, and 0.06 ± 0.02 for control animals ($p=0.34$). These findings demonstrate both systemic and portal venous administration of amifostine effectively protect hepatocytes

from ionizing radiation without compromising tumor cell kill in a clinically relevant animal model, and amifostine may be a selective normal tissue radioprotectant in liver cancer.

The possible benefits of using amifostine in combination with radiation therapy include reducing treatment-related toxicity and escalation of radiation dose in the curative treatment of cancer. Although several randomized clinical trials[51,52] have been conducted to determine amifostine protection in patients receiving radiation treatment for different cancers, its only approved use in combination with radiotherapy is as a protector against irradiation-induced xerostomia. This approval is based on the data from a large multi-center study in patients undergoing radiation therapy for head and neck cancer. Amifostine-treated patients demonstrated a statistically significant decrease in acute and chronic xerostomia compared to control patients. Another recent randomized trial in patients with lung cancer confirmed these results. Amifostine treatment significantly reduced pneumonitis and esophagitis, without decreasing tumor control. These and other clinical trials give strong support to the use of amifostine as a radioprotector. When given with radiation therapy for head and neck cancer, the recommended amifostine dose is 200 mg/m^2/day given as a slow IV push over 3 minutes, 15 to 30 minutes before each fraction of radiation therapy.

The liver appears to be a particularly promising organ for a radioprotective strategy using amifostine. As described previously, even a modest protective effect would permit a clinically meaningful increase in radiation dose to be delivered. In a small-scale study (internal protocol in progress), seven patients with diffuse intrahepatic cancer were treated using whole liver radiation with amifostine pretreatment. Patients received 150

mg/m^2 of amifostine prior to each dose of radiation, with a plan of radiation dose escalation. Treatment was delivered with concurrent hepatic arterial FdUrd. No patients developed RILD. There were no episodes of hypotension and no ≥ grade 3 nausea. The median survival of all patients was 10 months. Another preliminary study[53] showed that 19 of 203 patients treated with focal and whole liver radiation with amifostine pretreatment developed RILD without hepatic arterial FdUrd. From this study, patients with primary hepatobiliary cancers had a significantly greater risk of complication than those with colorectal cancer metastatic to the liver. These data suggest that amifostine administered systemically may protect the liver in patients with intrahepatic cancer who are undergoing whole liver radiation.

In summary, amifostine has the promise of being an effective radioprotector that could improve patient treatment outcomes and the quality of life. However, amifostine's radioprotective potential has materialized only in the treatment of head and neck cancer. Carefully designed preclinical and clinical trials may help to broaden the use of amifostine, for example, in liver cancer patients.

2.4 Pharmacokinetic properties of amifostine

The pharmacokinetic parameters of amifostine and WR-1065 in mice, rats, dogs, monkeys and humans are summarized in Table 2-1, 2-2 and 2-3. These results are discussed in more detail in the following sections below.

2.4.1 Absorption

The intravenous (IV) formulation of amifostine, used in virtually all clinical studies, is the sole formulation currently used for amifostine therapy in cancer patients. There is an important need for the development of an orally administered radioprotective drug. An

oral therapeutic agent can be administered more conveniently and used for the protection of critical body tissues against ionizing radiation. It might also protect human populations from the radiation hazards of nuclear events. However, oral administration of amifostine fails to protect monkeys and dogs, suggesting poor bioavailability of the drug. Besides the physicochemical properties of amifostine that have been described previously, various physiological factors such as gastric and intestinal transit time, drug binding, biotransformation in intestinal wall or liver are known to affect the rate and extent of amifostine absorption. It has been shown that amifostine suppresses stomach emptying and motility in the rhesus monkey.[54] Although the site of absorption of amifostine after oral administration is unknown, the main site of drug absorption is considered to be the small intestine. Another important cause of incomplete bioavailability of drugs is biotransformation in the intestinal wall or in the liver. When the extent of intestinal or hepatic extraction of the drug is high, only a small fraction of the drug absorbed from the intestine may actually reach the systemic circulation.

Characterization of amifostine and WR-1065 absorption in the rat small intestine[55,56] indicated that without an absorption enhancer (EDTA), a significant amount of parent compound (amifostine) was degraded in the small intestine presumably by dephosphorylation via alkaline phosphatase found in the brush border of the intestinal epithelium; WR-1065 was also extensively metabolized in the intestinal lumen and poorly absorbed. A decreased stability of amifostine and WR-1065 may increase the absorption of the radiolabeled compound, suggesting that the metabolites or degradation products of WR-1065 are better absorbed than the free thiol and parent compound. A pharmacokinetic study of amifostine and WR-1065 in the rhesus monkey,[57,58] with

different routes of administration (iv, intraduodenal, ip and portal), has shown that amifostine is not bioavailable after intraduodenal administration probably because of poor membrane permeability and metabolism by the intestinal tract and liver; low concentrations of free WR-1065 after intraduodenal administration revealed the drug's poor oral bioavailability.

Levi et al.[59] characterized the tissue activation of amifostine by the liver, gastrointestinal tract, lungs, and kidneys after systemic administrations of amifostine using sequential dose rates of 0.125, 0.500 and 1.00 μmol/min/kg in dogs. The experimental results demonstrated that amifostine is eliminated more extensively by the liver than by the gastrointestinal tract, lungs, or kidneys. Approximately 90% of the drug is extracted by the liver (i.e., converted to WR-1065). It is clear that poor oral bioavailability of amifostine may be due to this large first-pass effect by the liver. A greater understanding of the absorption of amifostine and its primary active metabolite, WR-1065, may be gained by characterization of the sites and extent of this organ-specific activation with WR-1065 alone.

Clinically, the blood and/or plasma concentrations of amifostine and WR-1065 are undetectable after oral administration of amifostine to the healthy subjects.[60] The bioavailability for the oral route could not be determined and this route of administration was unsuitable for further studies.

In conclusion, amifostine's poor bioavailability may have several explanations. Amifostine is readily hydrolyzed at gastric pH and suppresses gastric emptying. It is likely that the polar nature of amifostine limits its ability to cross lipoidal membrane

barriers found in the stomach and small intestine. Moreover, the small intestine and liver may be the sites of substantial drug metabolism.

2.4.2 Distribution

Preferred distribution of amifostine and/or WR-1065 in healthy tissues compared to tumor tissues is important in explaining amifostine selectivity. Several studies[61,62] of the distribution of amifostine made use of radiolabelled drug (primarily [^{35}S]-amifostine) and characterized the uptake of total [^{35}S]-amifostine radioactivity (amifostine plus its metabolites) from the bloodstream of experimental animals (primarily rats). Biodistribution of ^{35}S-labeled amifostine as a function of time after ip injection has shown that substantial tissue levels of ^{35}S were attained by 15 min and peaked at 30 to 60 min. The highest levels were obtained in kidney and submandibular salivary gland, with substantial levels in liver, gut, and lung. Whole brain and skin had the lowest levels of any normal tissues. A similar experiment using ^{35}S-labeled amifostine demonstrated that the labeled compound is rapidly cleared from the blood and appears in high concentration in normal tissues and in low concentration in several tumors. The distribution half-life of [^{35}S]-amifostine was very short - 5.5 min. The distribution of amifostine in normal tissues and tumors of rats, following both iv and ip injection, gave essentially identical results. Following administration (200mg/kg) of radiolabled amifostine, brain and spinal cord failed to accumulate detectable radioactivity over the 90-min test interval. In contrast, the lung, liver, heart and spleen initially contained less radioactivity than the serum, but by 15 min postinjection their concentrations exceeded that of the serum by factors of 1.5 to 2, indicating that these tissues are actively concentrating amifostine against a gradient. In the kidney, the levels of radioactivity were always higher than the serum levels. In the rat

tumors that were tested, radiolabel levels were significantly lower than in serum and slowly increased to equal decreasing serum concentrations 90 minutes after drug administration. From these observations, a facilitated transport process was suggested as the mechanism of uptake by the normal tissues studied versus passive absorption by tumors.

In a study of the distribution of WR-1065 after i.v. administration of 500 mg/kg amifostine to mice bearing tumors, Utley et al.[30] showed that maximal tissue concentrations of WR-1065 were achieved 5-15 min after injection. At 15 min after injection of [^{14}C]- amifostine, WR-1065 accounted for more than half of the total drug in all tissues (liver, kidney, lung, heart, muscle, spleen and salivary gland) except the tumor, where it accounted for one third of the total drug. This study showed that WR-1065 is rapidly produced from amifostine, that it is a major metabolite of the parent drug, and that the rate of disappearance of WR-1065 from tissues is very rapid in some cases. Concentrations rapidly decreased during the first 30 minutes in the lung and skin, and more slowly in the liver, whereas concentrations remained high for up to 3 hours in the salivary gland.

In a study by Shaw and coworkers,[63] the highest WR-1065 concentrations were found in the liver and kidney (965 and 2195 μmol/kg, respectively) 10 min after i.p. administration of 365 mg/kg amifostine to mice bearing tumor. In contrast, the heart and small intestine had lower peak values of 739 and 410 μmol/kg, respectively, at 30 minutes. Finally, WR-1065 accumulated in two experimental tumors at a significantly lower rate than it did in normal tissues. The pharmacokinetic behavior of amifostine was described in 13 patients with cancer who received 150 mg/m^2 intravenously.[64] After a

10-second bolus injection, there was a rapid biphasic decline in plasma drug concentration, with a distribution half-life of 0.88 minutes and an elimination half-life of 8.76 minutes. After a 15-minute infusion in another study in which 740mg/m^2 was administered to 10 patients with cancer, the average distribution half-life was 0.85 minutes. In humans, amifostine has a relatively small volume of distribution steady-state of 6.44 L, suggesting that the unmetabolized drug is largely confined to the intravascular compartment (primarily plasma). The plasma protein binding of the drug is also low; in studies in vitro, less than 4% of radioactively labeled amifostine was bound to albumin.[65]

In a study by Symon and coworkers[49] to determine liver protection by systemic or portal venous administration of amifostine in rats bearing tumor, portal venous delivery produced significantly less WR-1065 in the tumor compared to systemic administration (54 μM ± 36 vs. 343 μM ± 88, respectively, p = 0.03) although the levels of WR-1065 in the normal liver for systemic and portal venous delivery were found to be similar. This results in a significantly higher therapeutic index (i.e., mean liver/tumor concentration ratio) of WR-1065 for portal vein administration than for systemic venous administration. These findings support our hypothesis that compared to systemic administration, regional administration of amifostine may be advantageous in producing a higher normal to tumor WR-1065 ratio in liver.

2.4.3 Elimination

Amifostine is hydrolyzed to the free thiol, WR-1065, via a non-reversible process. In turn, WR-1065 is further oxidized to form disulfides with itself, proteins with thiol groups, and/or other endogenous thiols like glutathione and cysteine. The formation of

disulfides is a reversible process. Moreover, it was hypothesized that the disulfides serve as a depot for WR-1065. WR-1065 can undergo oxidation to form sulfonic acid or N-dealkylation to form cystamine. It was established in vitro that amifostine is dephosphorylated to form WR-1065, and that alkaline phosphatase is responsible for this process in several cell lines.[66] Following dephosphorylation, WR-1065 and the symmetrical disulfide (WR-33278) are then accumulated by cells in a ratio of 10:1, respectively.

Studies that investigated amifostine and/or WR-1065 metabolism have been conducted in mice,[55,56,63] dogs,[59,67,68] monkeys[57,58] and humans.[64,69,70] All these mammalian species share the similar extensive and rapid clearance of amifostine from the bloodstream as reflected by the short elimination half-lives observed. In monkeys,[57,58] conversion of amifostine to the thiol proceeded extremely rapidly since the peak concentration of WR-1065 occurred immediately after termination of the infusion of amifostine. Moreover, AUC values of amifosine and WR-1065 could account for only half of the radiolabel AUC values, suggesting the presence of unidentified metabolites in the plasma. In addition to WR-1065, several drug-related species were identified as metabolites of the parent drug and were present in the tissues of mice: they included WR-33278, the symmetrical disulfide of WR-1065 and the mixed disulfides (WR-1065-cysteine and WR-1065-glutathione).

In the study[59] in dogs to characterize the various tissues' activation of amifostine described previously (i.e., 0.125, 0.500 and 1.00 μmol/min/kg), the hepatic extraction of amifostine remained high at 90%, whereas gastrointestinal extraction decreased from 43 to 12~15% with increasing dose. Pulmonary extraction of amifostine was low at 7%,

whereas renal extraction was intermediate at 57%. Approximately 90% of the drug is extracted by the liver (i.e., converted to WR-1065), suggesting that the liver may preferentially take up the active free thiol and be protected extensively against the toxicities of radiation. Based on the clearance parameters above, amifostine exhibits saturable metabolism in the gastrointestinal tract (9.8 to 2.8~3.3 ml/min/kg) and the whole body (52.6 to about 37.3 ml/min/kg) as the doses increased in dogs. It is also worth notice that amifostine has a minimal extraction by the gastrointestinal tract (i.e., less than 15%) at concentrations likely to be achieved during clinical dosing. These conclusions formed the basis on which the study of liver radioprotection by regional delivery of amifostine is proposed.

In another metabolic study of amifostine,[71] it was found that small quantities of cysteamine were produced in mouse tissues following amifostine administration. However, cysteamine was not present in the blood 30 minutes after amifostine administration. These results support the hypothesis that WR-1065 undergoes N-dealkylation to form cystamine. A disposition study of WR-1065 in monkey[58] showed that free WR-1065 AUC values accounted for only 18.2% of the total WR-1065 AUC values, indicating rapid binding to endogenous thiols. It is further demonstrated that disulfide formation is a reversible reaction by measuring free WR-1065 levels in plasma following the administration of the symmetrical disulfide (WR-33278) to a beagle dog.[67,68]

The pharmacokinetics of amifostine in human have similar characteristics to that of animal models.[64,69,70,72] For example, amifostine and the free active thiol metabolite WR-1065 are cleared rapidly from the plasma. Second, the enzyme alkaline phosphatase

is responsible for the clearance of amifostine from the blood stream with immediate conversion to WR-1065. Finally, amifostine demonstrates nonlinear kinetics. In patients who received 150 mg/m^2 of amifostine intravenously, the elimination half-life is 8.76 minutes and less than 6% of the parent drug remained in the plasma compartment within 6 min after drug administration. AUC values for patients who received the 910 mg/m^2 dose (3,852 ± 1,363 μmol/min/L) are 2.6-fold higher than the values obtained for patients who received the 740 mg/m^2 dose (1,506 ± 665 μmol/min/L). The expected ratio for linear pharmacokinetic behavior is 910/740 =1.23, suggesting that amifostine exhibits nonlinear kinetic behavior.[72]

Only small amounts of amifostine and its metabolites are excreted in the urine.[70] In 7 patients receiving a 15-minute infusion of amifostine 740 mg/m^2, the average of percentage of the total administered amifostine dose recovered in the urine after 45 minutes was 1.05, 1.38 and 4.2% for amifostine, WR-1065 and WR-33278, respectively. Similar amounts of amifostine and metabolites (< 3% of the administered dose) were found in the urine after 45 minutes in 6 patients receiving a 150-mg/m^2 bolus dose of amifostine.[64] The rapid elimination, small volume of distribution, and limited amount of drug and metabolites recovered in the urine suggest that amifostine is rapidly dephosphorylated and then enters cells as WR-1065.

2.4.4 Drug-Drug interaction

The rapid elimination of amifostine from the plasma reduces the potential for drug interactions with antineoplastic agents, which are administered ≥ 15 minutes after infusion of amifostine. Still, amifostine does appear to influence the pharmacokinetics of

some chemotherapeutic agents, although the clinical significance of these changes is either minimal or not yet determined.

In patients receiving carboplatin (400 or 500 mg/m^2) or cisplatin (70 mg/m^2) therapy,[73,74] pretreatment with amifostine (910-740 mg/m^2) appears to reduce the renal clearance of these drugs. Mean values of the pharmacokinetic parameters of three cisplatin species (total, non protein-bound, and unchanged platinum) after treatment with and without amifostine indicate that amifostine had only a minor influence on the pharmacokinetics of cisplatin in plasma, resulting in an increase in the terminal half-life of cisplatin that is not protein-bound (0.77 hr with amifostine vs. 0.57 hr without amifostine). This effect was hypothesized to be due to a direct effect of amifostine on kidney function, because a transient increase in serum creatinine levels was observed in patients receiving the drug.

Table 2.1. Pharmacokinetic parameters of amifostine in dogs and monkeys ($\overline{X} \pm$ SD)

	Dogs[77] (IV 10min, n=4)	Monkeys[67] (IV 10min, n=5)
Dose	150 mg/kg	120-150 mg/kg
$T_{1/2}$	$T_{1/2(\beta)}$: 16.0 min	$T_{1/2}$: 8-15 min
C_{max}	800-900 μg/ml	477 μg/ml
V_d	120 ml/kg	
CL	11.0 ± 1.3 ml/min/kg	43.5 ± 13.4 ml/min/kg

Table 2-2: Pharmacokinetic parameters of WR-1065 in dogs and monkeys ($\overline{X} \pm$ SD)

	Dogs[67] (n=3)	Monkeys[58]	
		10-Min infustion (n=3)	120-Min infustion (n=3)
Dose	38.8 mg/kg (IV 10min)	60 mg/kg	60 mg/kg
$T_{1/2}$ terminal	81.4 min	207 min	201 min
V_c (L/kg)	0.532 ± 0.226	0.375 ± 0.877	2.81 ± 1.12
V_{ss} (L/kg)	2.27 ± 0.898	3.02 ± 2.42	9.54 ± 5.37
CL (ml/min/kg)	64 ± 6.9	64.1 ± 7.17	76.2 ± 20.4
AUC (μM∗hr)		117 ± 13.8	102 ± 27.4

Table 2-3 Pharmacokinetic parameters of amifostine in humans ($\overline{X} \pm$ SD)

Dose / Parameter	150 mg/m^2 (IV 10s, n=13)	200 mg/m^2 (IV 7.5min, n=12)	740 mg/m^2 (IV 15min, n=10)	740 mg/m^2 (IV 15min, n=5)	910 mg/m^2 (IV 15min,n=7)
V_d (L)	V_c : 3.50 ± 0.90 V_{ss}: 6.44 ± 1.46			8.7 ± 2.7	7.4 ± 2.2
$T_{1/2}$ (min)	$T_{1/2(\alpha)}$: 0.88 ± 0.12 $T_{1/2(\beta)}$: 8.76 ± 2.03	15.4 ± 9.6	$T_{1/2(\alpha)}$: 0.85	1.5 ± 0.4	2.7 ± 0.8
C_{max} (μmol/L)		104.9 ± 30.9		100 ± 44	235 ± 77
CL (L/min)	2.17 ± 0.39	1.48 ± 0.46		4.3 ± 1.8	2.1 ± 0.8
AUC (μmol/min/L)		1187 ± 351		1506 ± 665	3852 ± 1363
Amifostine urinary excretion (%)	0.69 ± 0.31		1.05		
WR-1065 urinary excretion (%)	2.64 ± 1.18		1.38		
Reference	64	60	70	65	65

References

1. O' Connell, M.J., Nagorney, D.M., Bernath, A. M., Schroeder, G., Fitzgibbons, R.J., Mailliard, J. A., Burch, P., Bolton, J.S., Colon-Otero, G. and Krook, J. E. Sequential intrahepatic fluorodeoxyuridine and systemic fluorouracil plus leucovorin for the treatment of metastatic colorectal cancer confined to the liver. *J Clin Oncol*, 16: 2528-2533, 1998.

2. Hughes, K. S., Simon, R., and Songhorabodi, S. Resection of the liver for colorectal carcinoma metastases: a multi-institutional study of indications for resection. *Surgery*, 103: 278-288, 1987.

3. McShan, D.L., Fraass, B.A., and Lichter, A. S. Full integration of the beam's eye view concept into computerized treatment planning. *Int. J. Radiat. Oncol. Biol. Phys*, 18: 1485-1494, 1990.

4. Lawrence, T. S., Tesser, R.J., and Ten Haken, R. K. An application of dose volume histograms to the treatment of intrahepatic malignancies with radiation therapy. *Int. J. Radiat. Oncol. Biol. Phys*, 19: 1041-1047, 1990.

5. Lawrence, T. S., Ten Haken, R. K., Kessler, M.L., Robertson, J.M., Lyman, M.T., LaVigne, M. L., Duross, D. J., Brown, M. B., Andrews, J. C., Ensminger, W.D. and Lichter, A. S. The use of 3-D dose volume analysis to predict radiation hepatitis. *Int. J. Radiat. Oncol. Biol. Phys*, 23: 781-788, 1992.

6. McGinn, C. J., Ten Haken, R. K., Ensminger, W. D., Walker, S., Wang, S. and Lawrence, T. S. Treatment of intrahepatic cancers with radiation doses based on a normal tissue complication probability model. *J Clin Oncol*, 16: 2246-2252, 1998.

7. Dawson, L.A., McGinn, C. J., Ten Haken, R. K., Ensminger, W. and Lawrence, T. S. Escalated focal liver radiation and hepatic artery floxuridine for unresectable liver malignancies. *J Clin Oncol*, 18: 2210-2218, 2000.

8. Shargel, Leon and Yu, Andrew B.C. Applied Biopharmaceutics & Pharmacokinetics, 1999.

9. Lawrence TS, Robertson JM, Anscher MS, Jirtle RL, Ensminger WD and Fajardo LF. Hepatic toxicity resulting from cancer treatment. *Int. J. Radiat. Oncol. Biol. Phys*, 31: 1237-1248, 1995.

10. Herscher LL, Cook JA, Pacelli R, Pass HI, Russo A and Mitchell JB. Principles of chemoradiation: theoretical and practical considerations. *Oncology*, 13: 11-22, 1999.

11. Links M and Lewis C. Chemoprotectants: a review of their clinical pharmacology and therapeutic efficacy. *Drugs*, 57: 293-308, 1999.

12. Davidson DE, Grenan MM and Sweeney TR. Biological characterization of some improved radioprotectors, in *radiation sensitizers*. *Their use in the clinical management of caner* (Brady L ed) pp 309-320, 1980, Masson, New York, NY.

13. Weiss JF. Pharmacologic approaches to protection against radiation-induced lethality and other damamge. *Environmental Health Perspectives* 105: 1473-1478, 1997.

14. Felckenstein L, Swynnerton NF, Ludden TM and Mangold DJ. Bioavailability and newer methods of delivery of phosphorothioate radioprotectors. *Pharmac Ther*, 39: 203-212, 1988.

15. Risley JM, Van Etten RL, Shaw LM and Bonner H. Hydrolysis of S-2-(3-aminopropylamino) ethylphosphorothioate (WR-2721). *Biochemical Pharmacology*, 35: 1453-1458, 1986.

16. Calabro-Jones, P.M., Aguilera, J.A., Ward, J. F., Smoluk, G.D., and Fahey, R.C. Uptake of WR-2721 derivatives by cell in culture – Identification of the transported form of the drug. *Cancer Res*, 48: 3634-3640, 1988.

17. Stewart, B.H., Amidon, G. L., and Brabec, R. K. Uptake of prodrugs by rat intestinal mucosal cells: Mechanism and pharmaceutical implications. *J. Pharm. Sci*, 75: 940-945, 1986.

18. Shaw, L.M., Bonner, H.S., Turrisi, A., Norfleet, A. L., and Glover, D.J. A liquid chromatographic electrochemical assay for S-2-(3-aminopropylamino) ethylphosphorothioate (WR-2721) in human plasma. *J Liq Chromatogr*, 7: 2447-2465, 1984.

19. Shaw, L.M., Bonner, H.S., Turrisi, A., Norfleet, A. L., and Kligerman, M. Measurement of S-2-(3-aminopropylamino) ethanethiol (WR-1065) in blood and tissue. *J Liq Chromatogr*, 9: 845-859, 1986.

20. Souid AK, Newton GL, Dubowy RL, Fahey RC and Bernstein ML. Determination of the cytoprotective agent WR-2721 (Amifostine, Ethyol) and it metabolites in human blood using monobromobimane fluorescent labeling and high-performance liquid chromatography. *Cancer Chemotherapy & Pharmacology*, 42: 400-406, 1998.

21. Feng Bai, Kirstein MN, Hanna, SK and Stewart CF. New liquid chromatographic assay with electrochemical detection for the measurement of amifostine and WR-1065, *J Chromatogr*, 772: 257-265, 2002.

22. Spencer CM, Goa KL. Amifostine: a review of its pharmacodynamic and pharmacokinetic properties, and therapeutic potential as a radioprotector and cytotoxic chemoprotector. *Drugs*, Dec; 50: 1001-31, 1995.

23. Grdina DJ, Kataoka Y, Murley JS. Amifostine: mechanisms of action underlying cytoprotection and chemoprevention. *Drug Metabol Drug Interact*, 16(4): 237-79, 2000.

24. Deneve WJ, Everrett CK, Suminski JE and Valeriote FA. Influence of WR-2721 on DNA cross-linking by nitrogen mustared in normal mouse bone marrow and leukemia cells in vivo. *Cancer Res*, 48: 6002-6005, 1988.

25. Treskes M, Holwerda U, Pinedo HM and van der Vijgh WJF. The chemical reactivity of the modulating agent WR2721 (ethiofos) and its main metabolites with the antitumor agents cisplatin and carboplatin. *Biochemical Pharmacology*, 42: 2125-2130, 1991.

26. Thompson DC, Wyrick SD, Holbrook DJ and Chaney SG. HPLC and ^{31}P NMR characterization of the reaction between antitumor platinum agents and the phosphorothioate chemoprotective agent S-2-(3-aminopropylamino) ethylphosphorothioic acid (WR-2721). *Biochemical Pharmacology*, 50: 1413-1419, 1995.

27. Snder, R.D. and Grdina, D.J. Further evidence that the radioprotective aminothiol, WR-1065, catalytically inactive mammalian topoisomerase II. Cancer Res, 60: 1186-1188, 2000.

28. Holwitt EA, Koda E and Swenberg CE. Enhancment of topoisomerase I – mediated unwinding of supercoiled DNA by the radioprotector WR-33278. *Radiation Res*, 124: 107-109, 1990.

29. Ramakrishnan N and Catravas GN. N-(2-mercaptoethyl)-1,3,-propanediamine (WR-1065) protects thymocytes from programmed cell death. *J Immunol*, 148: 1817-1821, 1992.

30. Utley JF, Seaver N, Newton GL and Fahey RC. Pharmacokinetics of WR-1065 in mouse tissue following treatment with WR-2721. *Int. J. Radiat. Oncol. Biol. Phys*, 10: 1525-1528, 1984.

31. Kennedy KA, Teicher BA, Rockwell S and Sartorelli AC. Chemotherapeutic approaches to cell populations of tumors, in molecular actions and Targets for cancer chemotherapeutic agents, pp85-101, Academic Press, New York.

32. Vaupel PW, Frinak S and Bicher HI. Heterogeneous oxygen partial pressure and pH distribution in C3H mouse mammary adenocarcinoma. *Cancer Res*, 41: 2008-2013, 1981.

33. Ensminger WD. Intra-arterial chemotherapy for the treatment of hepatic metastases. Principles and Practice of Oncology Updates, 1: 1, 1987.

34. Treskes M, Boven E, Holwerda U, Pinedo HM and van der Vijgh WJF. Time dependence of the selective modulation of cisplatin-induced nephrotoxicity by WR-2721 in the mouse. *Cancer Res*, 52: 2257-2260, 1992.

35. Glover D, Glick JH, Weiler C, Yuhas J and Kligerman MM. Phase I trials of WR-2721 and cis-platinum. *Int J Radiat Oncol Biol Phys*, 10: 1781-1784, 1984.

36. Glover D, Glick JH, Weiler C, Fox K, Turrisi A and Kligerman MM. Phase I/II trials of WR-2721 and cis-platinum. *Int J Radiat Oncol Biol Phys,* 12: 1509-1521, 1986.

37. Mollman JE, Glover DJ, Hogan WM and Furman RE. Cisplatin neuropathy: risk factors, prognosis, and protection by WR-2721. *Cancer*, 61: 2191-2195, 1988.

38. Kemp G, Rose P, Lurain J, Berman M, Manetta A, Roullet B, Homesley H, Belpomme D and Glick J. Amifostine pretreatment for protection against cyclophosphamide-induced and cisplatin-induced toxicities: results of a randomized control trial in patients with advanced ovarian cancer. *J Clin Oncol,* 14: 2101-2112, 1996.

39. Schuchter LM, Hensley ML, Meropol NJ and Eric P. 2002 update of recommendations for the use of chemotherapy and radiotherapy protectants: clinical practice guidelines of the American Society of Clinical Oncology. *J Clin Oncol*, 20(12): 2895-2903, 2002.

40. Budd GT, Ganapathi R, Bauer L, Murthy S, Adelstein D, Weick J, Gibson V, McLain D, Sergi J and Bukowski RM. Phase I study of WR-2721 and carboplatin. *European Journal of Cancer*, 29A: 1122-1127, 1993.

41. Wasserman TH, Phillips TL, Ross G and Kane LJ. Differential protection against cytotoxic chemotherapeutic effects on bone marrow CFUs by WR-2721. *Cancer Clin Trials*, 4:3-6, 1981.

42. Doz F, Berens ME, Spencer DR, Dougherty DV and Rosenblum ML. Experimental basis for increasing the therapeutic index of carboplatin in brain tumor therapy by pretreatment with WR-2721 compounds. *Cancer Chemotherapy and pharmacology* 28: 308-310, 1991.

43. Harris JW and Meneses JJ. Radioprotection of immunologically reactive T lymphocytes by WR-2721. *Int J Radiat Oncol Biol Phys*, 4: 437-440, 1978.

44. Millar JL, McElwain TJ, Clutterbuck RD and Wist EA. The modification of melphalan toxicity in tumor bearing mice by S-2-(3-aminopropylamino) ethylphosphorothioic acid (WR-2721). *American Journal of Clinical Oncology*, 5: 321-328, 1982.

45. Culy CR and Spencer CM. Amifostine: an update on its clinical status as a cytoprotectant in patients with cancer receiving chemotherapy or radiotherapy and its potential therapeutic application in myelodysplastic syndrome. Drugs, 61(5): 641-684, 2001.

46. Yuhas JM. Biological factors affecting the radioprotective efficiency of S-2-(3-aminopropylamino) ethylphosphorothioic acid (WR-2721). *Radiation Res*, 44: 621-628, 1970.

47. Jirtle, RL, Pierce LJ, Crocker, IR and Strom, SC. Radiation protection of rat parenchymal hepatocytes with S-2-(3-aminopropylamino) ethylphosphorothioic acid. Radiother Oncol, 4: 231-237, 1985.

48. Jirtle, RL, Anscher, MS, and Alati, T. Radiation sensitivity of the liver. *Adv Radiat Biol*, 14: 269-311, 1990.

49. Symon, Z., Levi, M., Ensminger, W.D., Smith, D.E., and Lawrence, T.S. Selective radioprotection of hepatocytes by systemic and portal vein infusion of amifostine in a rat liver tumor model. *Int J Radiat Oncol Biol Phys*, 50: 473-478, 2001.

50. Alati, T., Eckl, P., and Jirtle, R.L. An in vitro micronucleus assay for determining the radiosensitivity of hepatocytes. *Radiat Res*, 119: 562-568, 1989.

51. Brizel, DM, Wasserman, TH, Henke M, et al. Phase III randomized trial of amifostine as a radioprotector in head and neck cancer. *J Clin Oncol*, 18: 3339-3345, 2000.

52. Antonadou, D., Coliarakis, N., Synodinou, M., Athanassiou, H., Kouveli, A., Verigos, C., Georgakopoulos, G., Panoussaki, K., Karageorgis, P. and Throuvalas, N. Randomized phase III trial of radiation ± amifostine in patients with advanced-stage lung cancer. *Int. J. Radiat. Oncol. Biol. Phys*, 51: 915-922, 2001.

53. Dawson, L A., Normolle, D., Balter, JM., McGinn, C. J., Lawrence, T. S., and Ten Haken, R. K. Analysis of radiation induced liver disease using the Lyman NTCP model. *Int. J. Radiat. Oncol. Biol. Phys*, 53: 810-821, 2002.

54. Dubois, A., Guetta, O., Laporte, J.L. and Conklin, J.J. Relation between gastric empyting and gastric motility in primates. *Gastroenterology*, 91: 1051A, 1986.

55. Geary RS, Swynnerton NF, Timmons SF and Mangold DJ. Characterization of ethiofos absorption in the rat small intestine. *Biopharm & Drug Dispos*, 12: 261-274, 1991.

56. Geary RS, Swynnerton NF, Timmons SF and Mangold DJ. Characterization of WR-1065 absorption in the rat small intestine. *Biopharm & Drug Dispos*, 12: 275-284, 1991.

57. Mangold DJ, Miller MA, Huelle, BK, Sanchez-Barona DO, Swynnerton NF, Fleckenstein L and Ludden TM. Disposition of the radioprotector ethiofos in the rhesus monkey; influence of route of administration. *Drug Metab and Dispos*, 17(3): 304-310, 1989.

58. Mangold DJ, Miller MA, Huelle, BK, Geary RS, Sanchez-Barona DO, Swynnerton NF, Fleckenstein L and Ludden TM. Pharmacokinetics and disposition of WR-1065 in the rhesus monkey. *Drug Metab and Dispos*, 18(3): 281-287, 1990.

59. Levi, M., Ensminger, W.D., et al. Regional pharmacokinetics of amifostine in anesthetized dogs: role of the liver, gastrointestinal tract, lungs and kidneys. *Drug Metab Dispos,* 30: 1425-1430, 2002.

60. Bonner, H.S. and Shaw L.M. New dosing regimens for amifostine: a pilot study to compare the relative bioavailability of oral and subcutaneous administration with intravenous infusion. J Clin Pharmacol, 42: 166-174, 2002.

61. Yuhas JM, Spellman JM, Jordan SW, Pardini MC, Afzal SMJ and Culo F. Treatment of tumors with the combination of WR-2721 and cis-dichlorodiammineplatinum (II) or cyclophosphamide. Br J Cancer, 42: 574-585, 1980.

62. Rasey, J.S., Nelson, N.J., Mahler,P., Anderson, K., Krohn, K.A., and Menard, T. Radioprotection of normal tissues against gamma rays and cyclotron neutrons with WR-2721-LD_{50} studies and ^{35}S-WR-2721 biodistribution. *Radiat Res*, 97: 598-607, 1984.

63. Shaw, L. M., Bonner, H.S., and Brown, D.Q. Metabolic pathways of WR-2721 (ethyol, amifostine) in the BALB/c mouse. *Drug Metab Dispos*, 22: 895-902, 1994.

64. Shaw LM, Turrisi AT, Glover DJ, et al. Human pharmacokinetics of WR-2721. *Int. J. Radiat. Oncol. Biol. Phys*, 12: 1501-1504, 1986.

65. Shaw L, Bonner H, Nakashima H and Lieberman R. Pharmacokinetics of amifostine in cancer patients: evidence for saturable metabolism [abstract]. *Proc Am Soc Clin Oncol*, 13: 144, 1994.

66. Purdie JW, Inhaber ER, Schneider H and Labelle JL. Interaction of cultured mammalian cells with WR-2721 and its thiol, WR-1065: implications for mechanisms of radioprotection. *International Journal of Radiation Biology & Related Studies in Physics, Chemistry & Medicine,* 43: 517-527, 1983.

67. Swynnerton NF, Huelle BK, Mangold DJ and Ludden TM. A method for the combined measurement of ethiofos and WR-1065 in plasma: application to pharmacokinetic experiments with ethiofos and its metabolites. *Int. J. Radiat. Oncol. Biol. Phys,* 12: 1495-1499, 1986.

68. Swynnerton NF, Huelle BK, Mangold DJ and Ludden TM. Measurement of WR-1065 in plasma: preliminary pharmacokinetics in the beagle. *Research Communications in Chemical Pathology & Pharmacology*, 54: 255-269, 1986.

69. Shaw LM, Bonner HS and Lieberman L. Pharmacokinetic profile of Amifostine. *Semin Oncol*, 23: 18-22, 1996.

70. Shaw LM, Glover D, Turrisi A, Brown DQ, Bonner HS, Norfleet LA, Weiler C, Glick JH and Kligerman MM. Pharmacokinetics of WR-2721, *Pharmac Ther*, 39: 195-210, 1988.

71. Butler JD, Gahl WA and Tietze F. Cystine depletion by WR-1065 in cystinotic cells. Mechanism of action. *Biochemical Pharmacology* 34: 2179-2185, 1985.

72. Shaw LM, Bonner HS, Schuchter L, Schiller J and Lieberman R. Pharmacokinetics of Amifostine: effects of dose and method of administration. *Semin Oncol*, 26(2), suppl 7, 34-36, 1999.

73. Korst AEC, Van der Sterre MLT, Gall HE, et al. Influence of amifostine on the pharmacokinetics of cisplatin in cancer patients. *Clin Cancer Res*, 4: 331-6, 1998.

74. Korst AEC, Van der Sterre MLT, Eeltink CM, et al. Pharmacokinetics of carboplatin with and without amifostine in patients with solid tumors. *Clin Cancer Res*, 3: 697-703, 1997.

75. Micha L. Regional pharmacokinetics of the cytoprotective agent amifostine. D.Phil. thesis, University of Michigan, 2001.

76. Van der Vijgh WJF and Peters GJ. Protection of normal tissues from the cytotoxic effects of chemotherapy and radiation by amifostine (Ethyol): Preclinical Aspects. *Seminars in Oncology*, 21: 2-7, 1994.

77. Swynnerton NF, Mangold DJ and Ludden TM. Measurement of ethiofos (WR-2721) in plasma: preliminary pharmacokinetics in the beagle. *J Liq Chrom*, 8: 2675-2687, 1985.

CHAPTER 3

DETERMINATION OF AMIFOSTINE AND WR-1065 IN BLOOD/PLASMA AND TISSUE SAMPLES BY HIGH-PERFORMANCE LIQUID CHROMATOGRAPH COUPLED WITH ELECTROCHEMICAL DETECTOR

Abstract

In order to measure the concentrations of amifostine and WR-1065 (i.e., active metabolite of the cytoprotective agent amifostine) in blood/plasma and/or tissue (liver, tumor) samples, a high-performance liquid chromatographic method coupled with electrochemical detectors (amperometric vs coulometric) was validated in our lab. Plasma samples containing prodrug amifostine were deproteinized by using trichloroacetic acid followed by chromatographic analysis using a mercury/gold thin film electrochemical detection liquid chromatography system. The limit of quantification of amifostine in plasma was 0.5μM. The amifostine to internal standard (WR-80855) peak height ratios were linear over the amifostine concentration range of 0.5 to 50 μM (R^2 = 0.999). With the same detector, WR1065 can be measured in deproteinized blood and/or tissue samples by perchloric/EDTA solution. In addition to that, WR1065 can also be determined by HPLC with coulometric detection (analytical cell: E_1=200mV and E_2=600 mV; guard cell: E_G=650mV). The limit of quantification of WR1065 in deproteinized blood was 0.05 μM. The WR1065 peak heights were linear over the WR1065 concentration range of 0.05 to 10 μM (R^2 = 0.999). Both methods should be valuable in

investigating the pharmacokinetic properties of amifostine and WR-1065 in preclinical and clinical studies. Furthermore, the application of a coulometric electrode is more efficient and requires less maintenance than amperometric methods.

Introduction

Amifostine [$H_2N(CH_2)_3NH(CH_2)_2SPO_3H_2$; MW = 214] is a cytoprotective agent that is currently used to reduce the renal toxicity of cisplatin in patients with advanced ovarian cancer or non-small cell lung cancer, and to reduce the incidence of moderate to severe xerostomia in patients undergoing radiation treatment for head and neck cancer [1]. To offer protection, amifostine is effective only after it has been dephosphorylated by alkaline phosphatase in tissues to its pharmacologically active metabolite, WR-1065[2] [$H_2N(CH_2)_3NH(CH_2)_2SH$; MW = 134]. To better understand the pharmacokinetic–pharmacodynamic properties and relationship of amifostine and WR-1065, it is important to have an assay method that is accurate, precise and sensitive. In terms of thiols' detection, it is necessary that biological specimens are collected and processed in a manner that assures drug stability because the thiol can rapidly be oxidized to form disulfides. Both amifostine and WR-1065 are not very stable in biological specimens because it rapidly forms inactive disulfides. Moreover, they are small, hydrophilic compounds with properties that are similar to that of endogenous free thiols. Thus, it is a challenge to specifically and sensitively measure both amifostine and WR-1065 in biological matrices. In this specific study, both amifostine and WR-1065 are analyzed using high-performance liquid chromatography (HPLC), coupled to electrochemical detection [3, 4, 5, 6, 7, 8].

The principle of electrochemical detection of eluted solutes in high performance liquid chromatrography (HPLC) is similar to many other analytical electrochemical techniques: current due to oxidation or reduction of a compound is measured at a controlled potential

and the current is directly proportional to the concentration. We used both amperometric and coulometric types of electrochemical detector to measure concentration of amifostine and/or WR1065 in biological samples. An amperometric detector is a detector equipped with a thin film Hg/Au working electrode together with a Ag/AgCl reference electrode. When the thiols pass the surface of the electrode, the reaction $2RSH + Hg \rightarrow Hg(SR)_2 + 2H^+$ will happen on the surface of the working electrode to genetrate the current which can be recorded by HPLC system. A coulometric detector consists of dual analytical cell contains two porous graphite electrodes in series. Typical designs of these two kinds of LCEC detector were shown on Fig 3.1. Comparison of efficiency and features of these two detectors was also done in this study.

The HPLC methods were validated for assay of amifostine and WR-1065 in human blood samples and tissue sample, where biological samples were deproteinized by acidic buffer and 20 µl aliquot of supernatant was injected into HPLC after centrifuging, the method was specific, sensitive (limit of quantitation = 0.05 µM in deproteinized blood or 0.1 µM in whole blood for WR1065; and 0.5µM for amifostine in plasma), accurate (error $\leq$ 7.4 %) and reproducible (CV $\leq$ 6.9 %).

Materials and Methods

3.1. Chemical and reagents

Amifostine and WR-1065 standards were generously provided by the Drug Synthesis and Chemistry Branch, Developmental Therapeutics Program, Division of Cancer Treatment and Diagnosis, National Cancer Institute (Bethesda, Maryland). Perchloric acid 70% (redistilled) was obtained from the Aldrich Company (Milwaukee, WI). EDTA disodium salt was purchased from the Sigma Chemical Company (St. Louis, MO). HPLC grade acetonitrile, water, phosphoric acid and trichloroacetic acid were purchased from Fisher Scientific (Pittsburgh, PA). Other chemicals were obtained from standard sources and were of the highest quality available.

3.2. Sample processing

3.2.1. Amifostine in plasma by amperometric detector

Whole blood samples were immediately placed in prechilled Vacuette® EDTA tubes and centrifuged at 3400 g and 0~4°C for 5~10mins, and plasma was separated and stored at -70°C for subsequent analysis. On the day of analysis, the plasma samples were thawed, WR-80855 was added as an internal standard, an aliquot of 10% (w/v) trichloroacetic acid was then added to an aliquot of the sample in the ratio of 2 to 5 (v/v) to precipitate the plasma proteins. Samples were mixed together thoroughly and centrifuged at 40,000g for 3 mins at 0°C. A 20 µl aliquot of supernatant was injected into the HPLC.

3.2.2. WR1065 in whole blood by amperometric detector

Aliquots of whole blood were immediately placed in prechilled tubes containing an equivalent volume of 1M perchloric acid and 1g/L EDTA solution in order to precipitate the protein and stabilize WR-1065. Samples were mixed together thoroughly and then

centrifuged at 20,000 g for 5 mins at 0~4 °C. WR-251833 was added as an internal standard into the supernatant. A 20 µl aliquot of supernatant was injected into the HPLC.

3.2.3. WR1065 in tissue (liver and tumor) by amperometric detector

Liver and tumor samples were dissected, weighted and frozen rapidly by putting them in a liquid nitrogen bath for 1~3 min. The samples were stored at -70 °C for subsequent analysis. On the day of analysis, the samples were homogenized (1:5, w/v) in an ice-cold deproteinizing solution containing 1.0 M perchloric acid and 2.7 mM (1 g/L) disodium EDTA. The homogenate was then centrifuged at 40,000 g for 5 mins at 0°C and WR-251833 was added as an internal standard into the supernatant. A 20 µl aliquot of supernatant was injected into the HPLC.

3.2.4. WR1065 in human whole blood by coulometric detector

The whole blood samples were placed into prechilled tubes, containing ice-cold 1.0 M perchloric acid and 2.7 mM (1g/L) EDTA in a ratio of 1:1 (v/v), immediately after sampling. The mixture was then vortexed vigorously and centrifuged at 13,000 g for 8 mins at 4 °C. The supernatant was stored at -70 °C for subsequent analysis. On the day of analysis (less than 24 hrs), the samples were thawed, and a 20 µl aliquot of supernatant was injected into the HPLC.

3.3. Instrumentation

3.3.1. Amifostine in plasma by amperometric detector

The measurements of concentration of amifostine in plasma were performed on a Waters (Milford, Massachusetts) 515 isocratic HPLC pump. Amifostine and the internal standard WR-80855 were detected by a BAS (West Lafayette, Indiana) LC-4C amperometric detector equipped with a thin film mercury-gold amalgam working electrode. The Hg/Au

electrode potential was set at +0.15V with respect to the Ag/AgCl reference electrode and the range of the detector was set at 20nAFS. The analytical column, 4.6×250mm, 5μm particle size, C_{18} Symmetry® Waters (Milford, Massachusetts), was operated at room temperature. The amifostine chromatography protocol consists of an aqueous mobile phase containing 0.1M chloroacetic acid sodium salt and 1.5mM sodium octyl sulfate, pH 3.0 at a flow rate of 1ml/min. Peak identification was confirmed by comparing retention times in samples with authentic standards. Quantification was based on the peak height ratio of the compound and the internal standard.

3.3.2. WR1065 in whole blood by amperometric detector

The measurements of concentration of WR1065 in blood were performed on a Waters (Milford, Massachusetts) 515 isocratic HPLC pump. WR1065 and the internal standard WR-251833 were detected by a BAS (West Lafayette, Indiana) LC-4C amperometric detector equipped with a thin film mercury-gold amalgam working electrode. The Hg/Au electrode potential was set at +0.15V with respect to the Ag/AgCl reference electrode and the range of the detector was set at 50nAFS. The analytical column, 4.6×250mm, 5μm particle size, C_{18} Symmetry® Waters (Milford, Massachusetts), was operated at room temperature. The WR1065 chromatography protocol consists of a mobile phase containing 0.1M chloroacetic acid sodium salt and 1mM sodium octyl sulfate, pH 3.0, and 30% (v/v) methanol at a flow rate of 1ml/min. Peak identification was confirmed by comparing retention times in samples with authentic standards. Quantification was based on the peak height ratio of the compound and the internal standard.

3.3.3. WR1065 in tissue (liver and tumor) by amperometric detector

The measurements of concentration of WR1065 in tissue were performed on a Waters (Milford, Massachusetts) 515 isocratic HPLC pump. WR1065 and the internal standard WR-251833 were detected by a BAS (West Lafayette, Indiana) LC-4C amperometric detector equipped with a thin film mercury-gold amalgam working electrode. The Hg/Au electrode potential was set at +0.15V with respect to the Ag/AgCl reference electrode and the range of the detector was set at 0.1μAFS. The analytical column, 4.6×250mm, 5μm particle size, C_{18} Symmetry® Waters (Milford, Massachusetts), was operated at room temperature. The WR1065 chromatography protocol consists of a mobile phase containing 0.1M chloroacetic acid sodium salt and 1mM sodium octyl sulfate, pH 3.0, and 30% (v/v) methanol at a flow rate of 1ml/min. Peak identification was confirmed by comparing retention times in samples with authentic standards. Quantification was based on the peak height ratio of the compound and the internal standard.

3.3.4. WR1065 in human whole blood by coulometric detector

The WR1065 was detected by an ESA Coulochem III coulometric detector (Chelmsford, Massachusetts) equipped with two porous graphite electrode in series which are set at +600mv (E_2) and +200mv(E_1) respectively vs α-hydrogen/palladium reference electrode. The detector's range is set at 5μAFS. The analytical column, 4.6×250mm, 5μm particle size, C_{18} Symmetry® Waters (Milford, Massachusetts), was operated at 40°C. The WR-1065 chromatography protocol employed a mobile phase containing 0.1M chloroacetic acid sodium salt, 4mM sodium octyl sulfate, pH 3.0, and 40% (v/v) methanol running at 1ml/min. Peak indentification was confirmed by comparing retention times in samples with authentic standards. Quantification was based on the peak height ratio of the compound.

3.4. Calibration standards and quality controls

3.4.1. Standard solutions

The amifostine stock solution was made by dissolving 10 mg (100 mg) of amifostine in 10 ml (100 ml) water. The WR1065 stock solution was made by dissolving 10 mg of WR1065 in 10 ml 0.2 M perchloric acid/0.1 M chloroacetic acid (v/v: 3/1, adjust pH from 0.9 to 3 with 10 N NaOH) to prepare the standard stock solution of 1 mg/ml. The above stock solutions can be stored at −80 °C for at least one week.

For both amifostine and WR1065, 100 μl of 1 mg/ml stock solution diluted with the solution for its stock solution to 1 ml to prepare the working solution of 100 μg/ml (0.1 mg/ml), 20 μl (10 μl) of 1 mg/ml stock solution diluted with the solution for its stock solution to 1 ml to prepare the working solution 20 μg/ml (10 μg/ml), 200 μl of 10 μg/ml (100 μl of 20 μg/ml) diluted with the solution for its stock solution to 1 ml to prepare the working solution 2 μg/ml, 100 μl of 2 μg/ml diluted with the solution for its stock solution to 0.5 ml to prepare the working solution 0.4 μg/ml.

Amifostine calibration standards were prepared at the time of assay from the 10 μg/ml, 0.1 mg/ml and 1mg/ml aqueous working solution by making dilutions with blank plasma (~ 0.5ml) to obtain calibrators for the standard curve: 0.5, 1, 5, 10, 20, 50 μM. WR1065 calibration standards were prepared from 20 μg/ml, 2 μg/ml and 0.4 μg/ml working solution of WR1065 by making dilutions with blank deproteinized blood (~ 0.1ml) to obtain calibrators for the standard curve: 0.048, 0.0966, 0.24, 0.48, 2.4, 9.66 μM.

Stock solution of internal standard WR251833 was prepared by dissolving 5 mg of WR251833 in 5 ml aqueous solution containing 10 mmol/L Tris (M.W. 121.1), pH 7.4 adjusted by 6 N HCl, and 1 g/L sodium EDTA to make concentration of 1 mg/ml.

Working solution of 0.1 mg/ml and 20 μg/ml were prepared with 100 μl of 1 mg/ml stock solution diluted with the solution for its stock solution to 1 ml and 50 μl of 0.1 mg/ml solution diluted with the solution for its stock solution to 0.5 ml respectively. We fixed the concentration of internal standard WR251833 in WR1065 assay in deproteinized blood (~ 0.1ml) as 1 μg/ml and concentration of internal standard WR80855 in amifostine assay in plasma (~ 0.5ml) as 2 μg/ml.

Calibration data were best fitted to a power function described by the equation: $\ln(Y) = \text{slope} \cdot \ln(X) + y\text{-intercept}$, where ($Y$) is the peak height ratio of the amifostine or WR1065 and the internal standard or peak height of the compound and (X) is the concentration of the compound. Regression parameters (i.e., slope and y-intercept) were then used to calculate the concentration of WR-1065 in quality control samples and in vivo blood samples.

3.4.2. Quality control and assay validation

Amifostine and WR1065 quality control samples were prepared at the time of the analysis with blank plasma for amifostine at concentrations of 1, 10, 50μM or deproteinized blood for WR1065 at concentrations of 0.0966, 0.4831, 9.66 μM. The procedures developed for the quantitation of these two compounds were validated over 3 days by analysis of quality control samples to determine within- and between-day precision and accuracy. The limit of quantitation were defined as the ratio of signal-to-noise ≥ 3.

Results

Chromatography

Representative chromatograms of WR-1065 in deproteinized blood (with and without spiked compound) by amperometric detector are shown in Fig 3.2. Representative chromatograms of amifostine in plasma (with and without spiked compound) by amperometric detector are shown in Fig 3.3. For all of these measurements, no chromatographic peaks of the amifostine or WR1065 adduct were observed in blank plasma or deproteinized blood, indicating that endogenous compounds do not interfere with the compound to be detected with this method. Spiked samples clearly show a clean separation of WR-1065 or amifostine from the endogenous peaks that elute within 5 min after the injection. For those blood samples that were beyond the linear concentration range of quantitation, further dilution was achieved using blank plasma or blank deproteinized blood.

Assay validation

Standard curves of WR-1065 were linear over the 0.05–9.66 μM concentration range when prepared in deproteinized blood, as shown by the representative example in Fig 3.4. Assay validation on calibration standards of amifostine was presented in Table 3.1. Standard curves of amifostine were linear over the 0.5-50 μM concentration range when prepared in plasma, as shown by the representative example in Fig 3.5. Assay validation on calibration standards of WR1065 was presented in Table 3.2. Table 3.3 contains the mean results of WR-1065 quality control samples in deproteinized blood at three different concentrations (i.e., low, medium and high). Table 3.4 contains the mean results of amifostine quality control samples in plasma at three different concentrations (i.e., low, medium and high). Five replicates were evaluated within a day as well as two replicates among five days and, as shown in this table, precision and accuracy of the method were

good for the specific concentrations studied. Accuracy was represented by the percent relative error (%RE) of calibrations standards and quality control samples from their theoretical values using the Equation 2.1.

$$\%RE = (Concentration_{Observed} - Concentration_{Spiked})/Concentration_{Spiked} \times 100 \quad \text{Eq. 2.1}$$

Precision was evaluated by percent relative standard deviation (%RSD), which was calculated using Equation 2.2.

$$\%RSD = \text{Standard Deviation}/\text{Mean} \times 100 \quad \text{Eq.2.2}$$

In all cases, CV was $\leq 6.9\%$ and error was $\leq 7.4\%$, regardless of whether the determinations were made intraday or interday.

Discussion

Most published HPLC assays for WR-1065 have been based on electrochemical [5, 6, 8] or fluorescent detection [3, 4, 7, 9]. Because both amifostine and WR1065 are thiols, electrochemical detection was used mostly to directly measure concentrations of amifostine and WR1065 in biological samples in literature. Because electrochemical detector was used in this specific analysis, some electrolytes need to be included in the mobile phase. Literaturely, 0.1M chloroacetic acid was used as electrolytes in mobile phase, then adjust pH of aqueous phase to 3.0 with sodium hydroxide. However, we didn't get satisfactory chromatogram with these components in mobile phase. Because the aim is to form buffer system in the mobile phase, we changed to 0.1M chloroacetic acid sodium salt as electrolyte in mobile phase, then adjust pH of aqueous phase to 3.0 with phosphoric acid. We tried different acids to adjust pH value, and found both phosphoric and hydrochloric acid could generate good peak shape, but phosphoric acid can have more stable baseline. Retention time of compound can also be controlled by the

concentration of sodium octyl sulfate which is an ionpair agent in the mobile phase, this ability was indicated in the assay of different types of biological samples. The detailed mechanism of different mobile phase system need to be investigated, probably larger capacity of buffer system was formed with 0.1M chloroacetic acid sodium salt/phosphoric acid combination compared with 0.1M chloroacetic acid/sodium hydroxide system. Because amifostine is more polar than its active metabolite WR1065, we use pure aqueous mobile phase to control reasonable retention (6~7 min) compared with aqueous/organic phase mixture for the mobile phase of WR1065 analysis.

A significant advantage of electrochemical detection is the simple biological samples processing before injection into HPLC. Generally, liquid-liquid or solid-phase extraction can be used for lipophilic or hydrophilic compounds respectively, however, extraction procedure always involve multiple steps including extraction, condensation and so on. For unstable compounds, extraction is not very appropriate because we want inject this compound into HPLC column as soon as possible. Another biological samples processing method, that is, direct injection was used in this specific assay. As to the method of direct injection, plasma and/or blood proteins are first precipitated by acids or organic solvents, then supernatant will be injected into HPLC column after mixing and centrifuging. The success of this method will be dependent on the sensitivity of the detector and efficiency of protein precipitation. Electrochemical detector has higher sensitivity compared with UV and fluorescent detector, so the key point for this assay is to select appropriate solvent to precipitate the plasma protein as complete as possible to make chromatogram clear and longer life of analytical column. People from literatures use organic solvent acetonitrile to precipitate the plasma protein, however, with the method from the

literatures, we found serious interference with the compound we need detect and the amount of protein precipitated by acetonitrile is small and the color of protein precipitated appears reddish compared with protein precipitated by strong acid. It was reported[10] that for unit volume of plasma, the percentage plasma protein precipitated by 0.2 volume of 10% (w/v) trichloroacetic acid (TCA) is 99.7%; but only 13.4% by acetonitrile under same condition, the percentage plasma protein precipitated can reach 97.2% by acetonitrile until an equivalent volume of acetonitrile was added to the plasma (1:1). Based on this result from literature, we won't have lower limit of quantitation if we need precipitate the plasma protein as complete as possible by acetonitrile because we need add large volume of acetonitrile into plasma to precipitate the protein completely. We tried and selected 10% (w/v) TCA as protein precipitant in the assay of amifostine because it has much better efficacy of protein precipitation than that of acetonitrile. The only shortcoming of TCA precipitant is the acidic condition of supernatant (pH ~ 2.0) compared with that by acetonitrile precipitant (pH ~ 9.0) because amifostine is not very stable under acidic condition. In order to shorten the time amifostine stay in the acidic condition, we processed the plasma sample of amifostine right before the HPLC analysis and the results indicated that amifostine is detectable in plasma to 0.5 μM. From the literature report and analytical experience with WR1065 samples from our lab, we realized that significant degradation of WR-1065 occurs during sample preparation and storage (i.e., rapid oxidation while in plasma or blood), even at temperatures as low as −70 °C. Because WR1065 is relatively stable under acidic and low-temperature condition from the literature, as a result, blood samples containing WR1065 should be placed on ice and immediately mixed with the ice-cold solution of 1.0 M perchloric acid plus 2.7 mM

EDTA to precipitate the protein and damage some enzymes and oxidative substances to stabilize the WR1065 as much as possible. In addition to that, samples should be analyzed for WR-1065 within 12~24 h of collection. Concentration of perchloric acid in this deproteinizing solution will be dependent on the presence of a clear supernatant and more acidic condition achieved by higher concentration of perchloric acid. EDTA was used to bind with metal ion in the biological samples to lower the oxidative condition which results in the formation of disulfides from WR1065.

As to the electrochemical detector, the current generated depends upon concentration, fluid velocity, cell geometry, and electrode area for a given solute. Efficiency of electrochemical detectors for HPLC is strictly a matter of geometric design. A variety of flow-through electrochemical cells was developed and described theoretically. These include several basic geometries in LCEC detector design; tubular, thin layer, wall jet and coulometric porous. In our lab, we have two kinds of electrochemical detectors, one is thin-layer amperometric detector with which the solute flow over the surface of Hg/Au electrode, and reaction of $2RSH + Hg \rightarrow Hg(SR)_2 + 2H^+$ occurs. Based on this geometry of design and detection mechanism, that the efficiency of ampermetry which measures probably 15% of the electroactive species, should be less than real flow-through type of detectors results in the low intensity of the signal. However, because thiols will react with mercury on the electrode, the potential on the electrode should be low which can result in the less interference with the compound. Another is porous coulometric type of detector with which the solute flow through the porous graphite electrodes in series, and reaction of $2RSH \rightarrow RSSR + 2e^- + 2H^+$ occurs. Based on this type of geometry of design and detection mechanism, the conversion efficiency should be as complete as 100%, however,

the potential will be higher to induce that reaction which can probably result in more interferences in blank samples. However, the most important reason to make coulometric type is generally superior is much less maintenance work required for electrode compared with amperometric type. For this particular Hg/Au working electrode in amperometric detector, it is extremely difficult for novices to make results of assay reproducible because we need manually handle, polish and amalgamate the gold working electrode before and after each time of analysis. But once people get more experience with this type of detector, it is not a bad choice because low potential used with this type of detector can limit the number of endogenous substances oxidized or reduced. To some extent, the choice of different types of electrochemical detectors will be dependent on the time of developing the analytical method with the detector in hands.

In conclusion, we have described and validated an HPLC-electrochemical detection method for the measurement of amifostine and WR-1065 in biological samples. This method is specific, accurate, reproducible, and simple. With minor modifications of the published literature method, we have improved sensitivity compared with same electrochemical detection method in literature. This assay will be used to evaluate the extent of liver protection offered by systemic or regional administration of amifostine in preclinical models as well as in the clinic.

Table 3.1. Interday variability of slopes and intercepts derived from the standard curves of amifostine in plasma (the peak height ratios of WR 2721 to WR 80855 over the range of WR 2721 concentration in human plasma of 0.5 to 40 μM are plotted against WR 2721 concentration; lnC vs lnPHR)

	0.5μM	1μM	5μM	10μM	20μM	40μM	Slope	Intercept	R^2
Run 1 (11/24/03)	0.4836	1.006	5.5	11.03	20.91	38.125	1.1553	-1.4632	0.9987
	0.4626	0.9989	5.206	10.41	18.684	36			
Run 2 (11/25/03)	0.475	1.005	5.223	10.36	20.51	36.34	1.1407	-1.386	0.9988
	0.465	1.07	5.11	10.71	20.72	37.18			
Run 3 (11/26/03)	0.504	0.921	5.686	10.43	19.29	38.67	1.1113	-1.3109	0.9988
	0.522	0.921	4.994	10.78	18.94	39.41			
N	6	6	6	6	6	6	3	3	3
Mean	0.4854	0.9870	5.2865	10.62	19.8423	37.6208	1.1358	-1.3867	0.9988
S.D.	0.0234	0.0573	0.2578	0.2644	0.9815	1.3430	0.0224	0.0762	0.0001
%RSD (**Precision**)	4.8168	5.8075	4.8773	2.4899	4.9466	3.5698			
%RE (**Accuracy**)	-2.9267	-1.3017	5.73	6.2	-0.7883	-5.9479			

Table 3.2. Interday variability of slopes and intercepts derived from the standard curves of WR1065 in human deproteinized whole blood (the peak height ratios of WR1065 to WR 251833 over the range of WR1065 concentration in human deproteinized whole blood of 10 ng/ml (74 nM) to 1 μg/ml (7.4 μM) are plotted against WR 1065 concentration; lnPHR vs lnC)

	0.074 μM	0.148 μM	0.37 μM	0.74 μM	1.48 μM	3.7 μM	7.4 μM	Slope	Intercept	R^2
Run 1 (04/08/04)	0.0868	0.145	0.32	0.694	1.393	3.789	8.222	1.0022	-0.7696	0.9961
Run 2 (04/09/04)	0.0685	0.154	0.379	0.771	1.525	3.583	7.2	1.0459	-0.8948	0.9992
Run 3 (04/10/04)	0.081	0.137	0.359	0.743	1.417	3.991	7.281	1.0417	-0.5538	0.9987
N	3	3	3	3	3	3	3	3	3	3
Mean	0.08	0.15	0.35	0.74	1.45	3.79	7.57	1.03	-0.739	0.998
S.D.	0.01	0.01	0.03	0.04	0.07	0.2	0.57	0.024	0.172	0.002
% RSD (**Precision**)	11.87	5.85	8.51	5.30	4.87	5.39	7.51	2.341	-23.33	0.167
% RE (**Accuracy**)	6.44	-1.80	-4.68	-0.54	-2.36	2.37	2.27			

Table 3.3. HPLC assay validation for WR1065 in human deproteinized whole blood

	0.1 48 μM	1.48 μM	7.4 μM
Run 1 (04/08/04)	0.1589	1.433	8.168
	0.1561	1.467	8.496
	0.1325	1.469	8.28
Run 2 (04/09/04)	0.152	1.515	7.32
	0.155	1.493	7.4
	0.153	1.517	7.169
Run 3 (04/10/04)	0.146	1.316	8.017
	0.139	1.314	6.933
	0.149	1.238	6.551
N	9	9	9
Mean	0.15	1.42	7.59
S.D.	0.01	0.1	0.67
%RSD (**Precision**)	5.76	7.21	8.85
%RE (**Accuracy**)	0.71	-4.19	2.60

Table 2.4. HPLC assay validation for WR 2721 in human plasma

	1μM	10μM	40μM
Run 1 (11/24/03)	0.938	10.86	36.33
	0.961	10.655	35.32
	0.938	10.655	36.42
Run 2 (11/25/03)	0.9899	10.557	37.89
	0.8738	10.41	36.15
	1.031	11.75	36.95
Run 3 (11/26/03)	0.8138	10.42	37.02
	0.9914	9.795	37.81
	0.9418	10.75	39.53
N	9	9	9
Mean	0.942	10.650	37.047
S.D.	0.065	0.514	1.233
%RSD (**Precision**)	6.934	4.827	3.328
%RE (**Accuracy**)	-5.792	6.502	-7.383

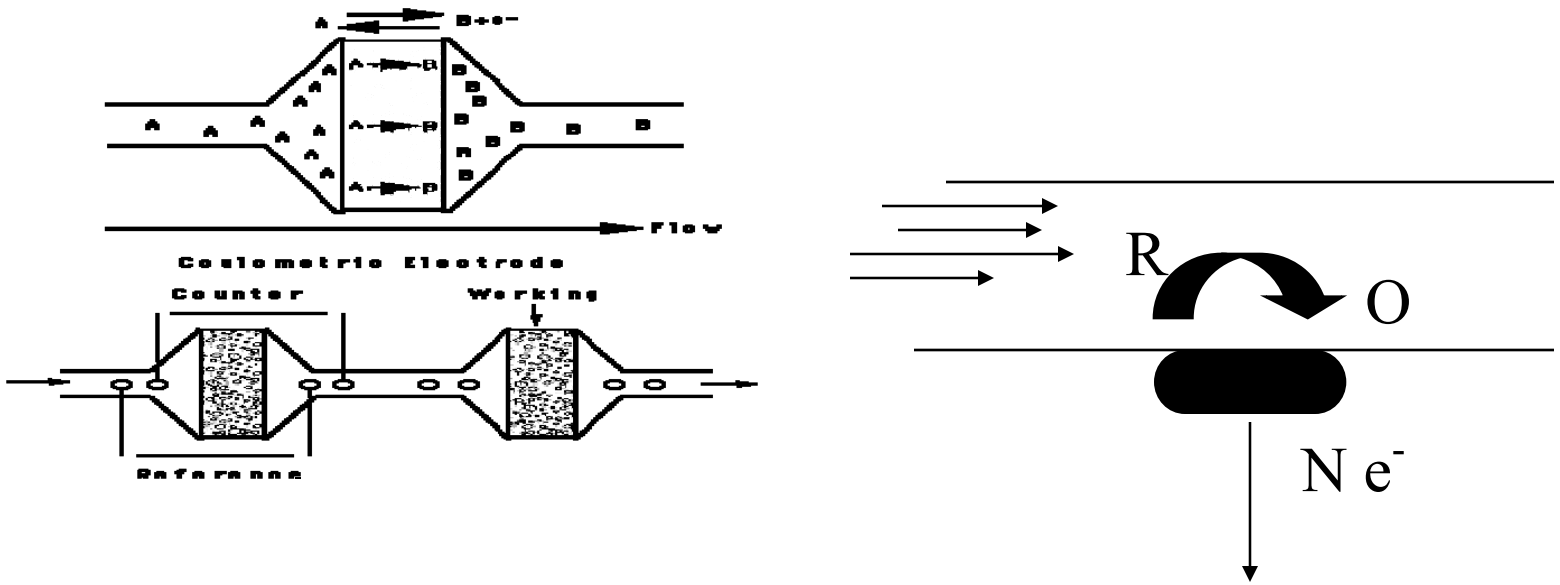

Figure 3.1. Typical designs of amperometric and coulometric detector

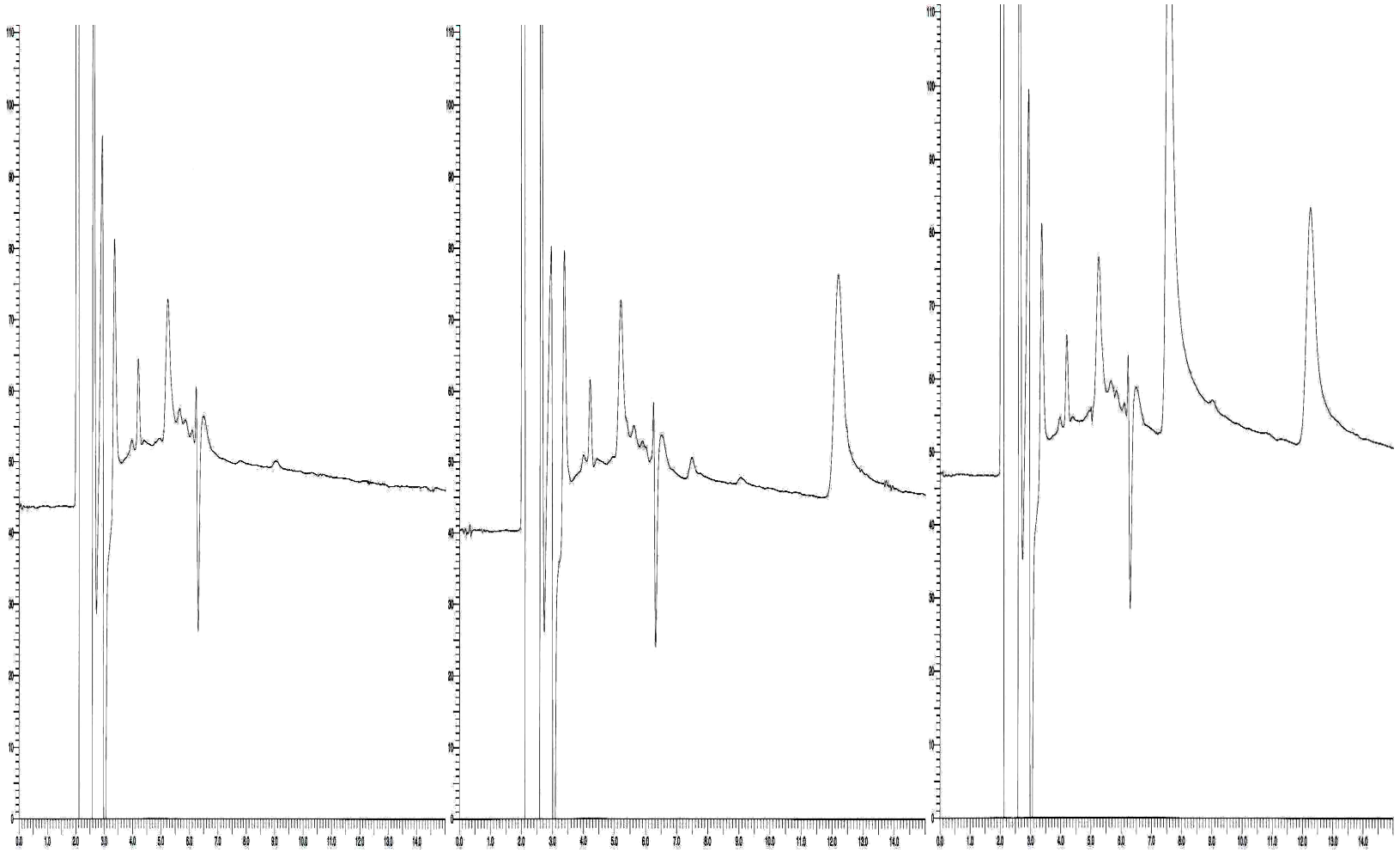

Blank human plasma 0.5μM Amifostine + 1ug/ml IS in plasma 10μM Amifostine+ 1μg/ml IS in plasm

Figure 3.2. Representative chromatograms of amifostine in plasma by amperometric detector

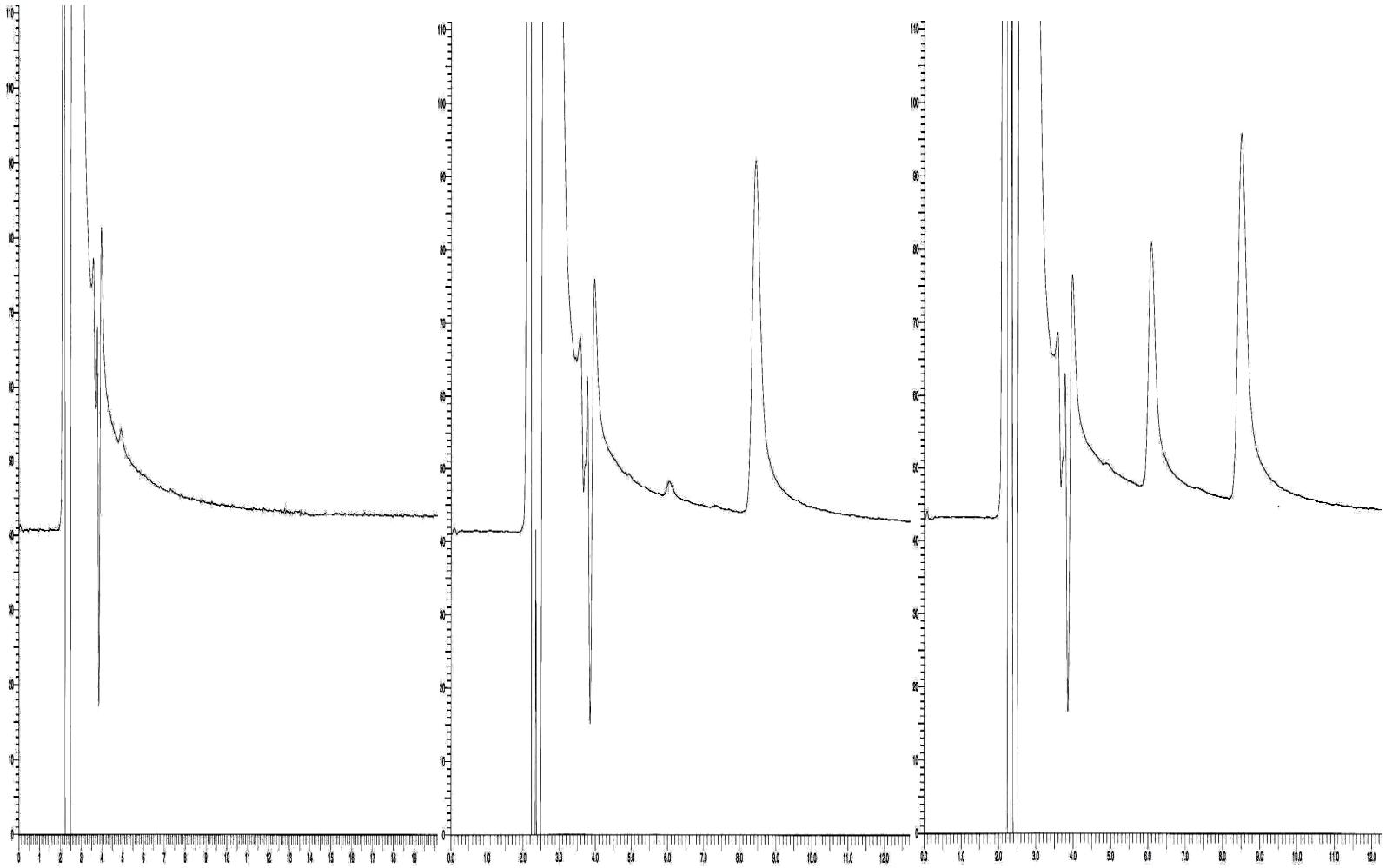

Blank human whole blood 0.15 μM WR1065 +0.5μg/ml IS in whole blood 1.5μM WR1065 + 0.5μg/ml IS in whole blood

Figure 3.3. Representative chromatograms of WR-1065 in deproteinized blood by amperometric detector

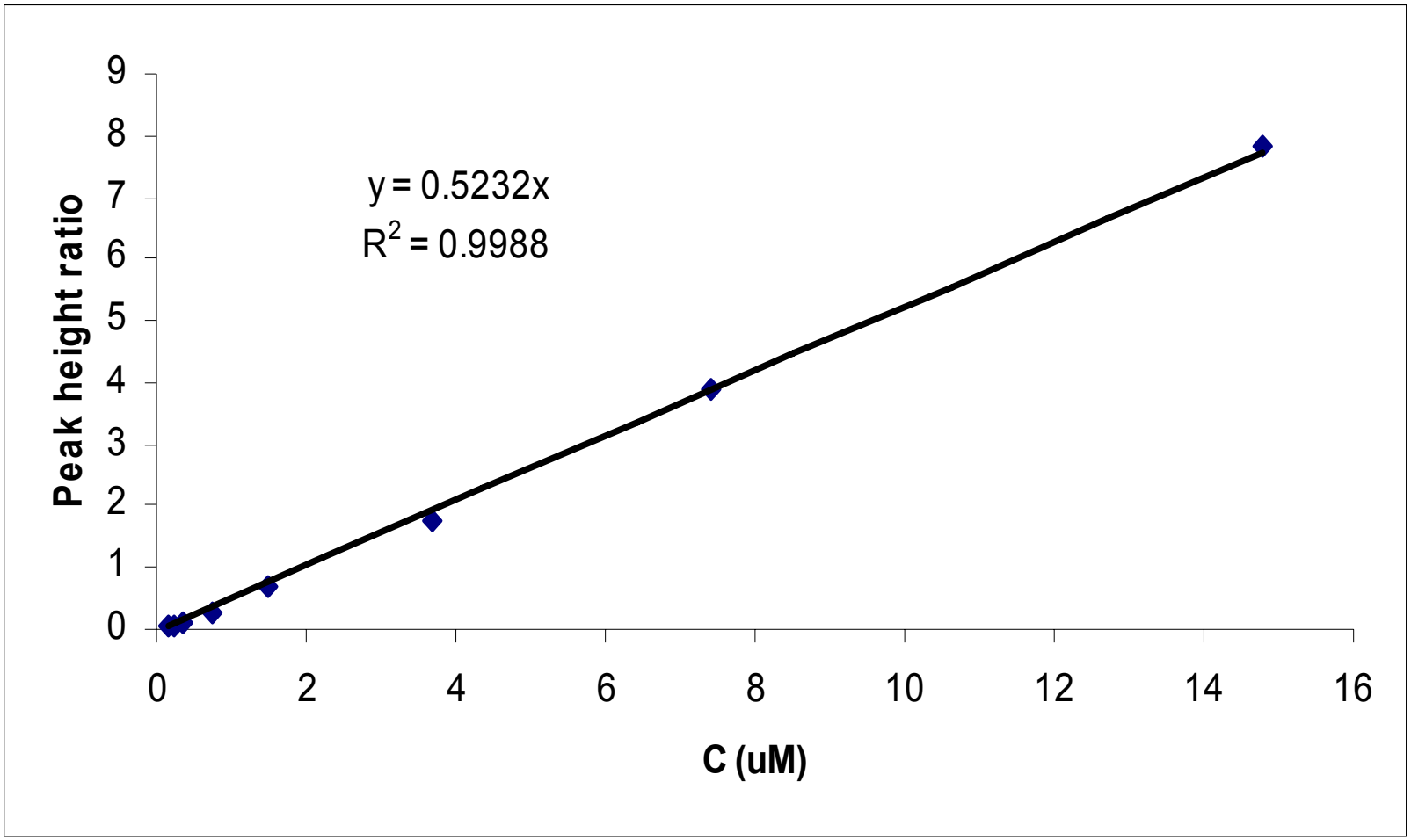

Figure 3.4. Representative example of standard curves of WR-1065 over 0.148-14.8 µM concentration range

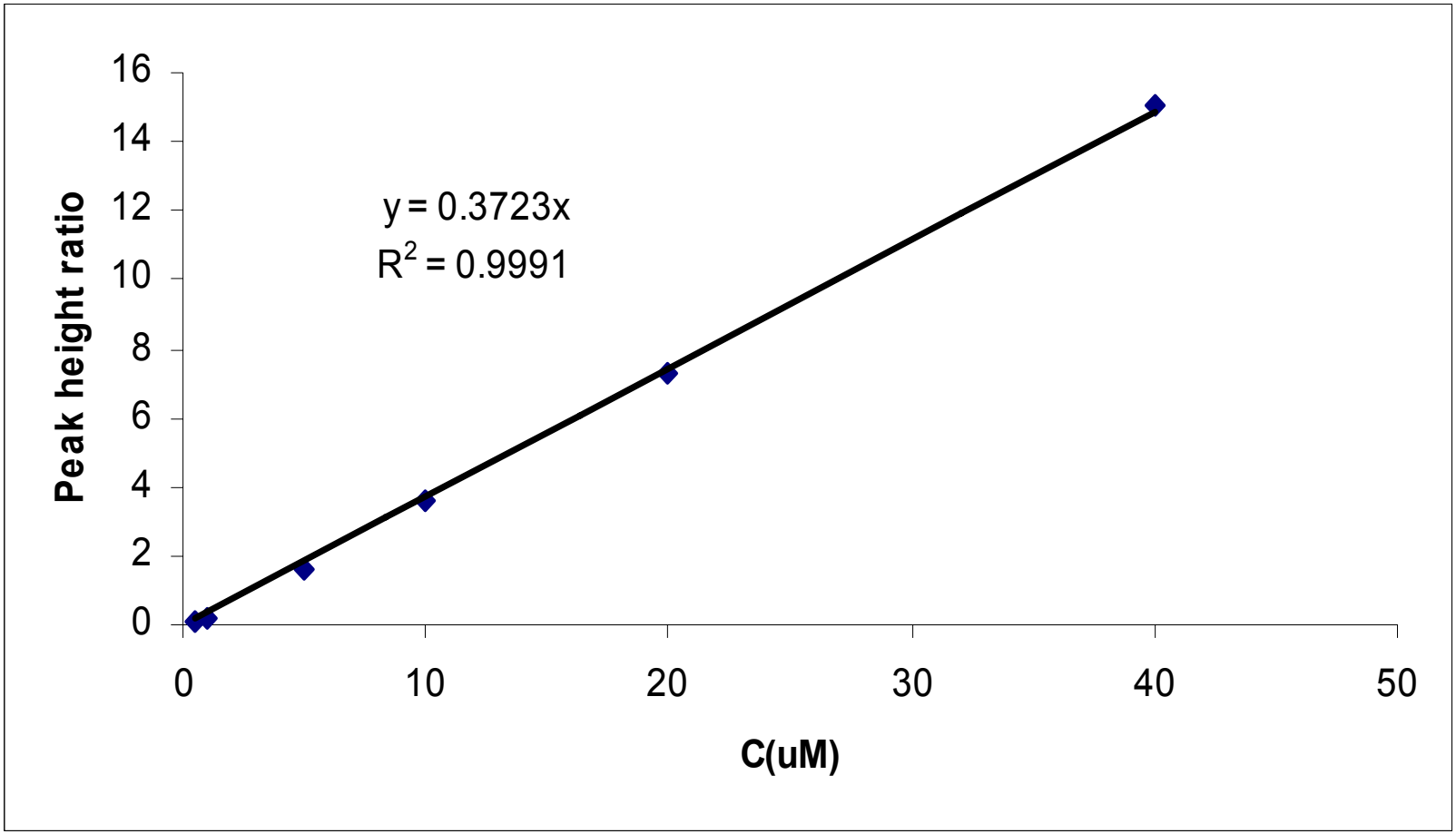

Figure 3.5. Representative example of standard curves of amifostine over 0.5-40 μM concentration range

References

1. Physicians' Desk Reference, 58th ed., Thomson PDR, Montvale, 2004, p. 1910.

2. Culy CR and Spencer CM. Amifostine: an update on its clinical status as a cytoprotectant in patients with cancer receiving chemotherapy or radiotherapy and its potential therapeutic application in myelodysplastic syndrome. Drugs, 61(5): 641-684, 2001.

3. Swynnerton NF, Huelle BK, Mangold DJ and Ludden TM. A method for the combined measurement of ethiofos and WR-1065 in plasma: application to pharmacokinetic experiments with ethiofos and its metabolites. *Int. J. Radiat. Oncol. Biol. Phys,* 12: 1495-1499, 1986.

4. Swynnerton NF, Huelle BK, Mangold DJ and Ludden TM. Measurement of WR-1065 in plasma: preliminary pharmacokinetics in the beagle. *Research Communications in Chemical Pathology & Pharmacology*, 54: 255-269, 1986.

5. Shaw, L.M., Bonner, H.S., Turrisi, A., Norfleet, A. L., and Glover, D.J. A liquid chromatographic electrochemical assay for S-2-(3-aminopropylamino) ethylphosphorothioate (WR-2721) in human plasma. *J Liq Chromatogr*, 7: 2447-2465, 1984.

6. Shaw, L.M., Bonner, H.S., Turrisi, A., Norfleet, A. L., and Kligerman, M. Measurement of S-2-(3-aminopropylamino) ethanethiol (WR-1065) in blood and tissue. *J Liq Chromatogr*, 9: 845-859, 1986.

7. Souid AK, Newton GL, Dubowy RL, Fahey RC and Bernstein ML. Determination of the cytoprotective agent WR-2721 (Amifostine, Ethyol) and it metabolites in human blood using monobromobimane fluorescent labeling and high-performance liquid chromatography. *Cancer Chemotherapy & Pharmacology*, 42: 400-406, 1998.

8. Feng Bai, Kirstein MN, Hanna, SK and Stewart CF. New liquid chromatographic assay with electrochemical detection for the measurement of amifostine and WR-1065, *J Chromatogr*, 772: 257-265, 2002.

9. Chen J, Lu Z, Lawrence TS, Smith DE. Determination of WR-1065 in human blood by high-performance liquid chromatography following fluorescent derivatization by a maleimide reagent ThioGloTM3. J Chromatogr B 819:161-167, 2005.

10. James B. Journal of Chromatography, 226: 455-460, 1981

CHAPTER 4

RELATIONSHIP BETWEEN AMIFOSTINE DOSE, ADMINISTRATION ROUTE (SYSTEMIC VS REGIONAL), AND SAMPLING TIME ON WR-1065 EXPOSURE IN THE LIVER OF TUMOR-BEARING RATS

ABSTRACT

The objective of the present study was to determine whether or not a higher liver to tumor ratio of the cyto- and radioprotective metabolite WR-1065 could be achieved following regional as opposed to systemic dosing of the inactive prodrug amifostine. Walker 256 cells were injected directly into the liver of male rats and focal tumors were allowed to grow for 12-14 days. Amifostine was then administered by a 3-min infusion into either the portal vein (i.e., regional) or femoral vein (i.e., systemic). The experiments were performed according to a central composite experimental design, with doses of 50, 125, 275, 425 and 500 mg/m^2 and post-treatment sampling times of 15, 21.5, 37.5, 53.5 and 60 min. Liver, tumor and blood samples were analyzed for WR-1065 by HPLC with electrochemical detection. Response surface regression models were fit to the log-transformed concentrations from regional and systemic experiments. The concentrations of WR1065 in the liver, tumor, blood, and liver to tumor ratio were not statistically different after regional or systemic dosing of amifostine in tumor-bearing rats ($p>0.05$). However, during both routes of drug administration, liver to tumor ratios were highest at the largest dose (500 mg/m^2, $p<0.0001$) and earliest sampling time (15 min, $p<0.0001$), achieving ratios of 4-5. Moreover, 2-D dose-response plots indicated that the kinetics of WR1065 were nonlinear. No significant differences were observed between regional and

systemic routes of administration for amifostine in tumor-bearing rats. However, it appears that the therapeutic index (i.e., liver to tumor ratio) of WR1065 may be optimized by increasing the amifostine dose within safe limits and by delivering radiotherapy 15 min after dosing.

INTRODUCTION

Cytoprotectant Amifostine protects almost all normal tissues from the cytotoxic effects of radiation and some chemotherapeutic agents.[4,5] It is a thiophosphate prodrug that is dephosphorylated to the free thiol active metabolite, WR-1065, by the plasma membrane bound enzyme alkaline phosphatase and WR1065 is the form of the drug taken by the cell.[6] The high alkaline phosphatase activity was localized in the endothelium of small arteries and arterioles at their origin from larger vessels.[7] As to the liver, it contains relatively less alkaline phosphatase compared with tissues such as the small intestine or kidney. In the liver of humans, the strongest activity was found in the sinusoids and the endothelium of the central and periportal veins which are in the central and peripheral part of the lobule but no alkaline phosphatase activity was found within hepatocytes. However, the localization of alkaline phosphatase in the human differs from that in the rat. No alkaline phosphatase activity in the sinusoids and low activity in the bile canaliculi of the rat. Periportal activity predominates in the rat.[8] A number of studies have attempted to characterize the mechanism of differential protection when amifostine is administered systemically. WR1065 may be actively absorbed by normal tissue cells and only passively absorbed by tumor cells. The polyamine transport system is probably responsible for the mediated uptake mechanism for WR1065 in the low micromolar concentration range and WR1065 is taken up by passive diffusion at high millimolar concentration level.[9,10] The selective uptake of WR-1065 may also be due to differences in the tissue microenvironment resulting in the slow entry of the free thiol into tumor masses. Tumors are often relatively hypovascular and have low interstitial pH, resulting

in low rates of prodrug activation by alkaline phosphatase. In addition, the distribution of alkaline phosphatase in capillaries and arterioles of normal tissues is extensive as compared with tumors. Thus, in tumors it is thought that both reduced metabolism of amifostine to the active protector WR-1065 and the low uptake of WR-1065 by the tumor result in a concentration of the free thiol that is much lower than that found in normal organs.[11,12] As a result, healthy tissue is protected from radiotherapy and chemotherapy while tumors with lower levels of the active metabolite are less protected. Transient hypotension, however, is the major dose-limiting adverse effect of amifostine. The main metabolic pathway of WR-1065 elimination involves the formation of symmetrical and nonsymmetrical disulfides that might serve as a depot for the active metabolite, free WR-1065.[13,14]

Compared with intravenous administration, regional chemotherapy may deliver high concentrations of drug to a desired target site while reducing the systemic exposure of drug. Amifostine may be a good candidate for regional drug delivery to the liver because it has a large clearance from the body and is eliminated more extensively by the liver than by the gastrointestinal tract, lungs, or kidneys.[15-17] Approximately 90% of the drug is extracted by the liver (i.e., converted to WR-1065), suggesting that the liver may preferentially take up the active free thiol, WR-1065.[18] We hypothesized that organs with high amifostine clearance and extraction ratio would have a high activation rate of amifostine to WR-1065 and, therefore, would be protected by amifostine.

Amifostine has shown in randomized trials to protect the kidney from cisplatin nephrotoxicity and the parotid gland from radiation due to the greater conversion of the drug to the active metabolite WR-1065 in the normal tissue than in the tumor. Protection

appears to result from scavenging oxygen-derived free radicals and hydrogen donation to repair damaged target molecules. Each of these mechanisms requires that the active metabolite be present at the time of radiation. WR-1065 may also affect the catalytic inactivation of topoisomerase II, which slows cell cycling, thus providing more time for DNA repair.[19] In order to optimize the use of amifostine as a radiation protector of normal liver, which will permit the safe delivery of higher doses of radiation for patients with both focal and diffuse disease, we performed preclinical studies to optimize selectivity and to estimate the appropriate dose of regional and/or systemic amifostine.

Amifostine is administered in the clinic at a dose of 200 ~ 350 mg/m^2 as IV bolus injection or 3-min infusion 15 ~ 30 min before the start of radiotherapy. In our preclinical study, the objective was to evaluate the potential advantage of amifostine regional administration to the liver and the relationship of selectivity (liver to tumor concentration ratio of WR1065) to the different doses and times after systemic and/or regional administration of amifostine. Thus, the concentrations of the active metabolite, WR-1065, were determined in the blood, liver and tumor of a tumor-bearing rat model at different times after both routes of administration under different doses. Rats received different doses of amifostine over an infusion period of 3 min either through the femoral vein (systemic dosing) or through the portal vein (regional dosing).

Materials and Methods

4.1 Animals

Male Sprague-Dawley rats weighting approximately 125-175g were obtained from Harlan Sprague Dawley, Inc. (Indianapolis, Indiana). They were housed in cages in a temperature-humidity controlled room with a 12 h light-dark cycle and fed with 5001 Rodent Diet (PMI Nutrition International, Inc. Brentwood, Mo). All animal procedures and study protocols were approved by the University of Michigan Committee on the Use and Care of Animals.

4.2 Tumor implantation

The rats were anesthetized using a 60 mg/kg intraperitoneal injection of pentobarbital. A mid-line abdominal incision was made starting at the xiphoid process and the liver was exposed. Walker 256 cells were grown in suspension cultures with RPMI media supplemented with 10% fetal calf serum and prepared for injection by suspension in phosphate buffered saline 7.4(PBS). The left lateral lobe (LL) of the liver was injected with tumor cells (~ 40µl) and the peritoneum and abdominal wall were closed. Focal tumors were allowed to grow for 12-14 days. The average weight of the tumors at the time of dosing was 0.385 g ± 0.343.

4.3 Experimental protocol

Tumor-bearing rats were divided randomly into two equal groups, each receiving amifostine either through the portal vein (regional) or the femoral vein (systemic). The rats were anesthetized using a 60 mg/kg intraperitoneal injection of pentobarbital and the femoral vein or portal vein was cannulated. Blood was drawn and seen in the cannula before dosing of amifostine. Approximate 1 ml of saline was injected over 60sec into the

portal vein and/or femoral vein to examine for leakage and to hydrate the animals before dosing of amifostine. A solution of amifostine (ALZA Pharmaceuticals, Palo Alto, or CA/US Bioscience, West Conchohocken, PA) at a dose of 50, 125, 275, 425 and 500 mg/m^2 was prepared in normal saline and administered as a 3-minute infusion using a syringe pump (Harvard Apparatus, South Natick, MA) set at 0.4 ml/min. Blood was obtained by cardiac puncture, and liver tissue and tumor samples were collected at 15, 21.5, 37.5, 53.5 and 60 min after initiating the drug infusion under different doses. The whole experiment consisted of two rotatable response surface designs centered at a dose of 275 mg/m^2 and a sampling time of 37.5 min. For each of the two modes (regional vs systemic) of administration, three animals were tested at each design point. Figure 4.1 displays this response surface design. Concentrations of WR1065 were assessed in blood, liver and tumor; the ratio of liver concentration to tumor concentration, the therapeutic index, was also evaluated.

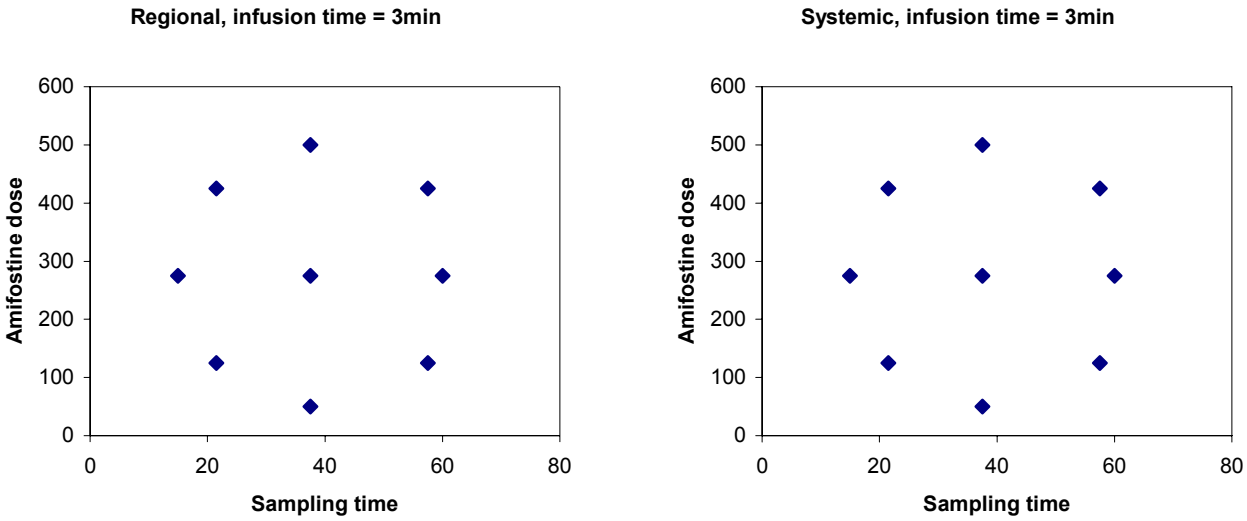

Figure 4.1. Response surface design

4.4 Assay for WR-1065[20]

Concentrations of free WR-1065 were measured in the blood and tissues of rats, as described briefly below and detailed information of analytical methodology can be found in chapter 3.

4.4.1 Sample preparation. Liver and tumor samples were dissected, weighed and frozen rapidly by putting them in a liquid nitrogen bath for 1 min. The samples were stored at -70°C for subsequent analysis. On the day of analysis, the samples were homogenized (1:5, w/v) in an ice-cold deproteinizing solution containing 1.0M perchloric acid and 2.7 mM (1g/L) disodium EDTA. The homogenate was then centrifuged at 40,000g for 5min (at 0°C) and WR-251833 was added as an internal standard into the supernatant. Blood samples were placed in tubes, containing ice-cold 1.0M perchloric acid and 2.7mM EDTA in a ratio of 1:1 (v/v), immediately after sampling. The mixture was then vortexed vigorously and centrifuged at 20,000g for 5min (at 0°C). The supernatant was stored at -70°C for subsequent analysis. On the day of analysis, the samples were thawed, WR-251833 was added as an internal standard, and a 20 μl aliquot was injected into the HPLC column. Using the described method, the limit of quantification was 0.25 μM. The linear range is 0.25 - 10 μM. The method was validated by measuring samples that were spiked with known concentrations of WR-1065 (0.5, 2.5 and 10μM) on three different days. The interday variability (precision) of WR-1065 was less than 10% and the accuracy (bias) was less than 2%.

4.4.2 HPLC analysis[22]. Analysis was performed on a Waters (Milford, Massachusetts) 515 isocratic HPLC pump. WR-1065 and the internal standard WR-251833 were detected by a BAS (West Lafayette, Indiana) LC-4C amperometric detector equipped with a thin

film mercury-gold amalgam working electrode. The Hg/Au electrode potential was set at +0.15V with respect to the Ag/AgCl reference electrode and the range of the detector was set at 0.1μAFS. The column, 4.6×250mm, 5μm particle size, C_{18} Symmetry® Waters (Milford, Massachusetts), was operated at room temperature. The WR-1065 chromatography protocol employed a mobile phase containing 0.1M chloroacetic acid sodium salt, 1mM sodium octyl sulfate, pH 3.0, and 30% (v/v) methanol running at 1ml/min. Peak indentification was confirmed by comparing retention times in samples with authentic standards. Quantification was based on the peak height ratio of the compound and the internal standard.

4.5 Statistics

All analyses were performed using SAS v9.1. The four endpoints (blood, liver, tumor, liver/tumor) were analyzed separately. Write y_{ijkl} as any endpoint, measured on the lth animal of the ith set (denoting regional [1] or systemic [2] infusion) at dose d_j and time t_k. Per the original experimental design, the response surface regression model was initially fit to all the data using SAS PROC RSREG or SAS PROC GLM:

$$E(y_{ijkl}) = \beta_{i0} + \beta_{i1} d_j + \beta_{i2} t_k + \beta_{i3} d_j t_k + \beta_{i4} d_j^2 + \beta_{i5} t_k^2$$

The expected value, $E(y_{ijkl})$, was plotted against dose and time. The null hypothesis of no difference between regional and systemic infusions is realized as:

Ho: $\beta_{10}=\beta_{20}$, $\beta_{11}=\beta_{21}$, $\beta_{12}=\beta_{22}$, $\beta_{13}=\beta_{23}$, $\beta_{14}=\beta_{24}$, $\beta_{15}=\beta_{25}$,

and can be tested using the CONTRAST statement in SAS PROC GLM. In a second analysis, the logarithmic transform was applied to the endpoints, and the analysis repeated with a reduced model:

$$E(\log(y_{ijkl})) = \beta_{i0} + \beta_{i1} d_j + \beta_{i2} t_k + \beta_{i3} d_j t_k$$

which was found to have a better fit than the original model. Issues with these models are explored in the Discussion.

Results

WR-1065 in liver The response surface of WR-1065 concentration in liver, after regional or systemic dosing of amifostine, is shown in Figure 4.2, where the tendency of both response surfaces to go up from the point with low dose and long sampling time to the point with high dose and short sampling time is observed. The maximal concentration in the liver was achieved with 500 mg/m^2 at 15min, regardless of the route of administration. The maximal concentration of WR-1065 in liver was 400 μM for femoral vein infusion and 275 μM for portal vein infusion. The F test indicates the difference between the two routes is statistically significant ($p = 0.02$). However, the response surfaces do not achieve a maximum within the experimental range. If we study the plots of concentration of WR-1065 in liver versus dose under different sampling time with two different dosing routes, which are shown in Figure 4.3, we see a very similar pattern of curves instead of straight lines in these two plots for femoral and portal vein infusion. The WR-1065 concentration in liver increases with dose, where the rate of increase depends upon the sampling time; the shorter the sampling time, the higher the WR-1065 concentration in liver and the steeper the curve. The WR1065 concentration in liver is dose dependent, which is shown by a disproportional increase in concentration with increased dose. The WR-1065 concentrations in liver versus time under different doses after regional or systemic dosing of amifostine are shown in Figure 4.4. As seen in this figure, the WR-1065 concentration in liver goes down as the sampling time increases and

the dose decreases. The earlier the sampling time, the higher the concentration of WR-1065 in the liver.

WR-1065 in tumor Response surface of the WR-1065 concentration in tumor is shown in Figure 4.5. That the maximal concentration in tumor is much lower than that obtained in liver tissue is demonstrated. However, there is no statistical difference between femoral and portal route regarding of the concentration of WR-1065 in tumor (F test; $p = 0.23$) within our experimental dose range. Dose-dependent feature can also be observed in the plot of the concentration of WR-1065 in the tumor versus dose (Figure 4.6), and the concentration of WR1065 in tumor increase with dose. In Figure 4.7, the concentration of WR1065 in tumor decrease with the time, however, its concentration increase with the time relative to the liver.

WR1065 liver to tumor ratio The response surface of WR-1065 concentration ratios for liver to tumor was shown in Figure 4.8. As shown in this figure, the maximal ratio is around 4~5 with both routes of administration, suggesting amifostine can selectively protect the normal tissue over tumor. Likewise, there is no statistical difference between these two administration routes regarding of the ratio of the concentration of WR-1065 in liver to tumor (F test; $p=0.96$) within this experimental range. In Figure 4.9, the concentration ratios of WR1065 in liver to tumor is increasing with the dose nonlinearly. And this ratio decrease with the time in Figure 4.10. Its highest value achieved at high dose and short time.

WR1065 in blood The response surface of the concentration of WR1065 in blood is shown in Figure 4.11. The F test ($p=0.87$) suggests there is no statistical difference between these two routes regarding of the concentration of WR-1065 in blood. We also

observed similar patterns with the concentration of WR1065 in blood with dose and time in Figure 4.12 and 4.13.

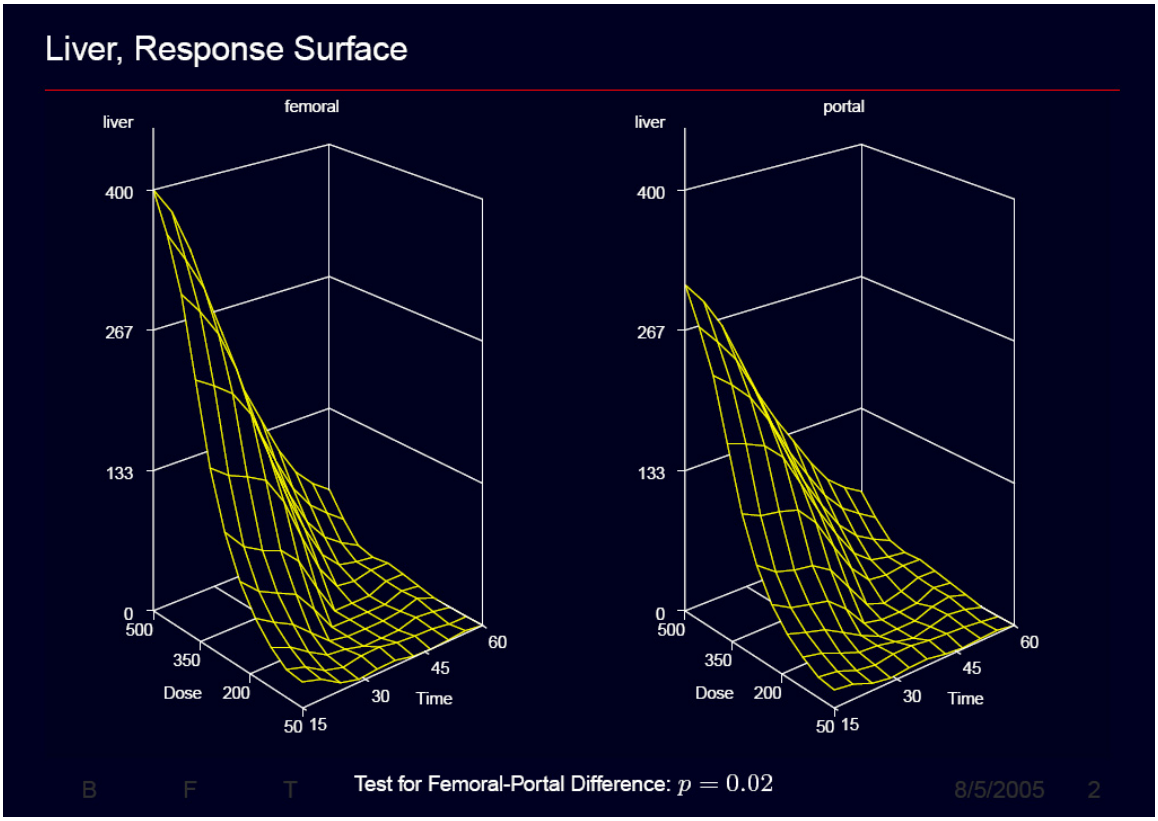

Figure 4.2. Response surface of WR1065 concentrations in liver

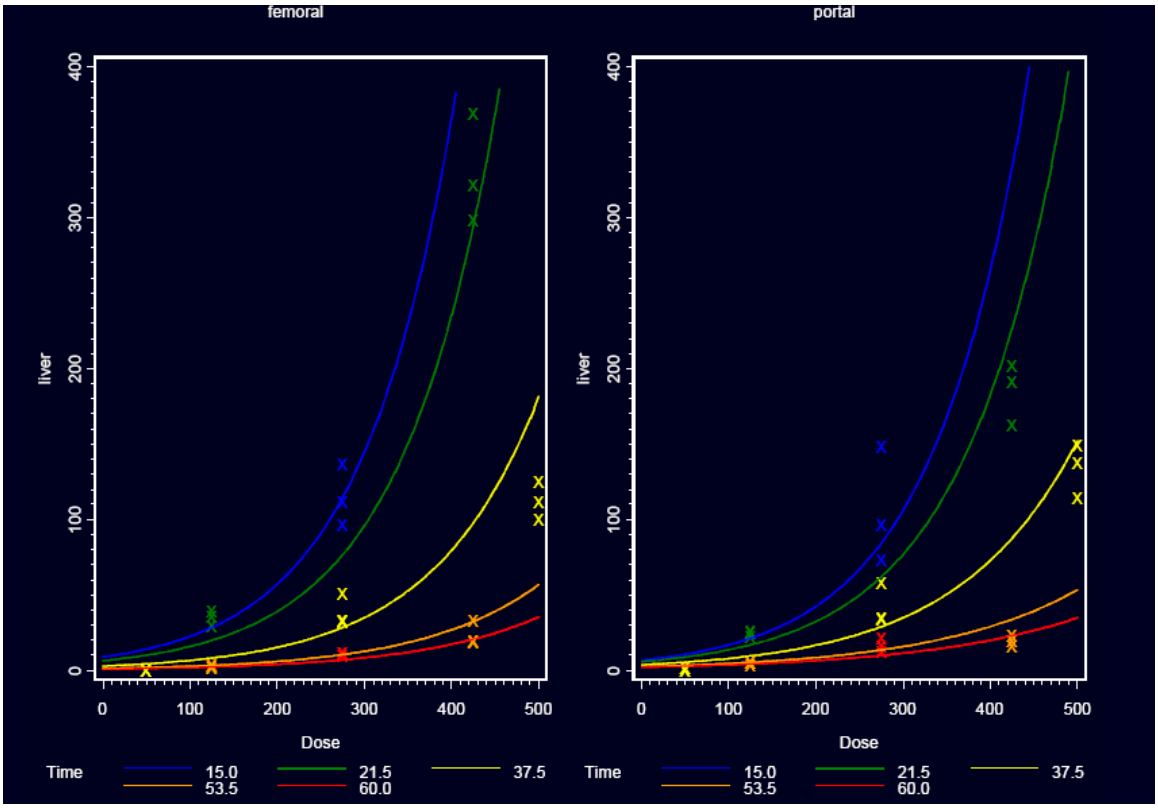

Figure 4.3. Liver concentrations of WR1065 as a function of dose for given sampling times

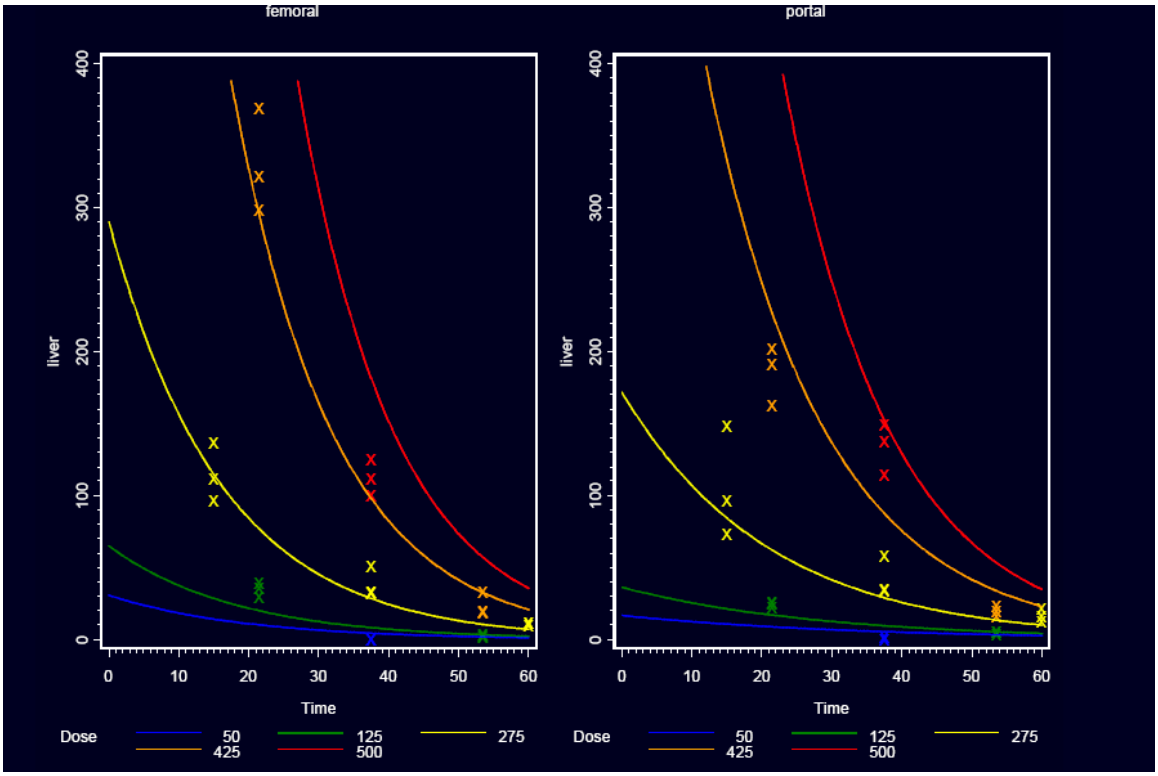

Figure 4.4. Liver concentrations of WR1065 as a function of sampling time for given doses

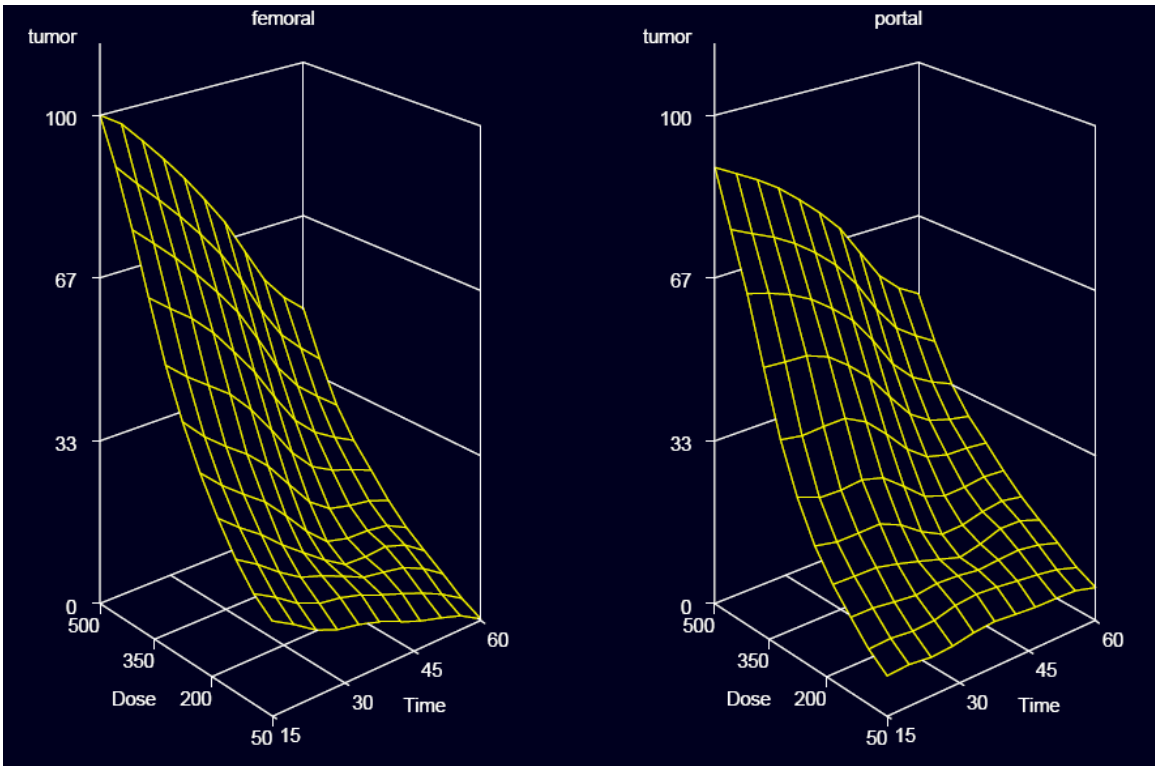

Figure 4.5. Response surface of WR1065 concentrations in tumor

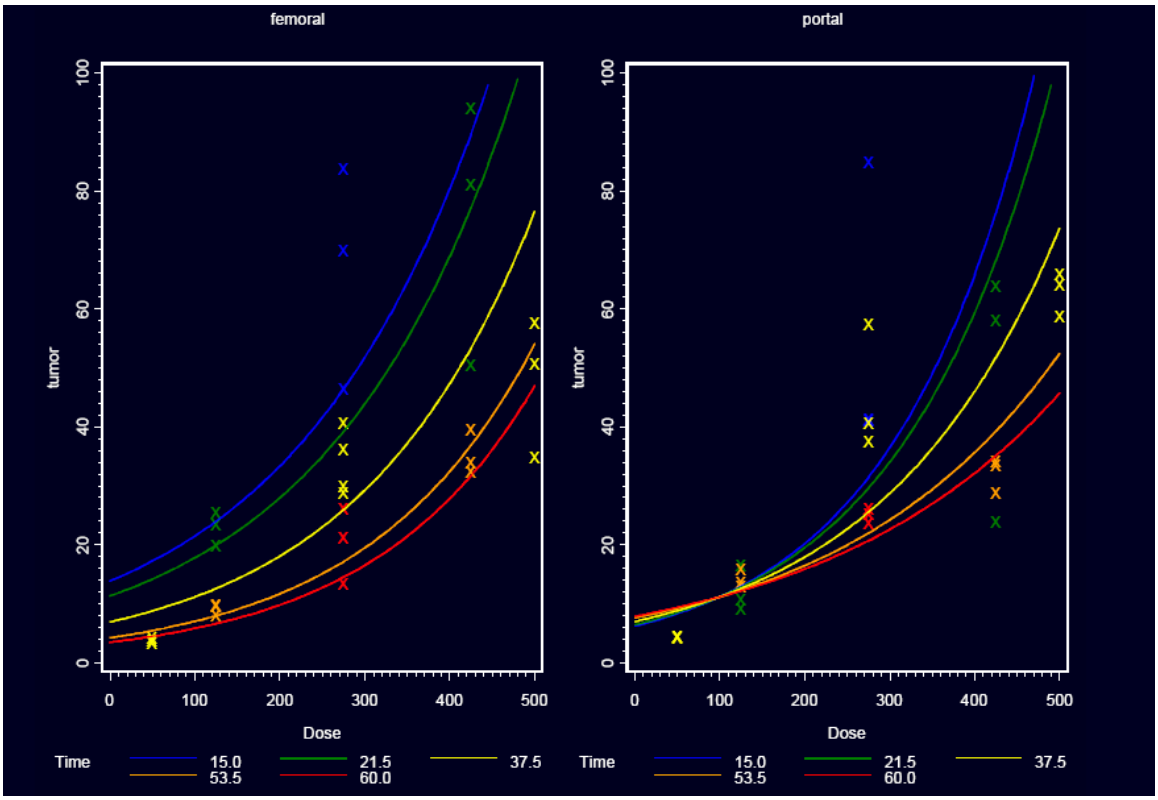

Figure 4.6. Tumor concentrations of WR1065 as a function of dose for given sampling times

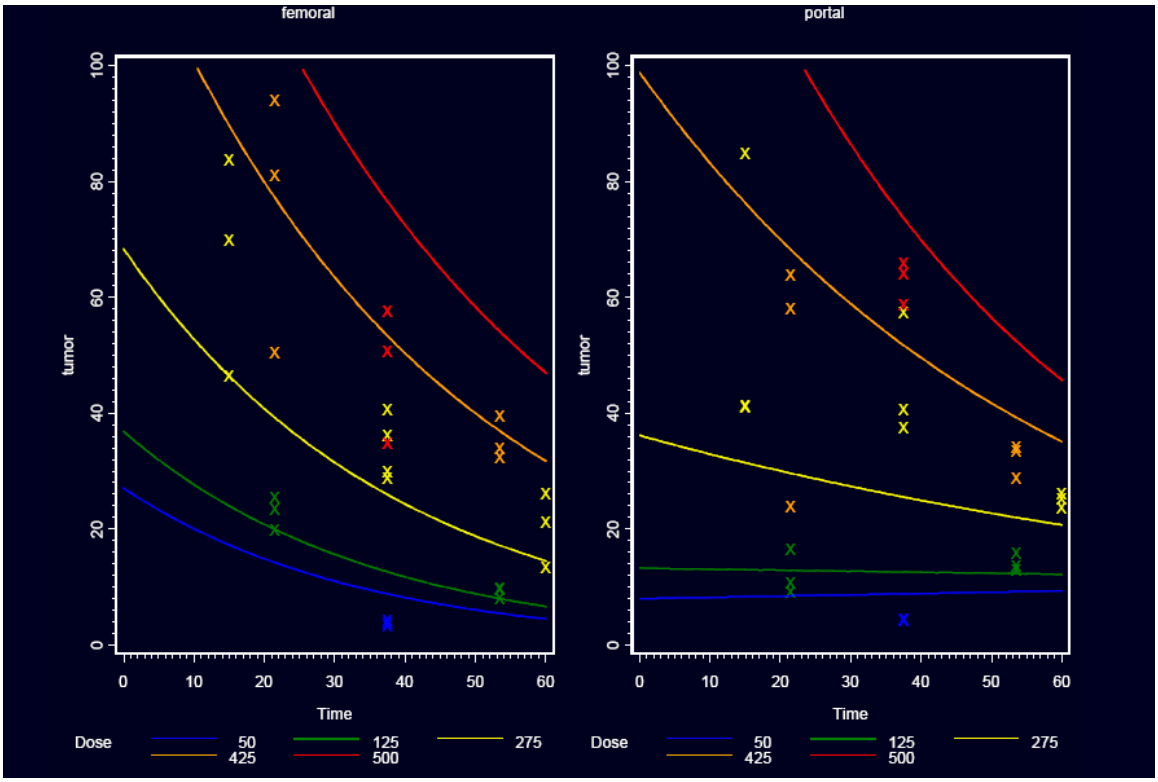

Figure 4.7. Tumor concentrations of WR1065 as a function of sampling time for given doses

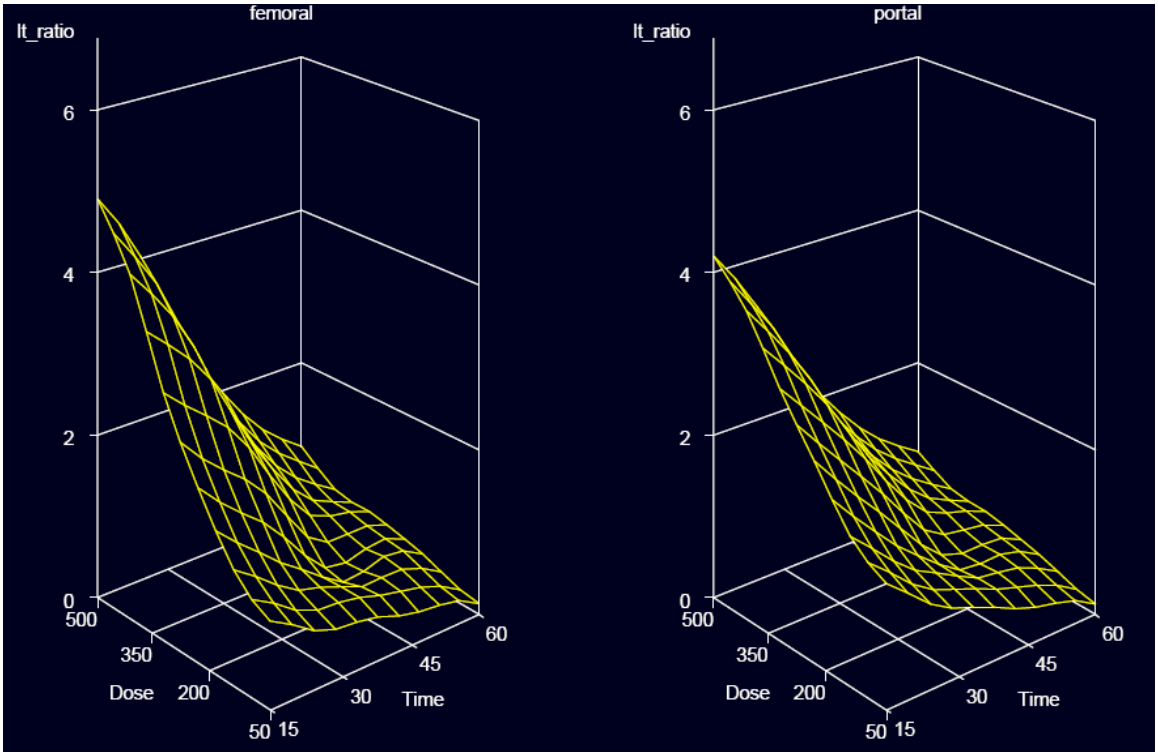

Figure 4.8. Response surface of WR1065 concentration ratios for liver to tumor

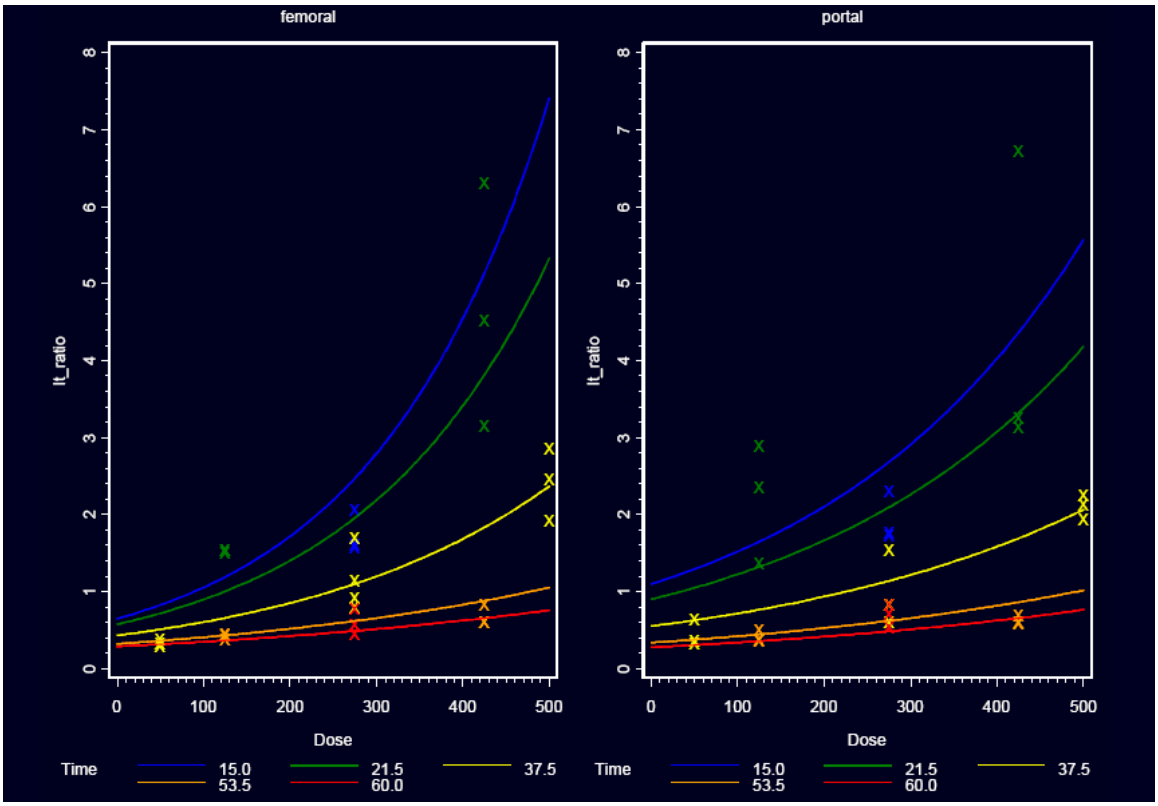

Figure 4.9. Liver/tumor concentration ratios of WR1065 as a function of dose for given sampling times

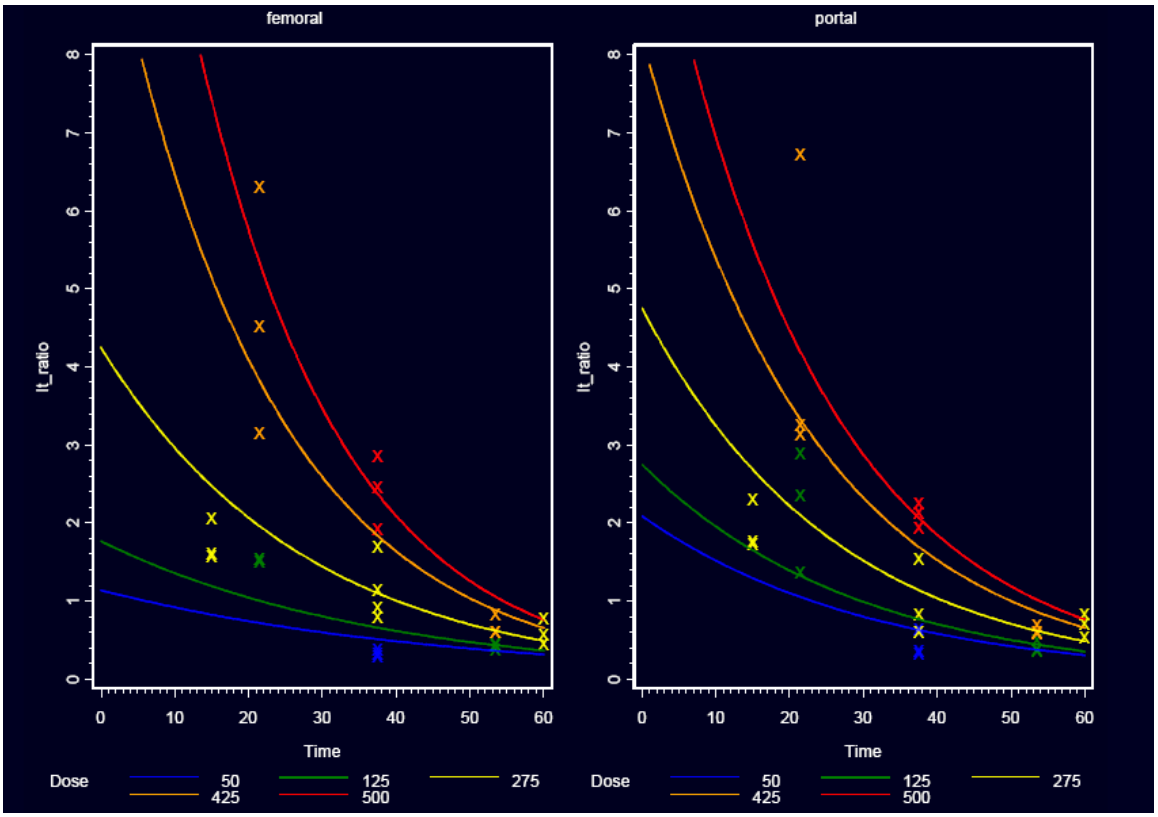

Figure 4.10. Liver/tumor concentration ratios of WR1065 as a function of sampling time for given doses

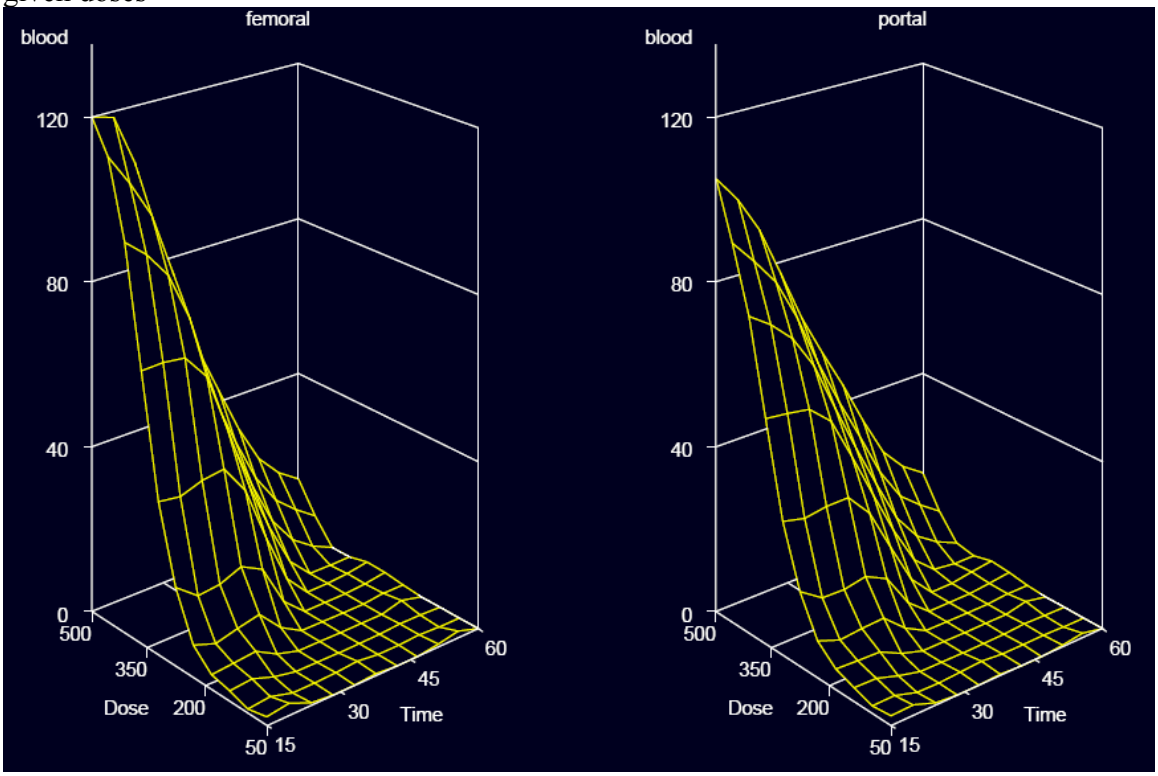

Figure 4.11. Response surface of WR1065 concentrations in blood

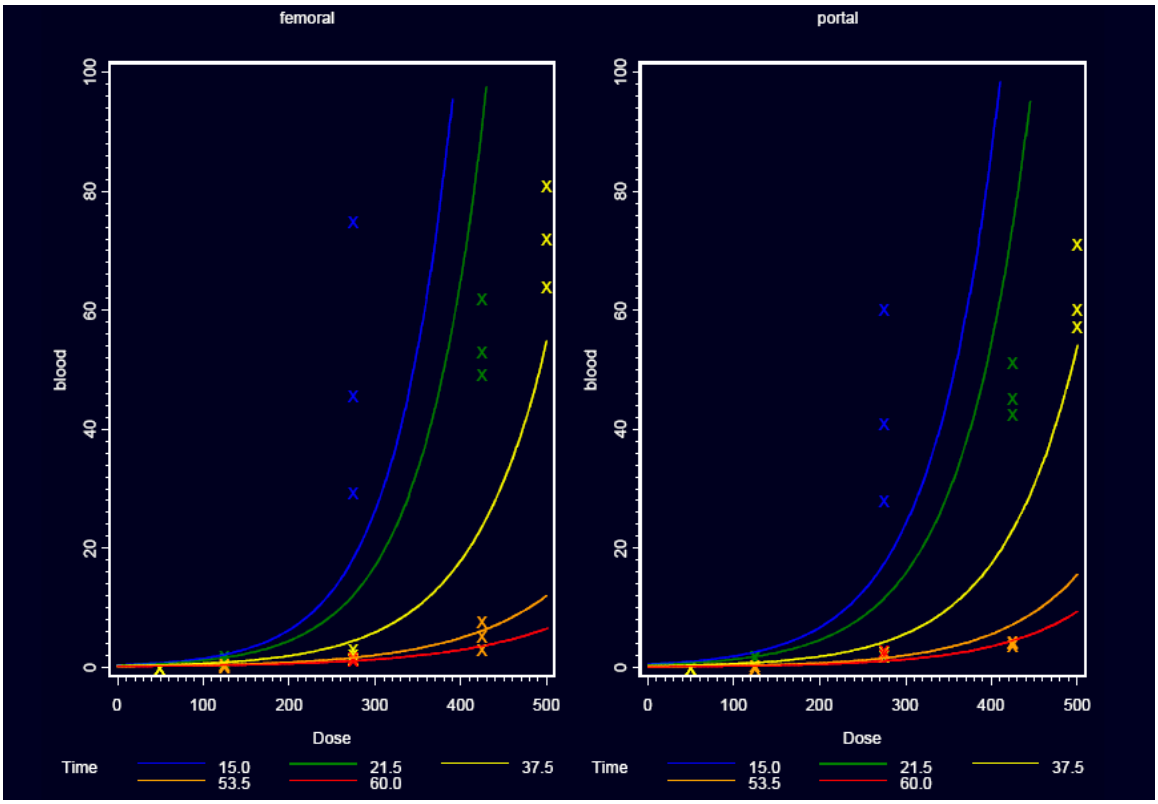

Figure 4.12. Blood concentrations of WR1065 as a function of dose for given sampling time

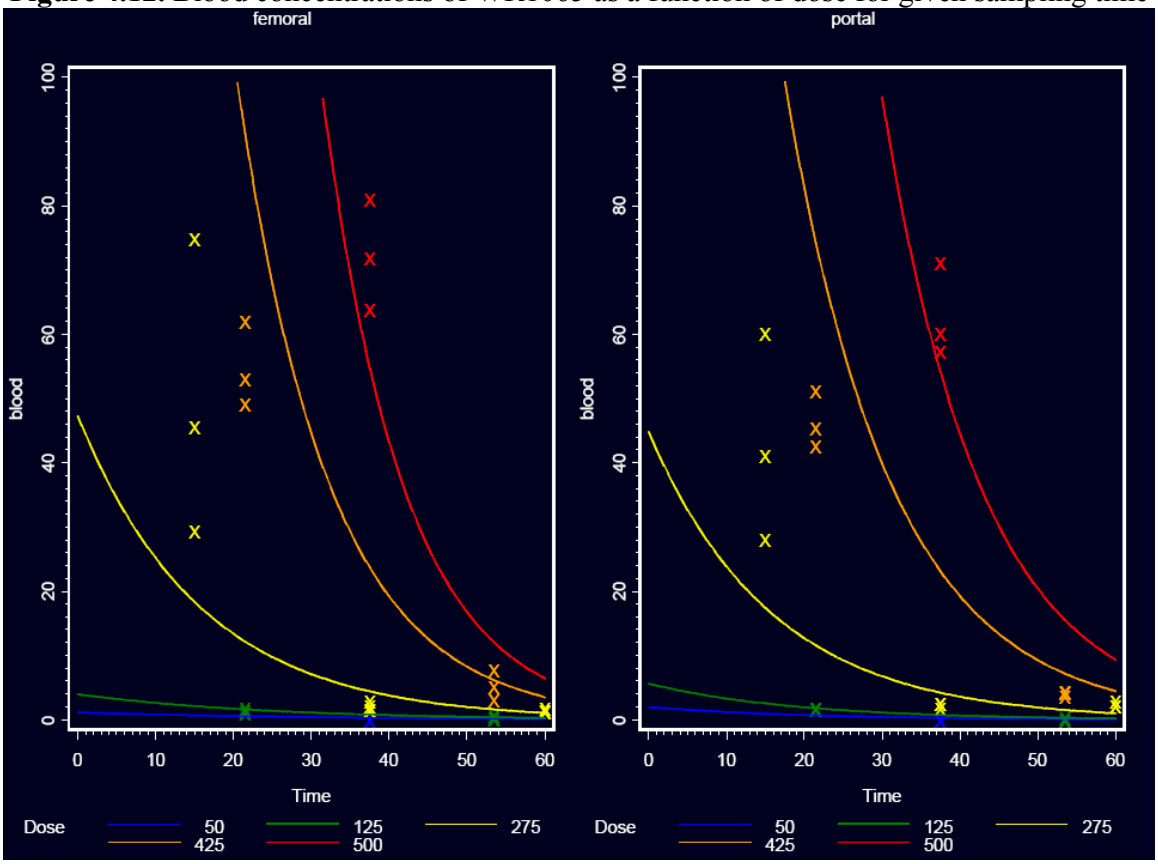

Figure 4.13. Blood concentrations of WR1065 as a function of sampling time for given doses

Discussions

Amifostine is administered at a dose of 200~350 mg/m^2 in the clinic as a 3-min infusion or IV bolus injection 15 -30 min before the start of radiotherapy. Based on this clinic setting during radiotherapy, we studied a dose range of 50 ~ 500 mg/m^2 with a sampling time up to one hour. We expected the optimum condition, i.e., the maximal value of the ratio of the concentration of WR-1065 in liver to tumor to be within this experimental range. We designed a second-order experiment which is shown in the Experimental protocol for this experimental range and originally proposed the second-order model, $E(y_{ijkl}) = \beta_{i0} + \beta_{i1}d_j + \beta_{i2}t_k + \beta_{i3}t_k d_j + \beta_{i4}d_j^2 + \beta_{i5}t_k^2$, to approximate the true response surface, because, if the maximum was obtained in the experimental range, it could be easily identified from the model. However, residual analysis (not shown) demonstrated significant lack of fit, and several of the response surface models displayed saddle points, rather than maxima. We achieved better fits to both regional and systemic data by logarithmically transforming the WR1065 concentrations, and determined that quadratic terms in dose and time destabilized the parameter estimation. This led us to our final model. The increased dose caused a disproportional increase of concentration, implicating non-linear pharmacokinetics of WR1065 and possible saturation of an elimination pathway(s) and/or uptake/retention in tumor, relative to liver. Higher ratios of WR1065 in liver to tumor can apparently be achieved at earlier sampling times regardless of administration route. This means we need to start radiation therapy as soon as possible after dosing of amifostine as long as no systemic toxicity. If we compare the concentration of WR1065 between liver and tumor at different time points, we can see that WR1065 concentrations in tumor exceed that in liver at later sampling points. This

supports above the conclusion that radiation is not acceptable at later times. Another aim of this experiment is to test if regional delivery of amifostine to the liver through the portal vein can generate higher concentration ratios of WR1065 in liver to tumor than that obtained by systemic delivery of amifostine through the femoral vein. Based on the test of equality of two models fitted by the data from portal and femoral vein infusion, respectively, we did not see a statistical difference between these two routes regarding of the ratio of WR1065 concentration in liver to tumor. Actually, we have had some preliminary preclinical results[23] which indicated that portal vein administration of amifostine increased WR1065 selectivity to the liver compared with systemic administration. This was demonstrated by the reduction of WR1065 tumor concentrations following regional dosing to as much as one-fifth the concentrations achieved following intravenous infusion. In that study, amifostine was administered at a dose of 200mg/kg as a 15min infusion to tumor-bearing rats either by femoral vein (systemic) or portal vein (regional) and tissue and blood samples were collected at 15, 20, 30, 45 and 60min after initiating the drug infusion. We observed the statistical difference between these two routes as to the WR1065 liver/tumor ratios at 30 and 45min sampling times. However, p.v. infusions of amifostine increased substantially the systemic exposure to WR1065, compared with i.v. infusion of the same dose. With the same schedule of amifostine: a 15-min infusion at 200mg/kg, we also evaluated whether systemic or portal venous administration of amifostine could protect the normal liver from the effects of ionizing radiation without compromising tumor cell kill in a same rat liver tumor model[17]. Both amifostine conditions (systemic vs regional) showed considerably less radiation effect than saline-treated controls; the two amifostine conditions did not differ. Based on these

previous results, we proposed to further investigate the significance of regional route over systemic administration and optimum condition of dose and timings in a more systematic fashion. We tried to optimized the schedule of amifostine with the dose and timings and compare the systemic and regional route of administration in this response surface experiment. Contrasted to our previous conclusions, we didn't see a statistical difference between these two routes, probably because previously, investigation was done with the single dose level which results in the limitation of the studies. In our current studies, the response surface was generated within a specific experimental range and the conclusion of no difference between regional and systemic dosing was made based on this more systematic study. For the benefit of clinical treatment, WR1065 concentration ratios for liver to tumor increase with the dose increase and this selectivity increase with the sampling time decrease are our main finding from this study.

References

1. Phillips TL. Sensitizers and protectors in clinical oncology. *Semin Oncol*, 8:65-81, 1981.

2. Links M and Lewis C. Chemoprotectants: a review of their clinical pharmacology and therapeutic efficacy. *Drugs*, 57: 293-308, 1999.

3. Hensley M, Schuchter LM, Lindley C, Meropol NJ, Cohen GI. American Society of Clinical Oncology: Clinical Practice Guidelines for the use of chemotherapy and radiotherapy protectants. *J Clin Oncol*, 17: 3333-3355, 1999.

4. Tannehill SP and Mehta MP. Amifostine and radiation therapy: past, present, and future. *Semin Oncol*, 23: 69-77, 1996.

5. Yuhas JM, Spellman JM and Culo F. The role of WR-2721 in radiotherapy and/or chemotherapy. *Cancer Clin Trials*, 3: 211-216, 1980.

6. Calabro-Jones, P.M., Aguilera, J.A., Ward, J. F., Smoluk, G.D., and Fahey, R.C. Uptake of WR-2721 derivatives by cell in culture – Identification of the transported form of the drug. *Cancer Res*, 48: 3634-3640, 1988.

7. Romanul,F.C.A., and Bannister, R. G. Localized areas of high alkaline phosphatase activity in endothelium of arteries. *Nature*, 195: 611-612, 1962

8. McComb, R. B., Bowers, Jr., G. N., and Posen, S. Alkaline Phosphatase, Chaps. 3 and 12. New York: Plenum Press, 1979

9. Newton, G. L., Aguilera, J. A., Kim,T., Ward, J.F. and Fahey, R.C. Transport of aminothiol radioprotectors into mammalian cells: passive diffusion versus mediated uptake. *Radiat Res*, 146, 206-215, 1996.

10. Mitchell, J.L.A., Judd, G.G., Diveley, R.R., Choe, C-Y and Leyser, A. Involvement of the polyamine transport system in cellular uptake of the radioprotectants WR1065 and WR-33278. *Carcinogenesis*, 16, 3063-3068, 1995.

11. Milas, L., Hunter, N., Reid, B.O., and Thames, J., H.D. Protective effects of S-2-(3-aminopropylamino) ethylphosphorothioic acid against radiation damage of normal tissues and a fibrosarcoma in mice. *Cancer Res*, 42: 18888-1897, 1982.

12. Rasey, J.S., Nelson, N.J., Mahler,P., Anderson, K., Krohn, K.A., and Menard, T. Radioprotection of normal tissues against gamma rays and cyclotron neutrons with WR-2721-LD_{50} studies and ^{35}S-WR-2721 biodistribution. *Radiat Res*, 97: 598-607, 1984.

13. Shaw, L. M., Bonner, H.S., and Brown, D.Q. Metabolic pathways of WR-2721 (ethyol, amifostine) in the BALB/c mouse. *Drug Metab Dispos*, 22: 895-902, 1994.

14. Yuhas, J.M. Active versus passive absorption kinetics as the basis for selective protection of normal tissues by S-2-(3-aminopropylamino) ethylphosphorothioic acid. *Cancer Res*, 40: 1519-1524, 1980.

15. Rasy, J. S., Grunbaum, A., Krohn, K.A., Menard, T. W., and Spence, A. M. Biodistribution of the radioprotective drug ^{35}S-labeled 3-amino-2-hydroxypropyl phosphorothioate (WR77913). *Radiat Res*, 102: 130-137, 1985.

16. Shaw LM, Bonner HS and Lieberman L. Pharmacokinetic profile of Amifostine. *Semin Oncol*, 23: 18-22, 1996.

17. Symon, Z., Levi, M., Ensminger, W.D., Smith, D.E., and Lawrence, T.S. Selective radioprotection of hepatocytes by systemic and portal vein infusion of amifostine in a rat liver tumor model. *Int J Radiat Oncol Biol Phys*, 50: 473-478, 2001.

18. Levi, M., Knol, J.A., Ensminger, W.D., Deremer, S.J., Dou, C., Lunte, S.M., Bonner, H.S., Shaw, L.M., and Smith, D.E. Regional pharmacokinetics of amifostine in anesthetized dogs: role of the liver, gastrointestinal tract, lungs and kidneys. *Drug Metab Dispos,* 30: 1425-1430, 2002.

19. Snder, R.D. and Grdina, D.J. Further evidence that the radioprotective aminothiol, WR-1065, catalytically inactive mammalian topoisomerase II. Cancer Res, 60: 1186-1188, 2000.

20. Shaw, L.M., Bonner, H.S., Turrisi, A., Norfleet, A. L., and Kligerman, M. Measurement of S-2-(3-aminopropylamino) ethanethiol (WR-1065) in blood and tissue. *J Liq Chromatogr*, 9: 845-859, 1986.

21. Shaw, L.M., Bonner, H.S., Turrisi, A., Norfleet, A. L., and Glover, D.J. A liquid chromatographic electrochemical assay for S-2-(3-aminopropylamino) ethylphosphorothioate (WR-2721) in human plasma. *J Liq Chromatogr*, 7: 2447-2465, 1984.

22. Shaw, L.M., Bonner, H.S., Turrisi, A., Norfleet, A.L., and Kligerman, M. Measurement of S-2-(3-aminopropylamino) ethanethiol (WR-1065) in blood and tissue. *J Liq Chromatogr*, 9: 845-859, 1986.
23. Levi, M., DeRemer S.J., et al. Disposition of WR-1065 in the liver of tumor-bearing rats following regional vs systemic administration of amifostine. *Biopharm. Drug Dispos*. 25: 27-35, 2004.

CHAPTER 5

RELATIONSHIP BETWEEN AMIFOSTINE DOSE, ADMINISTRATION ROUTE (INTRAVENOUS VS SUBCUTANEOUS), AND SAMPLING TIME ON WR-1065 EXPOSURE IN THE LIVER OF TUMOR-BEARING RATS

ABSTRACT

The objective of the present study was to determine if a higher liver-to-tumor ratio of the cytoprotective metabolite WR-1065 could be achieved following intravenous as opposed to subcutaneous dosing of the inactive prodrug amifostine. Amifostine was administered either by subcutaneous or intravenous route into rats bearing liver tumors. The experiment employed a central composite design, with doses of 100-1000 mg/m^2 and post-treatment sampling times of 5-60 min. Liver, tumor and blood samples were analyzed for WR-1065 by HPLC with electrochemical detection. Liver-to-tumor ratios were highest at the larger doses (550-1000 mg/m^2) and earliest sampling time (5 min), achieving ratios of 6-8 after intravenous dosing. Liver and blood concentrations of WR-1065 were highest at the first sampling time and decreased steadily over time, although tumor levels were relatively constant with respect to time. Following subcutaneous dosing of amifostine, the highest ratios (i.e., 4-6) were achieved at the higher doses (550-1000 mg/m^2) and sustained until 20 min post-dosing. Liver and tumor concentrations of WR-1065 were initially low, but increased over time, reaching a plateau for liver at 40-60 min, and continuing to rise for tumor. Blood levels were relatively constant over time. These results suggest that the therapeutic selectivity (i.e., liver to tumor ratio) of WR1065

may be optimized by increasing the amifostine dose within safe limits and by delivering radiotherapy ≤15 min after IV administration. The subcutaneous route may be a reasonable alternative when dosed 5-20 min before liver radiotherapy.

INTRODUCTION

Amifostine protects almost all normal tissues from the cytotoxic effects of radiation and some chemotherapeutic agents [1,6]. It is a thiophosphate prodrug that is dephosphorylated to the free thiol active metabolite, WR-1065; by the plasma membrane bound enzyme alkaline phosphates [4]. Amifostine may be actively absorbed by normal tissue cells and only passively absorbed by tumor cells [3]. The selective uptake of WR-1065 and/or amifostine may also be due to differences in the tissue microenvironment resulting in the slow entry of the free thiol into tumor masses. Tumors are often relatively hypovascular and have low interstitial pH, resulting in low rates of prodrug activation by alkaline phosphates. In addition, the distribution of alkaline phosphates in capillaries and arterioles of normal tissues is extensive as compared with tumors. Thus, in tumors it is thought that both reduced metabolism of amifostine to the active protector WR-1065 and the low uptake of WR-1065 and/or amifostine by the tumor result in a concentration of the free thiol that is much lower than that found in normal organs [2,5]. As a result, healthy tissue is protected from radiotherapy and chemotherapy while tumors with lower levels of the active metabolite are less protected. The main metabolic pathway of WR-1065 elimination involves the formation of symmetrical and nonsymmetrical disulfides that might serve as a depot for the active metabolite, free WR-1065 [10].

Radiation therapy has played a minor role in the conventional management of patients with intrahepatic malignancies because the dose of radiation that can be delivered is limited by normal tissue toxicity referred to as radiation-induced liver disease (RILD).

For patients with focal intrahepatic cancers, three-dimensional treatment planning has permitted the delivery of high doses of radiation, leading to improved local control and, possibly, survival. However, many patients have disease that is too diffuse to be treated with focal techniques. Amifostine has been shown in randomized trials to protect the kidney from cisplatin nephrotoxicity and the parotid gland from radiation due to the greater conversion of the drug to the active metabolite WR-1065 in the normal tissue than in the tumor. Protection appears to result from scavenging oxygen-derived free radicals and hydrogen donation to repair damaged target molecules. WR-1065 may also affect the catalytic inactivation of topoisomerase II, which slows cell cycling, thus providing more time for DNA repair [8]. In order to optimize the use of amifostine as a radiation protector of normal liver, which will permit the safe delivery of higher doses of radiation for patients with both focal and diffuse disease, we performed nonclinical study to optimize selectivity and to estimate the appropriate dose of intravenous and/or subcutaneous amifostine.

The IV administration of 200 to 350 mg/m^2 amifostine 15-30 minutes before each radiotherapy fraction is the usual recommended schedule for radioprotection. However, IV administration requires the availability of a day clinic attached to the radiotherapy unit, and a specialized nurse to treat the potential side effects related to amifostine infusion, such as acute hypotension and severe nausea and vomiting. Moreover, it can be difficult to administer the drug, transport the patient and initiate RT within the approved 15-to-30-minute time frame. Clearly, a simpler but equally effective mode of administration would make amifostine more convenient for both the patient and the practitioner. Subcutaneous administration of amifostine could potentially reduce the side

effects of the drug and be significantly more convenient for both patients and radiation oncologists. Amifostine is not currently approved for SC administration in the United States. However, evaluation of administration via this route is ongoing in the settings of chemotherapy and fractionated radiation therapy. To be clinically useful, the SC route would have to be as effective as IV administration.

In our nonclinical study, the objective was to evaluate the potential advantage of amifostine subcutaneous administration to the liver and the relationship of selectivity (liver to tumor concentration ratio of WR1065) to the different doses and times after intravenous and/or subcutaneous administration of amifostine. Thus, the concentrations of the active metabolite, WR-1065, were determined in the blood, liver and tumor of a tumor-bearing rat model at different times after both routes of administration under different doses.

Material and Methods

5.1 Chemicals

Amifostine and WR1065 standards were generously provided by the division of experimental therapeutics, department of chemical information, Walter Reed Army Institute of Research (Silver Spring, Maryland). Amifostine (bulk) was provided by ALZA Pharmaceuticals (Palo Alto, CA). Perchloric acid 70% (redistilled) was obtained from Aldrich Company (Milwaukee, WI). EDTA disodium salt was purchased from the Sigma Chemical Company (St. Louis, MO). HPLC grade methanol, water, phosphoric acid were purchased from Fisher Scientific (Pittsburgh, PA).

5.2 Animals

Male Sprague-Dawley rats weighting approximately 125-175g were obtained from Harlan Sprague Dawley, Inc. (Indianapolis, Indiana). They were maintained in a temperature-humidity controlled room on a 12 h light-dark cycle with access to 5001 Rodent Diet (PMI Nutrition International, Inc. Brentwood, Mo) and water. All animal procedures and study protocols were approved by the University of Michigan Committee on the Use and Care of Animals.

5.3 Tumor implantation

Rats were anesthetized using a 60 mg/kg intraperitoneal injection of pentobarbital. A mid-line abdominal incision was made starting at the xiphoid process and the liver was exposed. Walker 256 adenosarcoma cells were grown in suspension cultures with RPMI media supplemented with 10% fetal calf serum and prepared for injection by suspension

in phosphate buffered saline 7.4(PBS). The left lateral lobe (LL) of the liver was injected with tumor cells (~ 30μl) and the peritoneum and abdominal wall were closed for recovery. Tumors were allowed to grow for ~14 days.

5.4 Experimental protocol

Tumor-bearing rats were divided randomly into two equal groups and were anesthetized using a 60 mg/kg intraperitoneal injection of pentobarbital. For intravenous administration, femoral vein was cannulated and blood was drawn and seen in the cannula before dosing of amifostine. Approximate 1 ml of saline was injected over 60 sec into femoral vein to examine for leakage and to hydrate the animals before dosing of amifostine. For subcutaneous administration, Amifostine is injected into the center of the 'tent' made by pinching the skin over the back of the rats. A solution of amifostine at a dose of 100, 232, 550, 868 and 1000 mg/m^2 was prepared in normal saline and injected as a bolus dose either through subcutaneous administration or intravenous administration (femoral vein). Blood was obtained by cardiac puncture, and liver tissue and tumor samples were collected at 5, 13.05, 32.5, 51.95 and 60 min after initiating the drug administration under different doses. The whole experiment was designed with the method of central composite design centered at a dose of 550 mg/m^2 and a sampling time of 32.5 min. The levels and design are given in Table 5.1 and Table 5.2. For each of the two modes (IV vs SC) of administration, at least three animals were tested at each design point. Concentrations of WR1065 were assessed in blood, liver and tumor; the ratio of liver concentration to tumor concentration, the therapeutic selectivity, was also evaluated.

5.5 Determination of WR-1065[7]

Liver and tumor tissue samples were dissected, weighed and were homogenized (1:5, w/v) in an ice-cold deproteinizing solution containing 1.0M perchloric acid and 2.7 mM (1 g/L) disodium EDTA; blood samples were placed in tubes, containing same deproteinizing solution in a ratio of 1:1 (v/v), immediately after sampling. All mixture was then centrifuged at 20,000g for 5min (at 4°C) and the supernatant were stored at -70°C for subsequent analysis. On the day of analysis, WR-251833 was added as an internal standard into the supernatant and a 20 μl aliquot was injected into Waters (Milford, Massachusetts) Symmetry® C_{18} column (4.6×250mm, 5μm). Assay was performed with a Waters 515 isocratic HPLC pump coupled with a BAS (West Lafayette, Indiana) LC-4C amperometric detector equipped with a thin film amalgamated working electrode. The Hg/Au electrode potential was set at +0.15V with respect to the Ag/AgCl reference electrode and the range of the detector was set at 0.1μAFS. Mobile phase was 0.1M chloroacetic acid sodium salt and 1mM sodium octyl sulfate, pH 3.0, mixed with 30% (v/v) methanol. The flow rate was 1ml/min. The limit of quantification of this analytical method was 0.25 μM with the linear range of 0.25 - 10 μM. Quantification was based on the peak height ratio of the compound and the internal standard.

5.6 Data Analysis

All analyses were performed using SAS v9.1. The four endpoints (concentration of WR1065 in blood, liver, tumor and concentration ratio of WR1065 in liver to tumor) applied with logarithmic transform were analyzed separately. Write y_{ijkl} as any endpoint, measured on the lth animal of the ith set (denoting IV [1] or SC [2] injection) at dose d_j and time t_k. The final model of different endpoints was determined by stepwise selection from initial response surface regression model, $E(\log(y_{ijkl})) = \beta_{i0} + \beta_{i1} d_j + \beta_{i2} t_k +$

$\beta_{i3}\, d_j t_k + \beta_{i4}\, d_j^2 + \beta_{i5}\, t_k^2$, using SAS PROC REG. The null hypothesis of no difference between IV and SC injection is realized as: H_o: $\beta_{10}=\beta_{20}$, $\beta_{11}=\beta_{21}$, $\beta_{12}=\beta_{22}$, $\beta_{13}=\beta_{23}$, $\beta_{14}=\beta_{24}$, $\beta_{15}=\beta_{25}$, and can be tested using the CONTRAST statement in SAS PROC GLM.

Results

WR-1065 in liver

WR-1065 concentrations in liver versus time profiles under different doses (100-1000 mg/m^2) after intravenous or subcutaneous dosing of amifostine are shown in Figure 5.1. As seen in this figure, following intravenous dosing of amifostine, WR-1065 concentration in liver was highest at the earliest sampling time (5 min) and decreased steadily over time for all doses; the concentration of WR1065 in liver was directly proportional to doses. Amifostine doses of 868 mg/m^2 and 1000 mg/m^2 did not produce significantly different WR-1065 concentrations in liver indicated by the confidence intervals. Following subcutaneous dosing of amifostine, the concentration of WR1065 in the liver was initially very low and increased over time, reaching a plateau at 40-60 min for all doses. As with intravenous dosing, liver concentrations of WR-1065 after subcutaneous administration was directly proportional to the dose and did not significantly differ between amifostine doses of 868 and 1000 mg/m^2. Statistical test (F test) indicated there is a significant difference between the routes of intravenous and subcutaneous administration regarding the concentration of WR1065 in liver ($P < 0.05$). When we plot concentration of WR-1065 in liver versus blood concentration of WR1065 for two different routes in Fig 5.5 (A), we observe a good correlation between liver concentration and blood concentration for both routes, and regression lines for two different routes indicate they are similar regarding this correlation. The higher the blood concentration is, the higher the liver concentration is.

WR-1065 in tumor

The concentrations of WR-1065 concentrations in tumor over time by dose after intravenous or subcutaneous dosing are shown in Figure 5.2. Following the intravenous administration of amifostine, the WR-1065 concentration in tumor was relatively constant with respect to time, but increased with doses. Following subcutaneous dosing of amifostine, concentration of WR1065 in tumor was initially low, but continued to increase over time. Statistical test (F test) indicated there is a significant difference between the routes of intravenous and subcutaneous administration regarding the concentration of WR1065 in tumor ($P < 0.05$). In Fig 5.5 (B), we still observe a correlation between tumor concentration and blood concentration of WR-1065.

WR1065 liver to tumor ratio

Because Amifostine is a cytoprotective agent, higher concentration of WR1065 in liver compared to tumor which results in the higher selectivity which is the ratio of WR-1065 in liver to tumor is expected. The ratio of WR1065 concentrations in liver to tumor versus time after intravenous or subcutaneous dosing of amifostine are shown in Figure 5.3. Following intravenous dosing of amifostine, the ratio increased with dose, and was highest at the earliest sampling time (5 min), decreasing steadily over time for all doses. To achieve higher ratio of WR1065, there is no observable significant difference within the range of doses of 550-1000 mg/m^2. Following subcutaneous dosing of amifostine, the ratio was also highest at the earliest sampling time (5 min) and sustained till 15 min, then decreased steadily with respect to time; the ratio is proportional to doses. There was no significant difference in the range of 550 and 1000 mg/m^2 for achieving higher ratio. Here is a significant difference between the routes of intravenous and subcutaneous administration regarding the ratio of WR1065 in liver to tumor ($P < 0.05$). We expect

higer liver-to-tumor ratio, but not very high blood concentration of WR-1065 which could result in the toxicity. Fig 5.5 (C) clearly indicate IV administration can achieve higher liver-to-tumor ratio compared to SC administration with relatively higer liver concentration than SC administration, there is a better correlation for IV administration between ration and liver concentration than SC administration. Highest ratio with SC administration doesn't mean we have higher liver concentration at the same time, partial because of much lower concentration of WR-1065 in tumor.

WR1065 in blood

The WR-1065 concentrations in blood versus time under different doses (100-1000 mg/m^2) after intravenous or subcutaneous dosing of amifostine are shown in Figure 5.4. Following intravenous dosing of amifostine, the WR-1065 concentration in blood was highest at the earliest sampling time (5 min) and decreased steadily over time for all levels of doses; the higher concentration of WR1065 in blood was generated with the higher dose in this study (550-1000 mg/m^2) and the concentration was low at the low levels of doses (100-232 mg/m^2). There is no significant difference observed in achieving high concentration of WR1065 in blood between 868 and 1000 mg/m^2. Following subcutaneous dosing of amifostine, blood levels were relatively constant within the range of time (5-60 min) in this study; the highest blood level was generated with the highest dose of 1000 mg/m^2 and the level of concentration of WR1065 in blood goes down as the dose decreases. To achieve higher concentration of WR1065 in blood with the route of subcutaneous administration, first two higher levels of doses, 868 and 1000 mg/m^2 didn't differ significantly. Statistical test (F test) indicated there is a significant difference between the routes of intravenous and subcutaneous administration regarding the

concentration of WR1065 in blood ($P < 0.05$). IV administration can result in higher ratio with higher blood concentration compared to SC administration in Fig 5.5 (D), but the big advantage of high ratio with IV administration will also be dependent on the acceptable blood level.

Discussion

Amifostine is administered at a dose of 200~350 mg/m^2 in the clinic as a 3-min IV infusion or bolus injection 15-30 min before the start of radiotherapy. Compared to IV administration, SC route presents some advantages over IV route when amifostine is used during fractionated radiotherapy because of its simplicity and reduced toxicities. Based on above clinic setting during radiotherapy, we studied a dose range of 100-1000 mg/m^2 with a sampling time up to one hour to explore the SC administration as an alternative route systemically. We expected the optimum condition, i.e., the maximal value of the ratio of the concentration of WR-1065 in liver to tumor to be within this experimental range.

We consider three factors which are dose, time and route to affect responses which are concentration of WR1065 in tissue and blood in this study. We designed a second-order response surface study which is shown in the Experimental protocol for this experimental range based on factorial experiments instead of one-factor-at-a-time approach and originally proposed the second-order linear model, $E(y_{ijkl}) = \beta_{i0} + \beta_{i1}d_j + \beta_{i2}t_k + \beta_{i3}t_k d_j + \beta_{i4}d_j^2 + \beta_{i5}t_k^2$, to approximate the true response surface, because, if the maximum was obtained in the experimental range, it could be easily identified from the model. By comparison with the one-factor-at-a-time approach, factorial design method requires less runs for the same precision in effect estimation and conclusion from this analysis can be more general. Comparison between IV and SC administration can be indicated by the test of coincidence of response surfaces which was generated in this study. However, residual analysis (not shown) demonstrated some lacks of fit, and several of the response surface models displayed saddle points, rather than maxima. We achieved better fits to both IV

and SC data by logarithmically transforming the WR1065 concentrations, and determined statistically significant independent variables to enter the model for different dependent variables in this study by stepwise model-selection method at the level of entry and stay both equals 0.05. And it also seems that regression model weighted by the inverse of the sample variances within replicates can produce better fit than ordinary least square. All of above investigations led us to our final model for each dependent variable in our study. Among our four response variables, we consider higher ratio of WR1065 concentration in liver to tumor with high enough concentration of WR1065 in liver as a good indicator of protection.

For the route of intravenous administration, higher ratios of WR1065 in liver to tumor can apparently be achieved at earlier sampling times. This means we need to start radiation therapy as soon as possible after dosing of amifostine as long as no systemic toxicity which is indicated by the concentration of WR1065 in blood. Because there is no observable difference among first three levels of doses (550, 868, 1000mg/m^2) in achieving high ratio and lower doses produce lower blood concentration of WR1065, we are more interested in the range of 550-868 mg/m^2 to generate good protection with acceptable toxicity. If we compare the concentration of WR1065 between liver and tumor at different time points, we can see that WR1065 concentrations in tumor were relatively constant over time, which results in the ratio is very dependent on the concentration of WR1065 in liver which is lower at later sampling points. This supports above conclusions that radiation is not acceptable at later times.

For the route of subcutaneous administration, blood levels were relatively constant over time and significantly lower than those from IV administration indicating less toxicity

with SC administration compared with IV administration. Higher ratio was also generated at earlier sampling time with SC administration and can be sustained for a period of time which can provide flexible time frame to start radiotherapy clinically. The mechanism of producing higher ratio at earlier time can be clear by studying the concentration profile of WR1065 in liver and tumor after SC administration. Initially, at the earlier sampling time, both WR1065 concentration in liver and tumor are low compared with later sampling times and concentration of WR1065 in liver is much higher than that in tumor. Concentration of WR1065 in tumor continue to increase with respect to time, but concentration of WR1065 in liver reached a plateau around 40-60 min. All of these results indicate that there will be no benefit if the radiotherapy start during the later time typically after 30 min, and probably the concentration of WR1065 in liver is low if we start radiotherapy during earlier time.

Based on our criterion of effectiveness of protection, IV administration is better than SC administration because the ratio generated by IV administration is higher than that from SC administration (6-8 vs. 4-6) at earlier sampling time and we can have high concentration of WR1065 in liver with IV administration during the time when the higher ratio can be observed. Another aim of this experiment is to test if SC administration of amifostine can be equivalent in generating concentration of WR1065 in liver, tumor, blood and concentration ratio of WR1065 in liver to tumor to that obtained by systemic delivery of amifostine through the femoral vein. Based on the test of equality of two models fitted by the data, we found a statistical difference between these two routes regarding all of above responses ($P<0.05$). The result indicated there exists significant difference between subcutaneous and intravenous routes of administration for amifostine

probably because there should be an absorption process of drug for subcutaneous administration. Because all maximum responses can be achieved at early time and higher dose with intravenous administration, with as low as possible blood level, 550mg/m^2 can still achieve ratio of 7~8 with much higher WR1065 concentration in liver than that with subcutaneous route with same dose (550 mg/m^2). In our current studies, the response surface was generated within a specific experimental range and the conclusion of difference between IV and SC dosing was made based on this more systematic study. For the benefit of clinical treatment, WR1065 concentration ratios for liver to tumor increase with the dose increase and this selectivity increase with the sampling time decrease are our main finding with IV administration from this study, the subcutaneous route offers a less complicated method of administering amifostine to patients and may be a reasonable substitute when dosed 5-20 min prior to liver radiotherapy.

References

1. McComb, R. B., Bowers, Jr., G. N., and Posen, S (1979) *Alkaline Phosphatase*. Plenum Press, New York.

2. Milas, L., Hunter, N., Reid, B.O., and Thames, J., H.D (1982) Protective effects of S-2-(3-aminopropylamino) ethylphosphorothioic acid against radiation damage of normal tissues and a fibrosarcoma in mice. *Cancer Res* 1888:1897 42.

3. Mitchell, J.L.A., Judd, G.G., Diveley, R.R., Choe, C-Y and Leyser, A (1995) Involvement of the polyamine transport system in cellular uptake of the radioprotectants WR1065 and WR-33278. *Carcinogenesis* 3063:3068 16.

4. Newton, G. L., Aguilera, J. A., Kim,T., Ward, J.F. and Fahey, R.C (1996) Transport of aminothiol radioprotectors into mammalian cells: passive diffusion versus mediated uptake. *Radiat Res* 206:215 146.

5. Rasey, J.S., Nelson, N.J., Mahler, P., Anderson, K., Krohn, K.A., and Menard, T (1984) Radioprotection of normal tissues against gamma rays and cyclotron neutrons with WR-2721-LD_{50} studies and ^{35}S-WR-2721 biodistribution. *Radiat Res* 598:607 97.

6. Romanul,F.C.A., and Bannister, R. G (1962) Localized areas of high alkaline phosphatase activity in endothelium of arteries. *Nature* 611:612 195.

7. Shaw, L.M., Bonner, H.S., Turrisi, A., Norfleet, A. L., and Kligerman, M (1986) Measurement of S-2-(3-aminopropylamino) ethanethiol (WR-1065) in blood and tissue. *J Liq Chromatogr* 845:859 9.

8. Snder, R.D. and Grdina, D.J (2000) Further evidence that the radioprotective aminothiol, WR-1065, catalytically inactive mammalian topoisomerase II. Cancer Res 1186:1188 60.

9. Tannehill SP and Mehta MP (1996) Amifostine and radiation therapy: past, present, and future. *Semin Oncol* 69:77 23.

10. Yuhas, J.M (1980) Active versus passive absorption kinetics as the basis for selective protection of normal tissues by S-2-(3-aminopropylamino) ethylphosphorothioic acid. *Cancer Res* 1519:1524 40.

TABLE 5.1. Factors and Levels

Factor	Coded and uncoded levels				
	-1.414	-1	0	1	1.414
A. Dose (mg/m^2)	100	232	550	868	1000
B. Time (min)	5	13.05	32.5	51.95	60
C. Route		IV		SC	

TABLE 5.2. Design matrix for central composite design

Treatment	A	B	C
1	-1	-1	-1
2	1	-1	-1
3	-1	1	-1
4	1	1	-1
5	0	0	-1
6	0	1.414	-1
7	0	-1.414	-1
8	1.414	0	-1
9	-1.414	0	-1
10	-1	-1	1
11	1	-1	1
12	-1	1	1
13	1	1	1
14	0	0	1
15	0	1.414	1
16	0	-1.414	1
17	1.414	0	1
18	-1.414	0	1

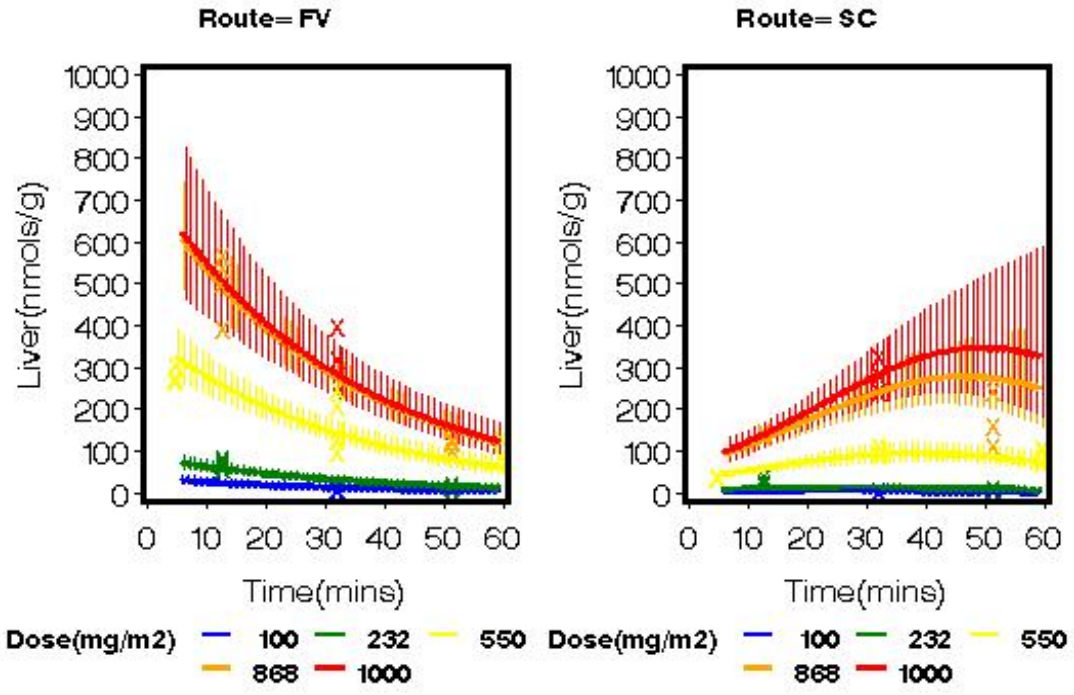

Fig. 5.1. Concentration-time profile of WR1065 in liver of tumor-bearing rats by doses

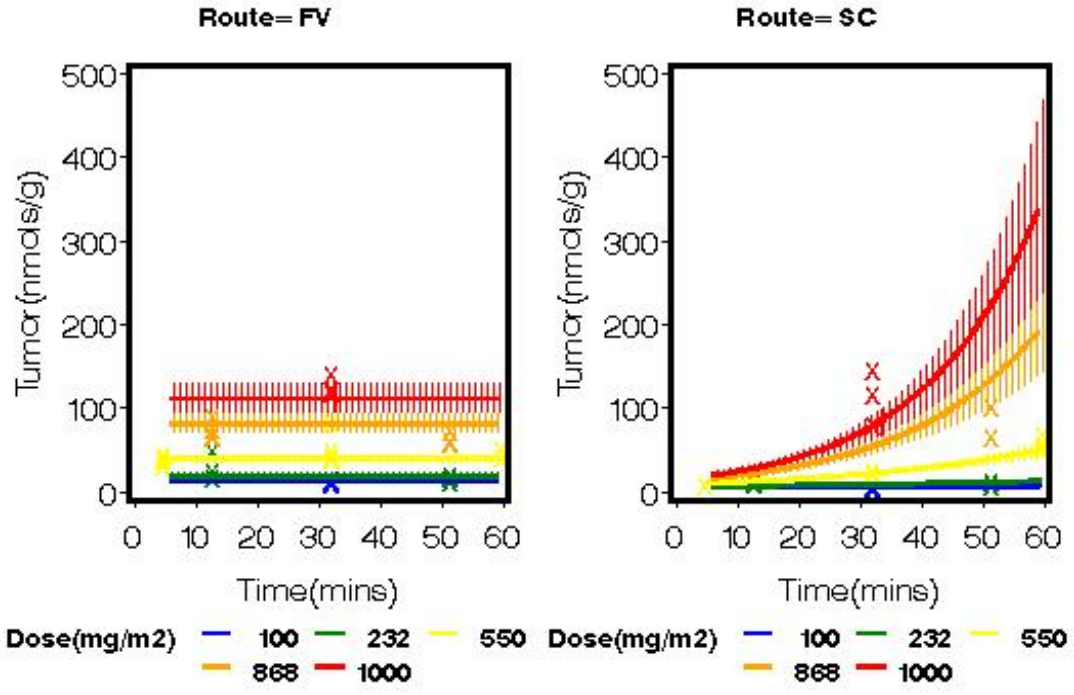

Fig. 5.2. Concentration-time profile of WR1065 in tumor of tumor-bearing rats by doses

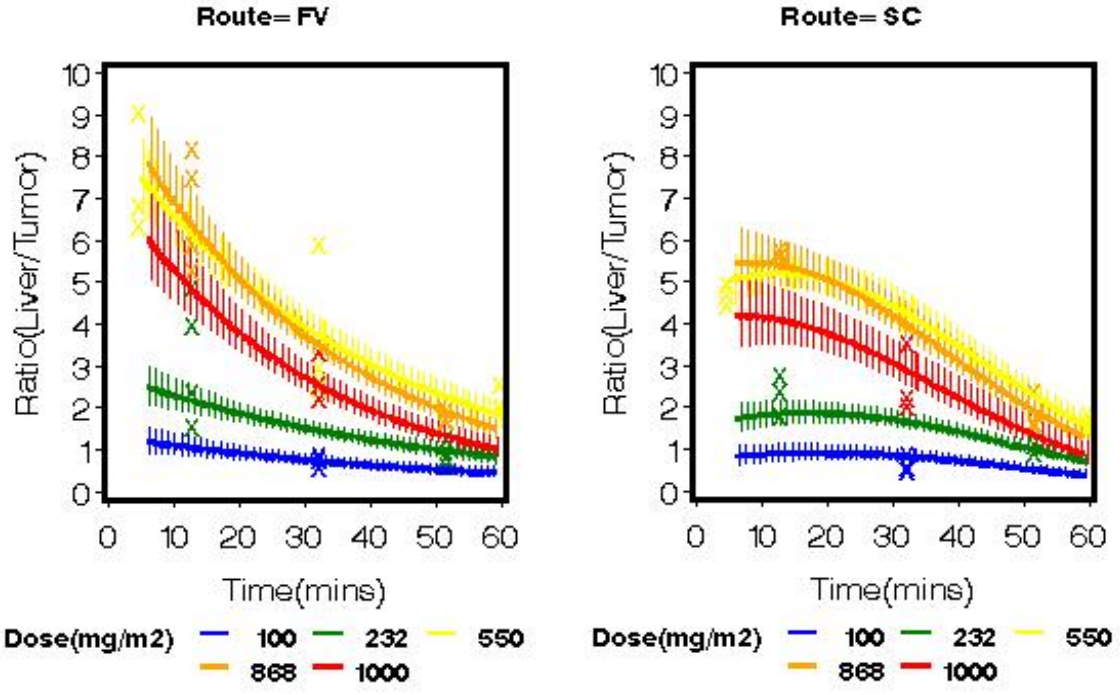

Fig. 5.3. Ratio-time profile of WR1065 in liver to tumor by doses

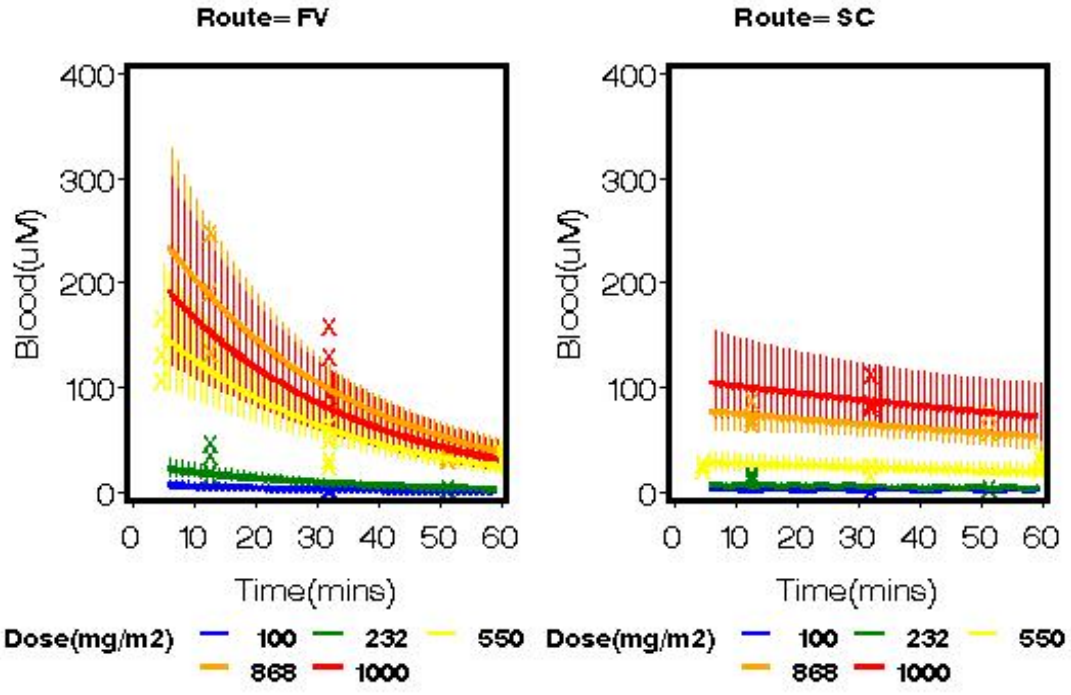

Fig. 5.4. Concentration-time profile of WR1065 in blood of tumor-bearing rats by doses

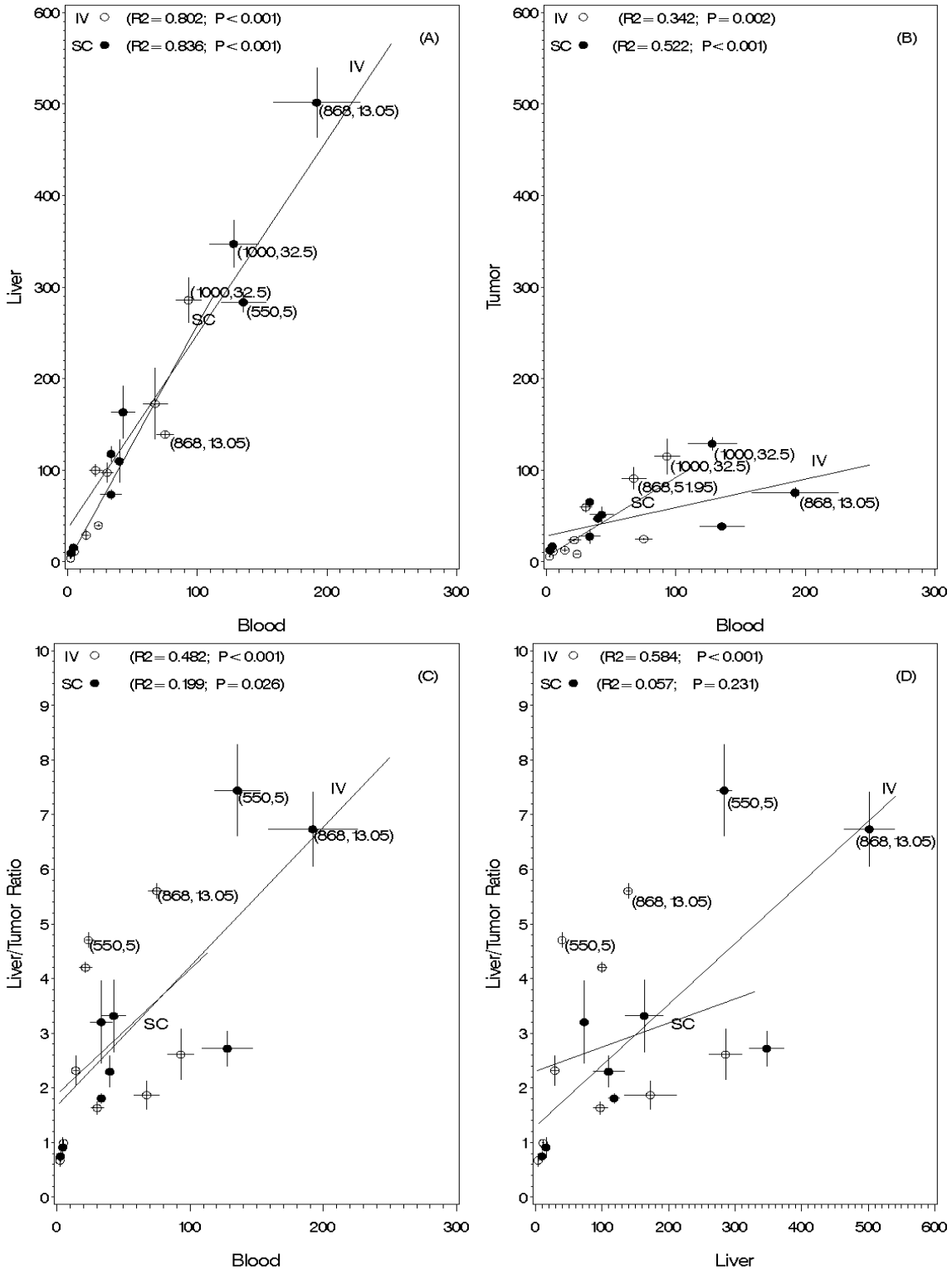

Fig. 5.5. Scatter plot of concentration of WR-1065 in (A) liver vs blood; (B) tumor vs blood; (C) liver-to-tumor ratio vs blood; (D) liver-to-tumor ratio vs liver, the number in parenthesis represent the dose and time on each point, the vertical and horizontal line on each point (mean value) represent the SEM of dependent and independent variables, respectively, regression lines are based on the predicted value of observation

CHAPTER 6

PHARMACOKINETICS OF AMIFOSTINE AND ITS METABOLITE WR-1065 IN PATIENTS WITH DIFFUSE INTRAHEPATIC CANCER

ABSTRACT

To investigate the pharmacokinetics of amifostine and its active metabolite WR1065 in liver cancer patients undergoing hepatic radiation, five patients received 340 mg/m^2 of amifostine by intravenous bolus injection, 15 min prior to delivery of fractional radiation. Serial blood samples were collected predose, at 1, 3, 5, 15, 30, 45 and 60 min, and at 2, 3, 4, 5 and 6 hr after dosing in patients on the first day of radiotherapy. High-performance liquid chromatography with electrochemical detection was used for the analysis of amifostine and WR1065 in plasma and blood samples, respectively, from this clinical study. The pharmacokinetics of amifostine and WR-1065 were analyzed simultaneously using the nonlinear mixed effect model NONMEM. One-compartment and two-compartment models were compared and the best model was selected based on the overall goodness-of-fit, structural model and residual model. The clearance of amifostine was 66.0 mL/min/kg, the volume of distribution was 0.31 L/kg and the half-life was 2.0 min. The clearance of WR1065 was 91.0 mL/min/kg, the central and peripheral volumes of distribution were 0.80 L/kg and 1.4 L/kg, respectively, and the terminal half-life was 75.6 min. The reliability of parameter estimation was acceptable and the interindividual variability was low. Amifostine has a short half-life, small volume of distribution and

large clearance indicating a rapid conversion to WR1065. The active metabolite WR-1065 has a longer half-life than the parent drug, and a larger volume of distribution, indicating extensive binding to tissues in the body. The large clearance of WR1065 suggests its rapid conversion to disulfide metabolites.

INTRODUCTION

Amifostine [Ethyol, WR2721] is an experimental drug that provides significant radioprotection to many normal tissues but provides little or no protection to many experimental tumors.[1-5] This selectivity is thought to be based on the preferential formation and uptake of the active metabolite WR-1065 in normal tissues, as the result of higher amount and activity of alkaline phosphatase, the enzyme which converts amifostine to the active metabolite WR-1065 and a higher pH condition compared to tumor tissues.[6-9] Amifostine has been shown in randomized trials to protect the kidney from cisplatin nephrotoxicity and the parotid gland from radiation due to the greater conversion of the drug to the active metabolite WR-1065 in the normal tissue than in the tumor. The liver appears to be a particularly promising organ for a radioprotective strategy using amifostine because the dose of radiation that can be delivered to patients with intrahepatic cancer is limited by normal tissue toxicity referred to as radiation-induced liver disease (RILD).[10] Based on described situation, even a modest increase in the dose of radiation that can be tolerated by the whole liver could benefit tens of thousands of patients a year. We hypothesize that the outcome of treatment can be improved further by the application of a radiation protector and we feel that the most promising radioprotector for the liver, based on both laboratory and clinical evidence, is the thiophosphate ester prodrug amifostine. To optimize the use of amifostine as a radiation protector of normal liver, we conducted a phase I trial of dose escalating radiation therapy with systemic amifostine for patients with focal and/or diffuse intrahepatic cancer. Our preclinical data demonstrate that, in fact, systemic administration

of amifostine produces more WR-1065 in the normal liver than in intrahepatic tumor, and this leads to radioprotection of the liver. For a better understanding of the mechanism of action and the metabolism of amifostine, pharmacokinetic studies of amifostine itself as well as its main metabolite WR-1065 may be of great importance. In this study, in order to obtain pharmacokinetic data for this dose, route, and schedule of amifostine and its metabolite in patients undergoing hepatic radiation, patients will receive 340 mg/m^2 prior to each fraction of radiation. The solution of drug will be injected intravenously, 15 minutes prior to delivery of radiation. The pharmacokinetics of systemically-injected amifostine will be determined in patients on the first day of radiotherapy. Serial blood samples will be obtained at predose, 1, 3, 5, 15, 30, 45 and 60 min, and at 2, 3, 4, 5 and 6 hr after dosing in patients. We expect the studies will provide the important information on the expected drug levels, exposure (AUC) and disposition (clearance, volume of distribution, half-life) of amifostine and WR-1065 after systemic delivery of drug. We anticipate that systemic administration of amifostine will result in enhanced liver protection following radiotherapy, with systemic drug concentration shown in patients to be safe.

Methods

6.1 Patients and study design

A total of 5 patients (86.1 ± 24.3 kg) with intrahepatic cancer entered a phase I trial of dose escalating radiation therapy with systemic administration of amifostine. All of these patients have adequate hepatic function, defined by a normal prothrombin time (PT) which measures the extrinsic pathway of coagulation and partial thromboplastin time (PTT) which measures the intrinsic pathway of coagulation or correctable with Vitamin K, 0.8 < INR < 1.2. Characteristics of patients in this study are shown in Table 6.1. Patients received 340mg/m^2 amifostine by IV bolus injection in one arm, 15 minutes prior to delivery of fractional radiation. The patient's weight and height was determined at baseline and the patient body surface area was calculated using the method of Dubois method and the appropriate dose of amifostine will be calculated. The radiation therapy was delivered in 2 Gy fractions once daily five days a week. The pharmacokinetics of systemically-administered amifostine was determined in patients on the first day of radiotherapy. Serial blood samples were collected from a peripheral vein in another arm at 0 (predose), 1, 3, 5, 15, 30, 45 and 60min, and at 2, 3, 4, 5, and 6hr after dosing.

6.2 Analytical methods[11-23]

A high-performance liquid chromatography (HPLC) method with electrochemical detection was used for the analysis of amifostine and its active metabolite WR1065 in this clinical study. For the analysis of amifostine[23], whole-blood samples were centrifuged at 3400g and 0°C for 5min, and the plasma was separated and stored at -70°C for subsequent analysis. On the day of analysis, the plasma samples were thawed, WR-80855 was added as an internal standard, an aliquot of 10% (w/v) trichloroacetic acid was

then added to an aliquot of the sample in the ratio of 2 to 5 (v/v) to precipitate the plasma proteins. Samples were mixed together thoroughly and centrifuged at 40,000g for 3mins at 0°C. A 20µl aliquot of supernatant was injected into the HPLC. For the analysis of WR1065[24], the whole-blood samples were placed into tubes, containing ice-cold 1.0 M perchloric acid and 2.7mM (1g/L) EDTA in a ratio of 1:1 (v/v), immediately after sampling. The mixture was then vortexed vigorously and centrifuged at 13,000g for 8min at 4°C. The supernatant was stored at -70°C for subsequent analysis. On the day of analysis (less than 24 hrs), the samples were thawed, and a 20µl aliquot was injected into the HPLC. Under the described method above, the limit of quantification of amifostine was 0.5µM. The amifostine to internal standard peak height ratios were linear over the amifostine concentration range of 0.5 to 50 µM (R^2 = 0.999). The within- and between-day accuracy of the assay varied from 5.8% to 7.4%, whereas the precision varied from 6.9% to 3.3%. The limit of quantification of WR1065 was 0.05 µM. The WR1065 peak heights were linear over the WR1065 concentration range of 0.05 to 10 µM (R^2 = 0.9991). The interday variability (precision) of WR-1065 was less than 10% and the accuracy (bias) was less than 2% by measuring samples spiked with known concentrations of WR1065 at 0.1, 0.5, 2.4, 10 µM. All analysis were performed on a Waters (Milford, Massachusetts) 515 isocratic HPLC pump. Amifostine and the internal standard WR-80855 were detected by a BAS (West Lafayette, Indiana) LC-4C amperometric detector equipped with a thin film mercury-gold amalgam working electrode. The Hg/Au electrode potential was set at +0.15V with respect to the Ag/AgCl reference electrode and the range of the detector was set at 50nAFS. The WR1065 was detected by an ESA Coulochem III coulometric detector (Chelmsford, Massachusetts)

equipped with two porous graphite electrode in series which are set at +600mv (E_2) and +200mv(E_1) respectively vs α-hydrogen/palladium reference electrode. The detector's range is set at 5μAFS. The analytical column, 4.6×250mm, 5μm particle size, C_{18} Symmetry® Waters (Milford, Massachusetts), was operated at room temperature. The amifostine chromatography protocol consists of a mobile phase containing 0.1M chloroacetic acid sodium salt and 1.5mM sodium octyl sulfate, pH 3.0 at a flow rate of 1ml/min. The WR-1065 chromatography protocol employed a mobile phase containing 0.1M chloroacetic acid sodium salt, 4mM sodium octyl sulfate, pH 3.0, and 40% (v/v) methanol running at 1ml/min. Peak indentification was confirmed by comparing retention times in samples with authentic standards.

6.3 Pharmacokinetic and covariate analysis

PK parameters of each patient were determined for amifostine and WR1065 by noncompartmental analysis with WinNonlin 5.0 (Pharsight, Mountain View, California). These parameters include the area under the concentration-time curve (AUC), maximal concentration (C_{max}), time to maximal concentration (t_{max}), volume of distribution (V_d), half-life ($t_{1/2}$), and clearance (CL). In addition to that, the pharmacokinetics of amifostine and WR-1065 were also evaluated simultaneously for 5 liver cancer patients using NONMEM VI 1.0 (GloboMax LLC, Hanover, MD) by use of the first-order conditional estimation with η-ε interaction. S-plus 7.0 (Insightful software, Seattle, WA) was used to visualize the data and for the purpose of model diagnosis. Covariates were plotted independently against the interindividual variability η_i and the method of locally weighted regression was used to visualize potential relations. The following covariates

were tested: body weight, age, gender and prothrombin time (PT). A significant covariate that most reduces the objective function will be left in the model.

6.4 Pharmacokinetic compartmental model

Amifostine and its active metabolite WR-1065 concentration (μM) vs time (min) data were fitted simultaneously. The pharmacokinetic model used is schematically depicted in Figure 6.1. The amifostine data were described by a one-compartment model with first-order elimination and IV bolus input, parameterized in terms of volume of distribution (V_1) and clearance to WR-1065 (CL_1). The formation of WR-1065 was described by a two-compartment model with the parameters of volume of the central compartment (V_2), volume of the peripheral volume (V_3), intercompartmental clearance (Q) and clearance of WR-1065 (CL_2). Interindividual variability of the pharmacokinetic parameters was described by a exponential error model: $\theta_i = \theta_{TV} \bullet e^{\eta i}$ for both amifostine and WR-1065; where θ_i is the individual value of the parameter of the ith subject, θ_{TV} is the typical value of the population estimate of θ_i, η_i is the difference between them and is assumed to be a random variable with zero mean and variance ω^2. The intraindividual variability was estimated by log-normal residual error model for both parent drug amifostine and metabolite. This means the model was fitted to log-transformed data and additive error term ε_i is a random variable with mean zero and variance σ^2.

6.5 Validation

The final model was validated by inspection of goodness-of-fit plots of observed versus individually predicted, observed versus population predicted, weighted residuals versus population predictions, and weighted residuals versus time. Also the internal validity of the pharmacokinetic model was assessed by the nonparametric bootstrap method.

Parameters obtained with the bootstrap replicates were compared with the estimates obtained from the original data set.

Results

Amifostine

The plasma concentration-time curves of amifostine of 5 patients are shown in Figure 6.2. The pharmacokinetic parameters of amifostine after an IV bolus dose from noncompartmental model with WinNonLin are summarized in Table 6.2. Following IV dose, the plasma concentration of amifostine decreased very rapidly, indicating that amifostine was rapidly converted into WR-1065. The mean values for half-life (3.4 ± 0.8 min) and clearance (52.5 ± 9.9 mL/min/kg) indicate that amifostine is quickly cleared from the plasma. The mean value of volume of distribution at steady-state (V_{ss}) of 8.4 L probably indicates that amifostine is primarily confined to the extracellular fluid. This is not unexpected given the very polar nature of amifostine. Population pharmacokinetic parameters from compartmental analysis are comparable to the results obtained from noncompartmental modeling. Based on the data collected and preliminary concentration vs time plot, we found the structural model of one-compartment with first-order elimination was the best fit for the data of amifostine. Clearance and volume of distribution of amifostine are 66.2 ± 3.89 ml/min/kg and 0.31 ± 0.04 L/kg respectively. Elimination half-life of amifostine is around 2 min. Inter-subject variability of clearance and volume of distribution of amifostine is low after including the covariate weight into the parameter model. Literaturely, amifostine has a small volume of distribution 3.5 - 8.7 L, half-life $t_{1/2} \leq$ 15mins, clearance is in the range of 1.5 to 4.3 L/min, the value of AUC is between 1187 and 3852 μmol/min/L from human pharmacokinetic studies [25].

WR-1065

The plasma concentration-time curves of WR-1065 of 5 patients are shown in Figure 6.3. The pharmacokinetic parameters of WR-1065 after an IV bolus dose of amifostine of these five patients from noncompartmental modeling are summarized in Table 6.3. In our analysis of WR-1065 pharmacokinetics in human, we assumed that the dose of WR-1065 is equal to that of amifostine which is 340mg/m^2 based on the fact that all of amifostine is converted by metabolism to WR-1065. The time to reach maximal concentration for WR-1065 is about 3 mins, confirms that amifostine is converted to WR-1065 very quickly. The maximal concentration of WR-1065 is lower than that of amifostine because the active metabolite has a larger volume of distribution. The clearance (81.7 ± 29.4 mL/min/kg) of WR-1065 is greater than that of amifostine. The elimination half-life is around 1.5hr. Amifostine does not bind to plasma proteins; however, at least 50% of WR-1065 is bound to proteins in plasma in the mouse [26]. WR-1065 can also rapidly form disulfides through oxidation. The large volume of distribution and the relatively long half-life indicates that WR-1065 is extensively bound in tissues. Two-compartment with first order elimination and absorption model was used for WR-1065 when we did population analysis compartmentally. Population estimates of clearance and volume of distribution of WR-1065 are larger than those of amifostine, indicating WR-1065 can form disulfide quickly and bound in tissues extensively. The half-life of WR-1065(0.693/β) is much longer than that of amifostine. No significant covariate was found to be responsible for the inter-subject variability of the PK parameters of WR-1065 and inter-subject variability of the parameters was low. The only reported WR-1065 results from human study are T_{max} between 1 and 4mins and C_{max} between 7.2 and 22μM [25].

Figure 6.4 and 6.5 show the diagnostic plots for amifostine and WR-1065 pharmacokinetic model. The relationship between predicted and observed value appears a straight line and we didn't observe significant trend on the plots of residuals vs predicted value for error model. The pharmacokinetic parameter values estimated by NONMEM and the method of bootstrapping are shown in Table 6.4. The fits of 100 bootstap replicates of the data set demonstrated the stability of the model.

Discussion

The pharmacokinetic study and a population pharmacokinetic model of amifostine and its metabolite WR-1065 are described. Furthermore, application of the population approach enables the characterization of interindividual variability as well as the source of this variability on the basis of covariate analysis. Because we have concentration data of both amifostine and WR-1065 and total 5 patients entered this study, we chose to estimate population PK parameters and simultaneously model amifostine and WR-1065 data. The selection of a pharmacokinetic model that fits the data best for each patient was based on the assessment of goodness-of-fit. Different weighting schemes ($w = 1, 1/y, 1/y^2$) were also applied, but no improvement in fit was observed. Goodness of fit was evaluated by the relative standard error of each parameter estimated (%CV), coefficient of determination, and a plot of residuals. Based on the above limitations and individual variability in clinical study, we choose to fit amifostine data with noncompartmental model. For WR-1065, data were also fitted by noncompartmental model. We used noncompartmental method to obtain some PK parameters of amifostine and WR-1065 because sometimes it is difficult to use one compartment model to fit all patients' data,

and PK parameters from noncompartmental model can serve as good initial estimates for late compartmental population analysis. The results indicated PK parameters from these two different models are very comparable. As to the choice of estimation method in population analysis, first-order (FO) method is recommended only when there are few observations per individual (e.g., 2-3). Because first-order conditional estimation (FOCE) and first-order conditional estimation with interaction (FOCEI) can be very sensitive to starting values and we have rich data (11 points) for each individual, we considered FOCEI method as our final estimate method for population analysis since FOCEI is appropriate whenever there are several observations per individual (> 5 points) and when the intraindividual error model depends on the individual mean, like proportional error or slope-intercept error model which are very common in the modeling of pharmacokinetic data. Proportional error and exponential error models are popular in dealing with intraindividual error, and they give the same results in estimation of parameters with NONMEM, however, the lognormal error model which we used in this study is better than above two because the geometric mean of an individual's response is estimated with lognormal error model and arithmetic mean of the individual's response is estimated with exponential error model, the lognormal error model is appropriate when the distribution of residuals is skewed and residual variability in the response is more than 30%. It is difficult to characterize the inter-subject variability (η) accurately in this study because we have a limited patients pool. A simultaneous fit is an excellent method for evaluating the overall parent and metabolite model because a priori mechanistic link between parent and metabolite is so strong in this study. It should be mentioned that non-linear regression programs (NONMEM) often give parameter estimates for unidentifiable

models and indicated that all was well therefore care must be taken to ensure all parameters are identifiable. When we fit simultaneously parent drug and metabolite concentrations it is not possible to estimate the volume of distribution of the metabolite and fraction of parent drug converted to metabolite separately. Without additional data we can either consider all drug is converted to metabolite or metabolite has same volume of distribution as parent drug. Based on the metabolic profile of amifostine, we think it is reasonable to assume that all amifostine is converted to metabolite (K_{10} = 0 in Figure 6.1), that is the dose of WR-1065 is same as that of amifostine, which was confirmed by preliminary NONMEM run. The experimental results have shown amifostine is cleared from the plasma and converted to WR1065 very quickly. WR1065 is extensively bound in tissue and has a very large V_d. The large clearance of WR1065 indicates that it can be oxidized to disulfides rapidly. That is also the reason why we need to analyze WR1065 samples immediately after collection. Because amifostine is more stable in plasma, we can process the samples in 1~2 days as long as the samples are stored under -70°C. In Summary, amifostine has a very short half-life, small volume of distribution and large clearance indicating that amifostine converted to WR1065 quickly; WR1065 has a longer half-life than amifostine, very large volume of distribution and large clearance indicating it converted quickly to symmetrical and mixed disulfides.

Table 6.1 Patient characteristics

Patient	Diagnosis	Dose (μmol)	Dose (mg/m^2)	Gender	Age (yrs)	Body Weight (kg)	Height (cm)	Body Surface Area (m^2)
LT	primary liver cancer	3371	340	F	44	110	163	2.1
CL	metastatic liver cancer from breast cancer	2544	340	F	48	55	165	1.6
JE	primary liver cancer	3611	340	M	54	110	178	2.3
DH	metastatic unknown primary	3060	340	F	53	85	165	1.9
RH	metastatic unknown primary	2961	340	M	69	70	178	1.9
Mean		3110			54	86	170	2.0
SD		407			10	24	8	0.3

Table 6.2. Noncompartmental analysis of amifostine

Patient	AUC min•μmol/L	CL (mL/min/kg)	V_z (L/kg)	MRT (min)	$T_{1/2}$ (min)
LT	672	45.5	0.25	4.6	3.9
CL	978	47.0	0.15	1.7	2.2
JE	485	67.7	0.43	4.5	4.4
DH	799	45.0	0.22	3.1	3.4
RH	739	57.3	0.27	2.8	3.3
Mean	735	52.5	0.26	3.3	3.4
SD	180	9.9	0.10	1.2	0.8

Table 6.3. Noncompartmental analysis of WR-1065

Patient	T_{max} (min)	C_{max} (μmol/L)	AUC (min●μmol/L)	CL (mL/min/kg)	V_z (L/kg)	MRT (min)	$T_{1/2}$ (min)
LT	5.0	28.5	562	54.4	5.3	34.8	68.0
CL	1.0	40.4	635	72.3	8.5	49.9	81.2
JE	3.0	16.2	336	97.5	19.3	58.4	137
DH	3.0	11.7	289	125	19.6	72.6	109
RH	3.0	35.3	710	59.5	7.1	41.8	82.2
Mean	3.0	26.4	506	81.7	12.0	51.5	95.5
SD	1.4	12.2	185	29.4	6.9	14.7	27.6

Table 6.4 Population pharmacokinetics.

Pharmacokinetic parameter	PK Model		Bootstrap	
	Estimate	CV%	Mean	CV%
CL_f (ml/min/kg)	66.2	5.8	65.7	6.7
V_1 (L/kg)	0.31	11.6	0.31	11.4
CL_m (ml/min/kg)	90.8	14.1	91.3	14.9
V_2 (L/kg)	0.80	23.3	0.82	24.3
V_3 (L/kg)	1.4	24.9	1.4	27.8
Q (CL_{23}=CL_{32}; ml/min/kg)	14.1	17.5	14.2	18.7
Interindividual variability				
η CL_f (%)	<1	<1	<1	<1
η V_1 (%)	24.8	59.5	22.1	65.1
η CL_m (%)	7.13	58.2	5.98	73.2
η V_2 (%)	<1	<1	<1	<1
η V_3 (%)	<1	<1	<1	<1
η Q (%)	<1	<1	<1	<1
Residual variability				
ε Amifostine (μM)	0.53	13.5	0.52	13.8
ε WR-1065 (μM)	0.4	5.1	0.37	9.2

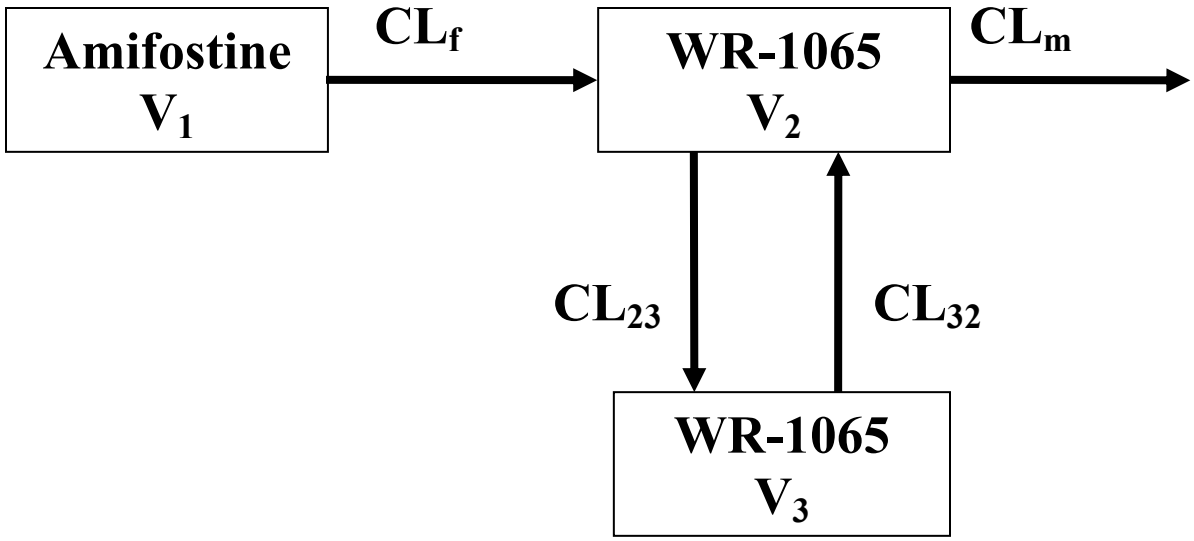

Figure 6.1. Schematic representation of the pharmacokinetic model for amifostine (parent) and its metabolites WR-1065

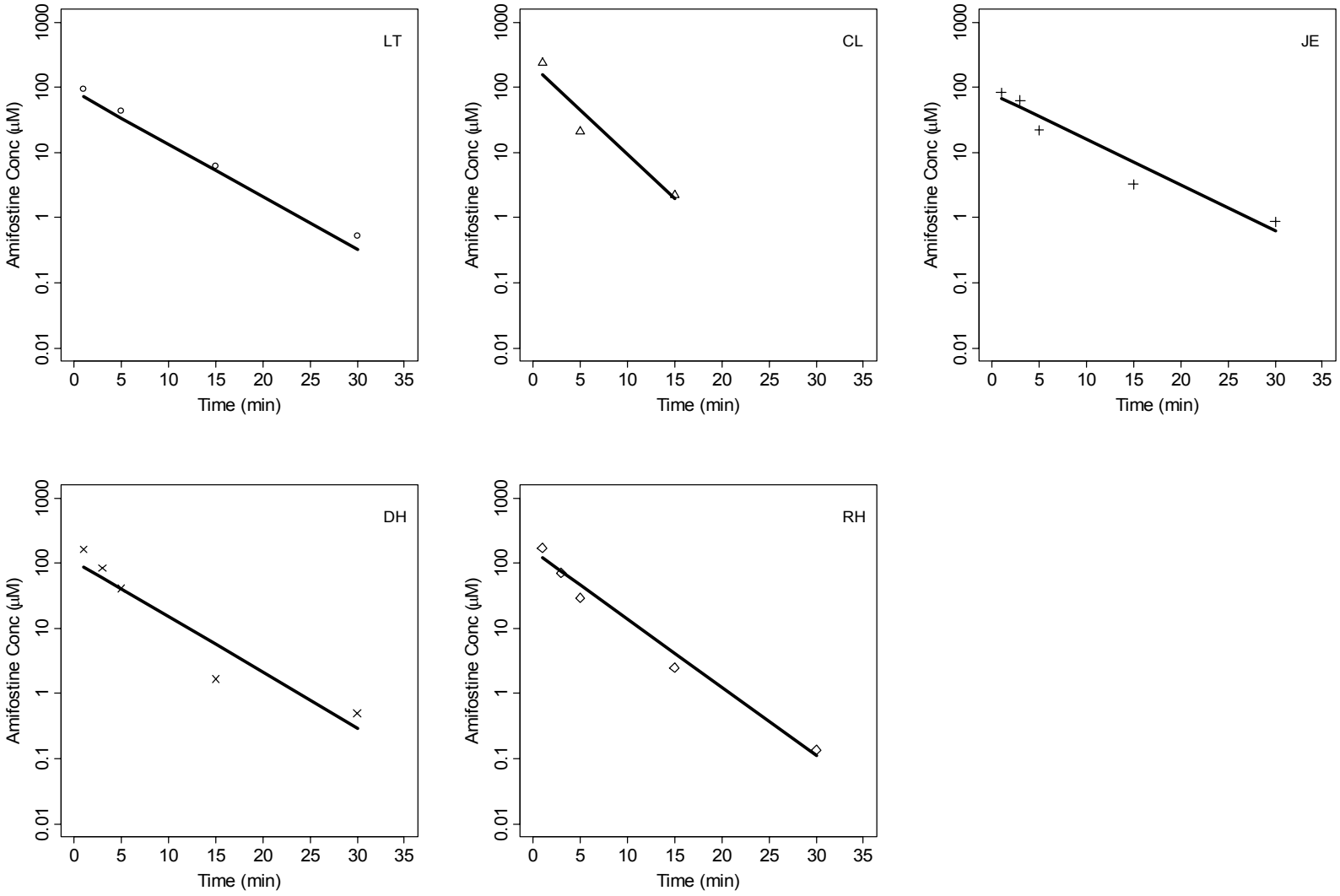

Figure 6.2. Blood concentration versus time profiles of amifostine in five liver cancer patients. Observed data are representated by symbols and the predicted data by solid lines.

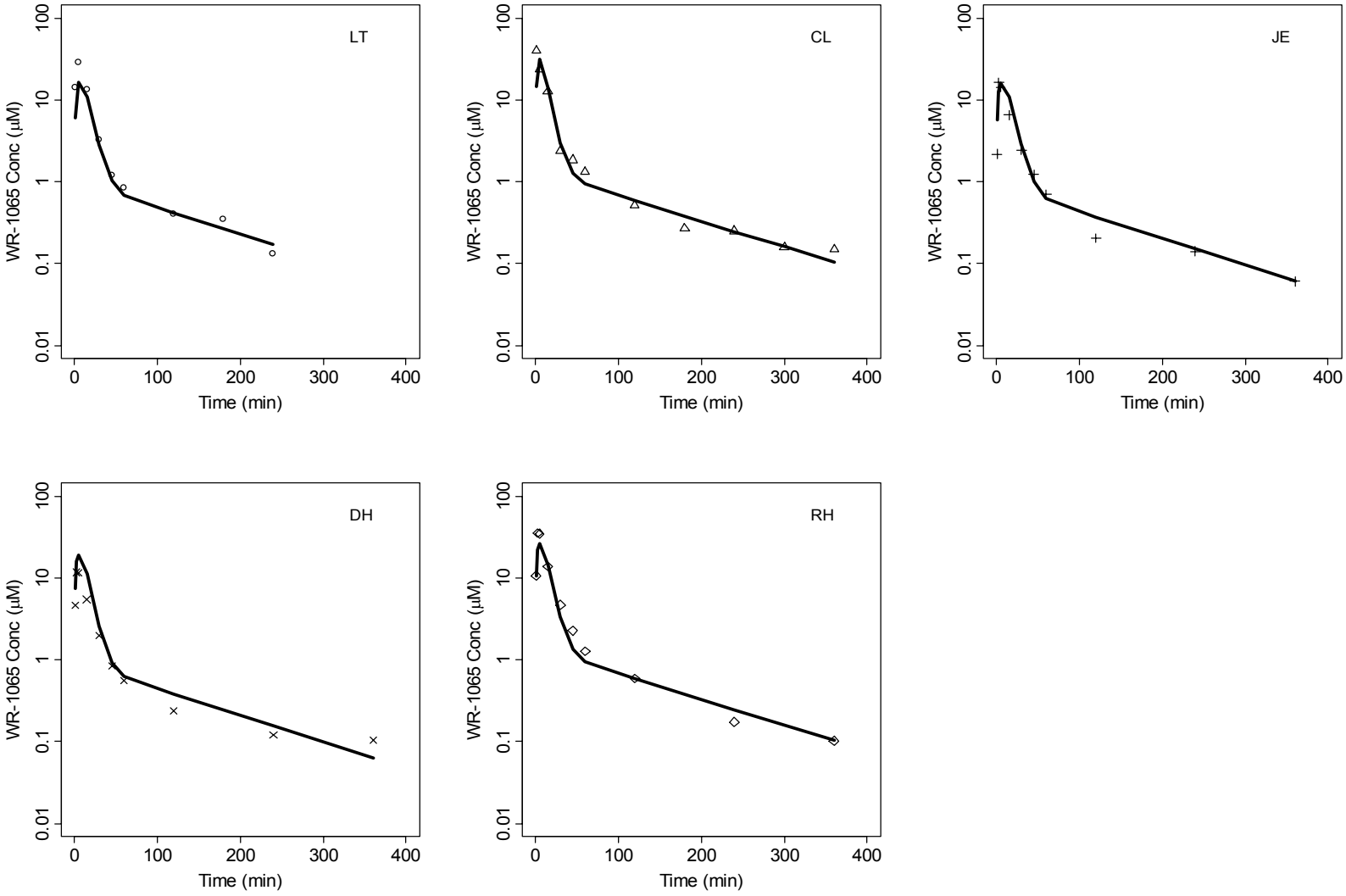

Figure 6.3. Blood concentration versus time profiles of WR-1065 in five liver cancer patients. Observed data are representated by symbols and the predicted data by solid lines.

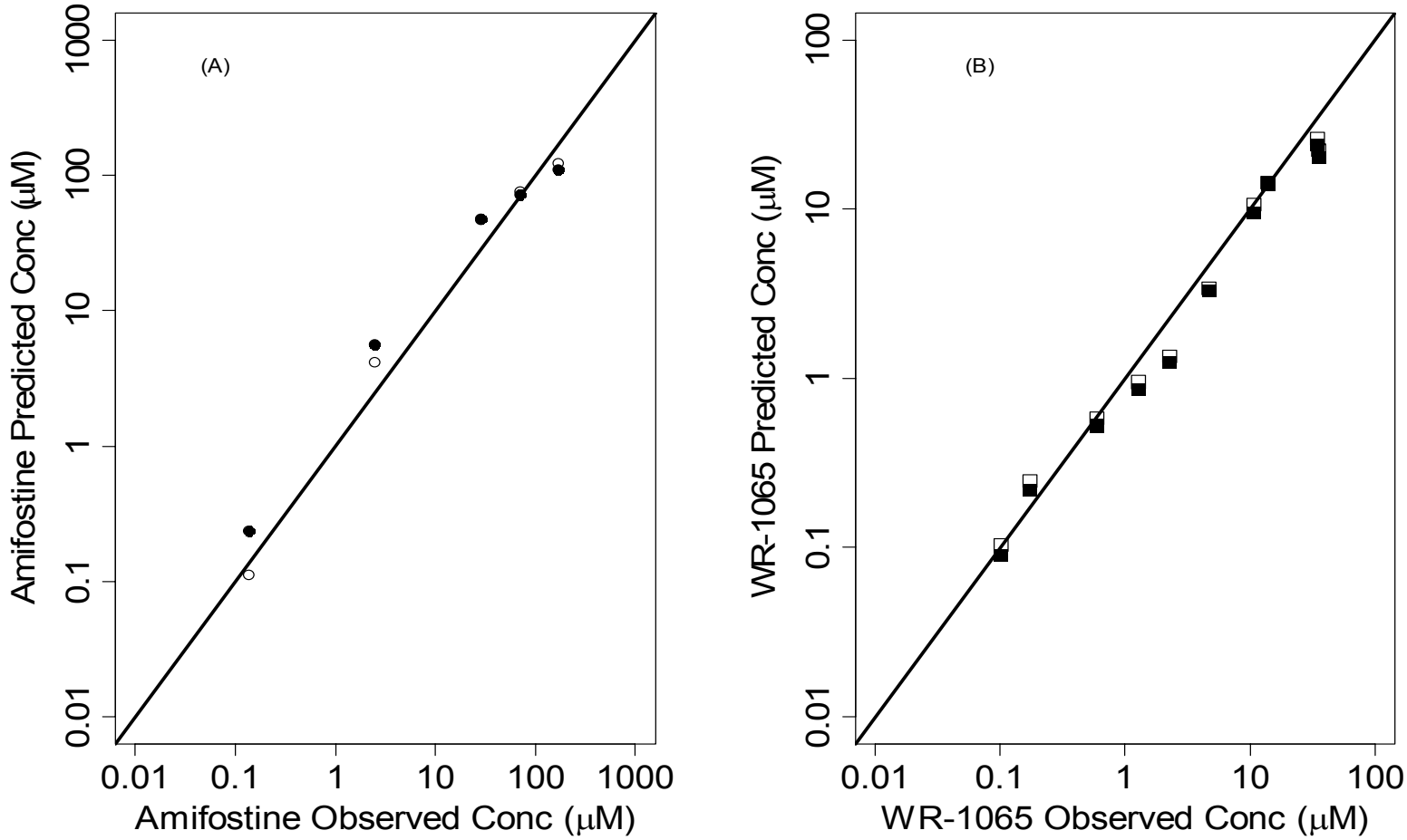

Figure 6.4. Observed versus predicted concentrations of (A) amifostine (circles) and (B) WR-1065 (squares), based on population predicted values (● ■) and individual predicted values (○ □)

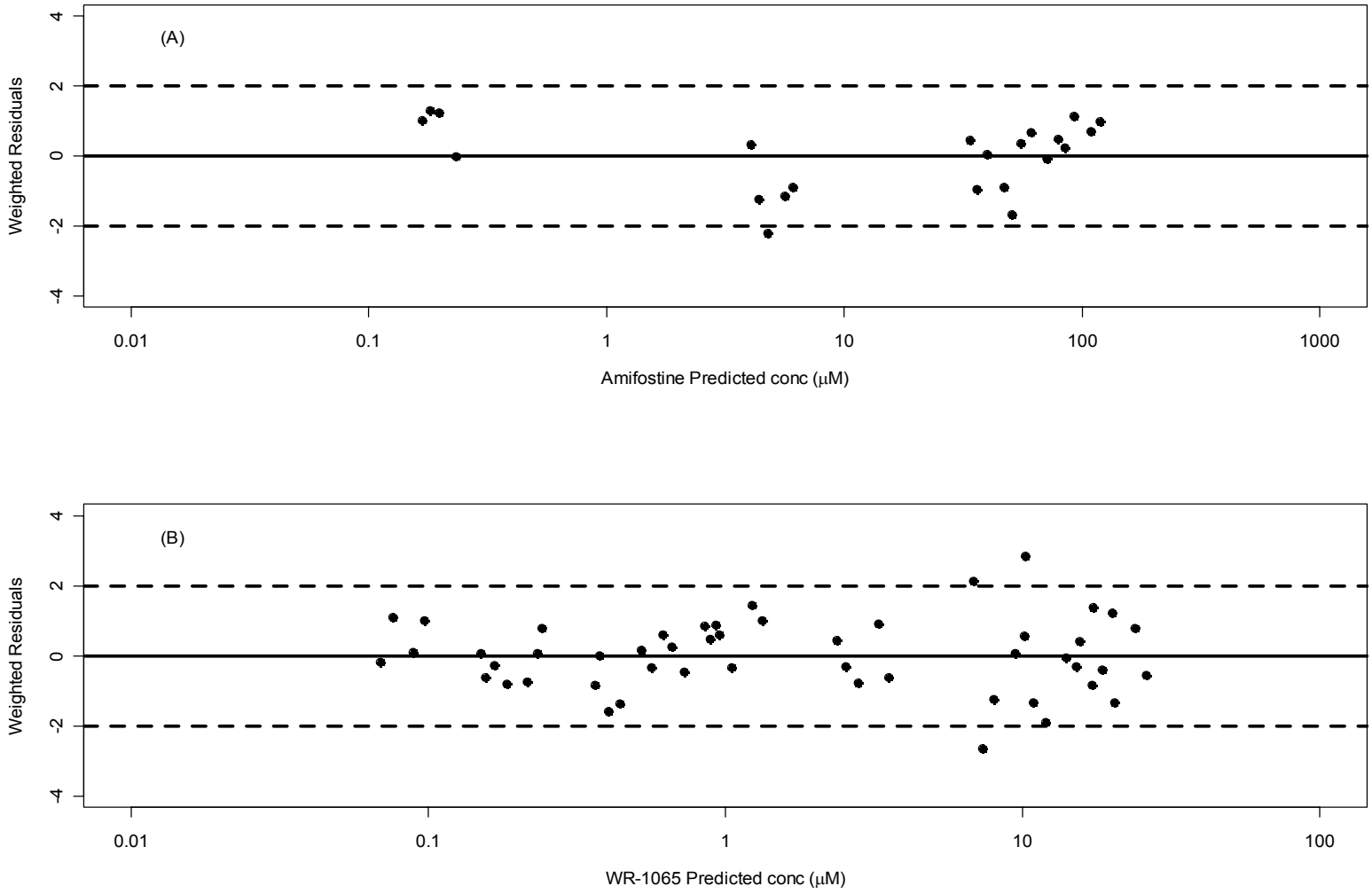

Figure 6.5. Diagnostic plots for amifostine (A) and WR-1065 (B), where the weighted residuals are shown as a function of predicted concentrations

Reference

1. Hensley M, Schuchter LM, Lindley C, Meropol NJ, Cohen GI. American Society of Clinical Oncology: Clinical Practice Guidelines for the use of chemotherapy and radiotherapy protectants. *J Clin Oncol*, 17: 3333-3355, 1999.

2. Tannehill SP and Mehta MP. Amifostine and radiation therapy: past, present, and future. *Semin Oncol*, 23: 69-77, 1996.

3. Yuhas JM, Spellman JM and Culo F. The role of WR-2721 in radiotherapy and/or chemotherapy. *Cancer Clin Trials*, 3: 211-216, 1980.

4. Milas, L., Hunter, N., Reid, B.O., and Thames, J., H.D. Protective effects of S-2-(3-aminopropylamino) ethylphosphorothioic acid against radiation damage of normal tissues and a fibrosarcoma in mice. *Cancer Res*, 42: 18888-1897, 1982.

5. Rasey, J.S., Nelson, N.J., Mahler,P., Anderson, K., Krohn, K.A., and Menard, T. Radioprotection of normal tissues against gamma rays and cyclotron neutrons with WR-2721-LD_{50} studies and ^{35}S-WR-2721 biodistribution. *Radiat Res*, 97: 598-607, 1984.

6. Shaw, L. M., Bonner, H.S., and Brown, D.Q. Metabolic pathways of WR-2721 (ethyol, amifostine) in the BALB/c mouse. *Drug Metab Dispos*, 22: 895-902, 1994.

7. Yuhas, J.M. Active versus passive absorption kinetics as the basis for selective protection of normal tissues by S-2-(3-aminopropylamino) ethylphosphorothioic acid. *Cancer Res*, 40: 1519-1524, 1980.

8. Calabro-Jones, P.M., Aguilera, J.A., Ward, J. F., Smoluk, G.D., and Fahey, R.C. Uptake of WR-2721 derivatives by cell in culture – Identification of the transported form of the drug. *Cancer Res*, 48: 3634-3640, 1988.

9. Rasy, J. S., Grunbaum, A., Krohn, K.A., Menard, T. W., and Spence, A. M. Biodistribution of the radioprotective drug ^{35}S-labeled 3-amino-2-hydroxypropyl phosphorothioate (WR77913). *Radiat Res*, 102: 130-137, 1985.

10. Ryan SV, Carrithers SL, Parkinson SJ, Skurk C, Nuss C, Pooler PM, Owen CS, Lefer AM. Hypotensive mechanisms of amifostine. *J Clin Pharm*, 36: 365-373, 1996.

11. Shaw LM, Bonner HS and Lieberman L. Pharmacokinetic profile of Amifostine. *Semin Oncol*, 23: 18-22, 1996.

12. Symon, Z., Levi, M., Ensminger, W.D., Smith, D.E., and Lawrence, T.S. Selective radioprotection of hepatocytes by systemic and portal vein infusion of amifostine in a rat liver tumor model. *Int J Radiat Oncol Biol Phys*, 50: 473-478, 2001.

13. Shaw, L.M., Bonner, H.S., Turrisi, A., Norfleet, A. L., and Kligerman, M. Measurement of S-2-(3-aminopropylamino) ethanethiol (WR-1065) in blood and tissue. *J Liq Chromatogr*, 9: 845-859, 1986.

14. Burns, J. A., Butler, J. C., Moran, J., and Whitesides, G. M. Selective reduction of disulfides by tris(2-carboxyethyl) phosphine. *J Org Chem*, 56: 2648-2650, 1991.

15. Shaw, L.M., Bonner, H.S., Turrisi, A., Norfleet, A. L., and Glover, D.J. A liquid chromatographic electrochemical assay for S-2-(3-aminopropylamino) ethylphosphorothioate (WR-2721) in human plasma. *J Liq Chromatogr*, 7: 2447-2465, 1984.

16. Levi, M., Knol, J.A., Ensminger, W.D., Deremer, S.J., Dou, C., Lunte, S.M., Bonner, H.S., Shaw, L.M., and Smith, D.E. Regional pharmacokinetics of amifostine in anesthetized dogs: role of the liver, gastrointestinal tract, lungs and kidneys. *Drug Metab Dispos,* 30: 1425-1430, 2002.

17. Snder, R.D. and Grdina, D.J. Further evidence that the radioprotective aminothiol, WR-1065, catalytically inactive mammalian topoisomerase II. Cancer Res, 60: 1186-1188, 2000.

18. Shaw, L.M., Bonner, H.S., Turrisi, A., Norfleet, A.L., and Kligerman, M. Measurement of S-2-(3-aminopropylamino) ethanethiol (WR-1065) in blood and tissue. *J Liq Chromatogr*, 9: 845-859, 1986.

19. Levi, M., DeRemer S.J., et al. Disposition of WR-1065 in the liver of tumor-bearing rats following regional vs systemic administration of amifostine. *Biopharm. Drug Dispos*. 25: 27-35, 2004.

20. Shaw, L.M., Bonner, H.S., Turrisi, A., Norfleet, A.L., and Glover, D.J. A liquid chromatographic electrochemical assay for S-2-(3-aminopropylamino)ethylphosphorothioate (WR-2721) in human plasma. *J Liq Chromatogr*, 7: 2447-2465, 1984.

21. Feng Bai, Kirstein MN, Hanna, SK and Stewart CF. New liquid chromatographic assay with electrochemical detection for the measurement of amifostine and WR-1065, *J Chromatogr*, 772: 257-265, 2002.

22. Shaw LM, Turrisi AT, Glover DJ, et al. Human pharmacokinetics of WR-2721. *Int. J. Radiat. Oncol. Biol. Phys*, 12: 1501-1504, 986.

23. Bonner H.S. and Shaw L.M. Measurement of both protein-bound and total S-2-(3-aminopropylamino)ethanethiol (WR-1065) in blood by high-performance liquid chromatography. *Journal of Chromatography B*, 739: 357-362, 2000.

APPENDICES

APPENDIX A

Data for chapter 4

Table A.1. Concentration of WR-1065 in liver, tumor, blood and ratio of concentration of WR-1065 in liver to tumor in tumor-bearing rats with systemic or regional dosing under central composite design

Dose	Time	Route	Rats	Blood	Liver	Tumor	Ratiolt	Ratiolb	Ratiotb
50	37.5	portal	1	0.154	3.08	4.56	0.68	20.00	29.61
50	37.5	portal	2	0.216	1.73	4.87	0.36	8.01	22.55
50	37.5	portal	3	0.18	1.93	4.81	0.40	10.72	26.72
50	37.5	femoral	1	0.21	1.69	4.11	0.41	8.05	19.57
50	37.5	femoral	2	0.274	1.47	4.54	0.32	5.36	16.57
50	37.5	femoral	3	0.23	1.32	3.74	0.35	5.74	16.26
125	21.5	portal	1	1.89	27.83	9.5	2.93	14.72	5.03
125	21.5	portal	2	2.08	26.2	11	2.38	12.60	5.29
125	21.5	portal	3	1.97	23.5	16.8	1.40	11.93	8.53
125	21.5	femoral	1	2.074	37.5	23.78	1.58	18.08	11.47
125	21.5	femoral	2	1.286	40.43	25.78	1.57	31.44	20.05
125	21.5	femoral	3	1.664	30.98	20.25	1.53	18.62	12.17
125	53.5	portal	1	0.284	5.43	14.08	0.39	19.12	49.58
125	53.5	portal	2	0.28	6.7	16.15	0.41	23.93	57.68
125	53.5	portal	3	0.516	6.95	13.25	0.52	13.47	25.68
125	53.5	femoral	1	0.94	4.89	10.11	0.48	5.20	10.76
125	53.5	femoral	2	0.42	3.5	8.37	0.42	8.33	19.93
125	53.5	femoral	3	0.56	4.52	9.88	0.46	8.07	17.64
275	15	portal	1	28.28	97.75	41.8	2.34	3.46	1.48
275	15	portal	2	60.36	74.73	41.58	1.80	1.24	0.69

275	15	portal	3	41.36	149.9	85.2	1.76	3.62	2.06
275	15	femoral	1	29.56	97.78	46.73	2.09	3.31	1.58
275	15	femoral	2	75.12	138.4	84.25	1.64	1.84	1.12
275	15	femoral	3	45.84	113.1	70.3	1.61	2.47	1.53
275	37.5	portal	1	2.74	36.58	57.71	0.63	13.35	21.06
275	37.5	portal	2	2.81	59.61	37.93	1.57	21.21	13.50
275	37.5	portal	3	2.14	35.05	40.87	0.86	16.38	19.10
275	37.5	femoral	1	1.81	52.3	30.32	1.72	28.90	16.75
275	37.5	femoral	2	1.76	33.5	40.97	0.82	19.03	23.28
275	37.5	femoral	3	3.2	34.58	36.5	0.95	10.81	11.41
275	37.5	femoral	4	2.32	34.29	29.19	1.17	14.78	12.58
275	60	portal	1	3.05	22.87	26.5	0.86	7.50	8.69
275	60	portal	2	2.476	17.84	24.02	0.74	7.21	9.70
275	60	portal	3	2.34	14.5	25.63	0.57	6.20	10.95
275	60	femoral	1	1.438	12.76	26.49	0.48	8.87	18.42
275	60	femoral	2	1.625	13	21.6	0.60	8.00	13.29
275	60	femoral	3	2	11.11	13.84	0.80	5.56	6.92
425	21.5	portal	1	42.88	203.48	64.25	3.17	4.75	1.50
425	21.5	portal	2	51.52	164.45	24.35	6.75	3.19	0.47
425	21.5	portal	3	45.56	192.48	58.45	3.29	4.22	1.28
425	21.5	femoral	1	49.44	299.7	94.38	3.18	6.06	1.91
425	21.5	femoral	2	62.26	370.3	81.45	4.55	5.95	1.31
425	21.5	femoral	3	53.32	323.1	50.95	6.34	6.06	0.96
425	53.5	portal	1	4.52	17.81	29.17	0.61	3.94	6.45
425	53.5	portal	2	4.4	24.95	34.52	0.72	5.67	7.85
425	53.5	portal	3	3.97	21.38	33.85	0.63	5.39	8.53
425	53.5	femoral	1	8	34.59	39.89	0.87	4.32	4.99

425	53.5	femoral	2	3.27	20.68	32.77	0.63	6.32	10.02
425	53.5	femoral	3	5.44	21.56	34.23	0.63	3.96	6.29
500	37.5	portal	1	60.32	116.23	59.03	1.97	1.93	0.98
500	37.5	portal	2	57.5	138.93	64.43	2.16	2.42	1.12
500	37.5	portal	3	71.32	150.85	66.18	2.28	2.12	0.93
500	37.5	femoral	1	72.24	101.5	35.2	2.88	1.41	0.49
500	37.5	femoral	2	64.22	113.1	57.9	1.95	1.76	0.90
500	37.5	femoral	3	81.16	126.95	51.1	2.48	1.56	0.63

APPENDIX B

SAS codes for chapter 4

```
/*************************read and creat data**********************/

PROC IMPORT OUT= WORK.rats1
            DATAFILE= "C:\Documents and Settings\zlu\Desktop\Rats Study\Rats1
study\rats1 data\rats1.xls"
            DBMS=EXCEL2000 REPLACE;
     SHEET="Sheet2$";
     GETNAMES=YES;
RUN;
proc sort data=rats1;
by vein dose time;
run;

options symbolgen;
%let v=femoral;
data rats1;
set rats1;
label dose='dose(mg/m2)'
      time='time(mins)'
            liver='liver(nmols/g)'
            tumor='tumor(nmols/g)'
            ratio='L/T ratio'
            blood='blood(uM)'
            ;
lliver=log(liver);
ltumor=log(tumor);
lratio=log(ratio);
lblood=log(blood);
vdum=(vein="&v");
run;
data rats1coded; set rats1;
time=(time-37.5)/16;
dose=(dose-275)/150;
run;

/************************comparison with full model*****************/
%let y=lratio;
%let model=%str(vdum|dose|time);
```

```
proc transreg data=rats1 details;
model boxcox(&y)=identity(&model);
run;

%macro doit;
proc glm data=rats1;
model &y=&model/solution;
%if &model=%str(vdum|dose|time) %then %do;
contrast  'test for coincidence' vdum 1 -1,
                          dose*vdum 1 -1,
                           time*vdum 1 -1,
                           dose*time*vdum 1 -1;
%end;
%else %do;
contrast  'test for coincidence' vdum 1 -1,
                          dose*vdum 1 -1,
                           time*vdum 1 -1,
                           dose*time*vdum 1 -1,
                           dose*dose*vdum 1 -1,
                            time*time*vdum 1 -1;
%end;
output out=rats1out p=yhat r=resid;
run;quit;
proc gplot data=rats1out;
plot &y*yhat;
plot resid*yhat;
plot resid*dose;
plot resid*time;
run;quit;
proc univariate data=rats1out normal;
var resid;
histogram;
qqplot/normal(mu=est sigma=est);
run;
%mend;
%doit



/**********data are splited**********/
%let a=f;
%let model=%str(dose|time);
data rats1&a; set rats1;
where vein="&v";
run;
proc transreg data=rats1&a details;
```

```
model boxcox(&y)=identity(&model);
run;
proc glm data=rats1&a;
model &y=&model;
output out=rats1&a.out p=yhat r=resid;
run;quit;
proc gplot data=rats1&a.out;
plot &y*yhat;
plot resid*dose;
plot resid*time;
plot resid*yhat;
run;
quit;
proc univariate data=rats1&a.out  normal;
var resid;
histogram;
qqplot/normal(mu=est sigma=est);
run;


/*************combine contour plot with spin surface plot************/


goptions reset=all ftext=swiss htext=6  gunit=pct border;
data grid;
do dose=50to 500 by 45;
do time=15 to 60 by 4.5;
ypred=exp(-0.162+ 0.00585*dose-0.01814*time-0.000065*dose*time);
output;
end;
end;
run;
%let nlevels=8;
%let colors='yellow vibg cyan green lime gold orange red';
proc means data=grid noprint min max;
var dose time ypred;
output out=range min=dmin tmin ymin
max=dmax tmax ymax;
run;
data _null_;
set range;
call symput('dmin',dmin);
call symput('dmax',dmax);
call symput('tmin',tmin);
call symput('tmax',tmax);
call symput('ymin',ymin);
```

```
call symput('ymax',ymax);
call symput('step',(ymax-ymin)/&nlevels);
call symput('floor', int(ymin-4));
call symput('ceil',int(ymax+2));
run;
proc sort data=grid;
by time dose;
run;
data plane1 surf1;
length function color $8;
retain xsys ysys zsys '2';
set grid;
by time;
x=time; y=dose; z=&floor;
if first.time then function='move';
else do;
function='draw'; size=2;
ncol=min(&nlevels,int(1+(ypred-&ymin)/&step));
color=scan(&colors,ncol);
end;
output plane1;
z=ypred; output surf1;
run;
proc sort data=grid;
by dose time;
run;
data plane2 surf2;
length function color $8;
retain xsys ysys zsys '2';
set grid;
by dose;
x=time; y=dose; z=&floor;
if first.dose then function='move';
else do;
function='draw'; size=2;
ncol=min(&nlevels,int(1+(ypred-&ymin)/&step));
color=scan(&colors,ncol);
end;
output plane2;
z=ypred; output surf2;
run;
data legend;
length function color $8;
retain xsys ysys zsys '2';
do legend=&ymin to (&ymax-&step) by &step;
x=&tmin; y=&dmax; z=legend;
```

```
function='poly'; style='solid';
ncol=min(&nlevels,int(1+(legend-&ymin)/&step));
color=scan(&colors,ncol);output;
z=legend+&step;
function='polycont'; output;
x=&tmin+1; output;
z=legend; output;
end;
run;
proc means data=rats1&a noprint mean nway;
class dose time;
var liver tumor ratio blood;
output out=meanout mean=lmean tmean rmean bmean;
run;

data back;
merge rats1&a meanout;
by dose time;
retain color 'purple' xsys ysys zsys '2';
function='label'; x=time; y=dose; z=ratio; size=1; text='X';  output;
function='move'; x=time; y=dose; z=rmean; size=1; output;
function='draw'; x=time; y=dose; z=&floor; size=2; output;
run;

data annoall;
set  surf1 surf2 plane1 plane2 legend back;
run;
data plotdata;
dose=&dmin; time=&tmin; ypred=&floor; output;
dose=&dmax; time=&tmax; output;
run;

%macro animate;
%local angle;
%do angle=0 %to 396 %by 36;
%if &angle=0 %then %do;
goptions reset=all gsfname=out dev=gifanim iteration=2 gsfmode=replace delay=100
cback=black  transparency disposal=background
       ftext=swissb htext=1.5;
title height=2 color=white  'by femoral vein';
filename out 'C:\Documents and Settings\zlu\Desktop\Rats Study\Rats1 study\rats1
results\ratiospinf.gif';
%end;
%else %do; goptions gsfmode=append; %end;
%if &angle=396 %then %do; goptions gepilog='3B'x;
%end;
```

```
proc g3d data=plotdata;
scatter dose*time=ypred/rotate=&angle shape='point'
xticknum=4 yticknum=4 zticknum=6 zmin=&floor zmax=9.0 ctext=white
annotate=annoall;
label dose='Dose(mg/m2)'
      time='Time(mins)'
      ypred='Ratio';
run;
%end;
%mend;
%animate


/*****************2-D plot by time with predicted values with labeled experimental
points*************/

data grid2t;
do time=15,21.5,37.5,53.5,60;
do dose=50 to 500 by 10;
ypred=exp(0.5543+ 0.00365*dose-0.031*time-0.000027*dose*time);
output;
end;
end;
run;
proc sort data=rats1&a;
by time dose;
run;
data anno2t;
length color1-color5 $8;
set rats1&a;
by time;
retain i 0 color1 'blue' color2 'green' color3 'yellow' color4 'orange' color5 'red' xsys ysys
'2';
array colors{*} color1-color5;
if first.time then i+1;
function='symbol'; x=dose; y=ratio; text='X'; color=colors{i}; style='swiss'; size=1.5;
output;
run;
ods listing close;
ods html file='C:\Documents and Settings\zheng lu\Desktop\Rats Study\Rats1 study\rats1
results\test.html'
      gpath='C:\Documents and Settings\zheng lu\Desktop\Rats Study\Rats1 study\rats1
results\';
```

```
goptions reset=all cback=black transparency disposal=background ctext=white
ftext=swissb htext=1.5;
goptions device=win target=winprtc;
title height=2 color=white  ' portal vein';

axis1 color=white
      width=20
                label=(font=swiss height=2)
      value=(font=swiss height=2)
      major=(width=2);
axis2 color=white
      width=20
                label=(a=90 font=swiss height=2)
      value=(font=swiss height=2)
      major=(width=3 height=1)
      order=0 to 8 by 1;
symbol1 c=blue i=spline v=none w=30;
symbol2 c=green i=spline v=none w=30;
symbol3 c=yellow i=spline v=none w=30;
symbol4 c=orange i=spline v=none w=30;
symbol5 c=red i=spline v=none w=30;
proc gplot data=grid2t;
plot ypred*dose=time/anno=anno2t haxis=axis1 vaxis=axis2;
label dose='Dose(mg/m2)'
      time='Time(mins)'
      ypred='Ratio';
run;quit;
ods html close;
ods listing;

/*****************2-D plot by dose with predicted values with labeled experimental
points*************/

data grid2t;
do time=15 to 60 by 5;
do dose=50, 125, 275, 425, 500;
ypred=exp(0.5543+ 0.00365*dose-0.031*time-0.000027*dose*time);
output;
end;
end;
run;
proc sort data=rats1&a;
by dose time;
run;
data anno2t;
length color1-color5 $8;
```

```
set rats1&a;
by dose;
retain i 0 color1 'blue' color2 'green' color3 'yellow' color4 'orange' color5 'red' xsys ysys
'2';
array colors{*} color1-color5;
if first.dose then i+1;
function='symbol'; x=time; y=ratio; text='X'; color=colors{i}; style='swiss'; size=1.5;
output;
run;
ods listing close;
ods html file='C:\Documents and Settings\zlu\Desktop\Rats Study\Rats1 study\rats1
results\test.html'
      gpath='C:\Documents and Settings\zlu\Desktop\Rats Study\Rats1 study\rats1
results\';

goptions reset=all cback=black transparency disposal=background ctext=white
ftext=swissb htext=1.5;
goptions device=win target=winprtc;
title height=2 color=white  ' portal vein';

axis1 color=white
      width=20
            label=(font=swiss height=2)
      value=(font=swiss height=2)
      major=(width=2);
axis2 color=white
      width=20
            label=(a=90 font=swiss height=2)
      value=(font=swiss height=2)
      major=(width=3 height=1)
      order=0 to 8 by 1;
symbol1 c=blue i=spline v=none w=30;
symbol2 c=green i=spline v=none w=30;
symbol3 c=yellow i=spline v=none w=30;
symbol4 c=orange i=spline v=none w=30;
symbol5 c=red i=spline v=none w=30;
proc gplot data=grid2t;
plot ypred*time=dose/anno=anno2t haxis=axis1 vaxis=axis2;
label dose='Dose(mg/m2)'
      time='Time(mins)'
      ypred='Ratio';
run;quit;
ods html close;
ods listing;
```

APPENDIX C

Data for chapter 5

Table C.1. Concentration of WR-1065 in liver, tumor, blood and ratio of concentration of WR-1065 in liver to tumor in tumor-bearing rats with intravenous or subcutaneous dosing under central composite design

Dose	Time	Route	Liver1	Liver2	Tumor1	Tumor2	Ratiolt	Blood	Ratiolb	Ratiotb
100	32.5	FV	1.95	11.7	2.24	13.44	0.87	4.87	2.4	2.76
100	32.5	FV	1.975	11.85	2.49	14.94	0.79	1.85	6.41	8.08
100	32.5	FV	0.93	5.58	1.6	9.6	0.58	1.73	3.23	5.55
100	32.5	SC	0.48	2.88	0.921	5.526	0.52	1.64	1.76	3.37
100	32.5	SC	0.66	3.96	0.736	4.416	0.9	2.79	1.42	1.58
100	32.5	SC	0.81	4.86	1.335	8.01	0.61	2.93	1.66	2.73
1000	32.5	FV	66.47	398.82	19.92	119.52	3.34	159.52	2.5	0.75
1000	32.5	FV	53.76	322.56	20.89	125.34	2.57	94.72	3.41	1.32
1000	32.5	FV	53.41	320.46	23.75	142.5	2.25	129.8	2.47	1.1
1000	32.5	SC	40.63	243.78	19.71	118.26	2.06	85.5	2.85	1.38
1000	32.5	SC	47.51	285.06	13.46	80.76	3.53	112.47	2.53	0.72
1000	32.5	SC	54.77	328.62	24.41	146.46	2.24	81.22	4.05	1.8
550	5	FV	46.19	277.14	7.24	43.44	6.38	131.64	2.11	0.33
550	5	FV	44.8	268.8	6.53	39.18	6.86	167.1	1.61	0.23
550	5	FV	50.81	304.86	5.59	33.54	9.09	108.03	2.82	0.31
550	32.5	FV	16.71	100.26	6.64	39.84	2.52	25.36	3.95	1.57
550	32.5	FV	21.57	129.42	7.2	43.2	3	31.02	4.17	1.39
550	32.5	FV	21.43	128.58	8.15	48.9	2.63			
550	32.5	FV	34.75	208.5	13.87	83.22	2.51	63.82	3.27	1.3
550	32.5	FV	41.72	250.32	7.02	42.12	5.94	51.02	4.91	0.83
550	60	FV	14.47	86.82	7.19	43.14	2.01	42.82	2.03	1.01
550	60	FV	22.18	133.08	8.59	51.54	2.58	36.94	3.6	1.4
550	5	SC	6.74	40.44	1.51	9.06	4.46	27.09	1.49	0.33
550	5	SC	6.32	37.92	1.34	8.04	4.72	22.04	1.72	0.36

550	5	SC	6.86	41.16	1.39	8.34	4.94	22.3	1.85	0.37
550	32.5	SC	15.51	93.06	3.62	21.72	4.28	17.15	5.43	1.27
550	32.5	SC	15.71	94.26	3.91	23.46	4.02	26.25	3.59	0.89
550	32.5	SC	18.82	112.92	4.37	26.22	4.31			
550	60	SC	18.31	109.86	11.52	69.12	1.59	37.75	2.91	1.83
550	60	SC	12.72	76.32	8.71	52.26	1.46	21.99	3.47	2.38
550	60	SC	17.68	106.08	9.54	57.24	1.85	31.68	3.35	1.81
232	13.05	FV	12.98	77.88	8.37	50.22	1.55			
232	13.05	FV	11.3	67.8	2.84	17.04	3.98	18.19	3.73	0.94
232	13.05	FV	10.3	61.8	4.29	25.74	2.4	46.44	1.33	0.55
232	13.05	FV	14.39	86.34	2.94	17.64	4.89	35.65	2.42	0.49
232	13.05	SC	3.65	21.9	2	12	1.83	14.45	1.52	0.83
232	13.05	SC	4.39	26.34	1.59	9.54	2.76	10.94	2.41	0.87
232	13.05	SC	6.53	39.18	2.75	16.5	2.37	17.79	2.2	0.93
232	51.95	FV	3.68	22.08	2.93	17.58	1.26	4.77	4.63	3.69
232	51.95	FV	1.37	8.22	2.19	13.14	0.63	3.51	2.34	3.74
232	51.95	FV	2.823	16.938	3.28	19.68	0.86	5.48	3.09	3.59
232	51.95	SC	2.07	12.42	2.21	13.26	0.94	5.29	2.35	2.51
232	51.95	SC	2.3	13.8	2.053	12.318	1.12	5.322	2.59	2.31
232	51.95	SC	1.32	7.92	1.42	8.52	0.93	5.18	1.53	1.64
868	51.95	FV	21.54	129.24	12.38	74.28	1.74	35.24	3.67	2.11
868	51.95	FV	20.43	122.58	10.33	61.98	1.98			
868	51.95	FV	16.99	101.94	9.93	59.58	1.71	31.81	3.2	1.87
868	51.95	SC	18.57	111.42	11.19	67.14	1.66	58.15	1.92	1.15
868	51.95	SC	27.01	162.06	17.156	102.936	1.57			
868	51.95	SC	40.79	244.74	17.18	103.08	2.37	77.03	3.18	1.34
868	13.05	FV	83.89	503.34	11.12	66.72	7.54	134.1	3.75	0.5
868	13.05	FV	94.39	566.34	11.52	69.12	8.19	192.7	2.94	0.36
868	13.05	FV	65.93	395.58	12.49	74.94	5.28	249.46	1.59	0.3
868	13.05	FV	90.2	541.2	15.22	91.32	5.93			
868	13.05	SC	22.68	136.08	3.91	23.46	5.8	65.74	2.07	0.36
868	13.05	SC	24.27	145.62	4.29	25.74	5.66	87.82	1.66	0.29
868	13.05	SC	22.67	136.02	4.238	25.428	5.35	72.18	1.88	0.35

APPENDIX D

SAS codes for chapter 5

```
/*************************read and creat data**********************/

PROC IMPORT OUT= WORK.rats2
            DATAFILE= "C:\Documents and Settings\zlu\Desktop\Rats Study\Rats2
study\rats2 data\062206"
            DBMS=EXCEL2000 REPLACE;
     SHEET="sheet1$";
     GETNAMES=YES;
RUN;
proc sort data=rats2;
by route dose time;
run;
options symbolgen;
%let r=SC;
data rats2;
set rats2;
label dose='dose(mg/m2)'
      time='time(mins)'
            liver2='liver(nmols/g)'
            tumor2='tumor(nmols/g)'
            ratio='L/T ratio'
            blood='blood(uM)'
            ;
lliver=log(liver2);
ltumor=log(tumor2);
lratio=log(ratio);
lblood=log(blood);
rdum=(route="&r");
run;
data rats2coded; set rats2;
time=(time-32.5)/19.45;
dose=(dose-550)/318;
run;
```

```
/************************comparison with full model*****************/
%let y=lblood;
%let model=%str(vdum|dose|time);

proc transreg data=rats1 details;
model boxcox(&y)=identity(&model);
run;

%macro doit;
proc glm data=rats1;
model &y=&model/solution;
%if &model=%str(vdum|dose|time) %then %do;
contrast  'test for coincidence' vdum 1 -1,
                          dose*vdum 1 -1,
                           time*vdum 1 -1,
                          dose*time*vdum 1 -1;
%end;
%else %do;
contrast  'test for coincidence' vdum 1 -1,
                          dose*vdum 1 -1,
                           time*vdum 1 -1,
                          dose*time*vdum 1 -1,
                          dose*dose*vdum 1 -1,
                           time*time*vdum 1 -1;
%end;
output out=rats1out p=yhat r=resid;
run;quit;
proc gplot data=rats1out;
plot &y*yhat;
plot resid*yhat;
plot resid*dose;
plot resid*time;
run;quit;
proc univariate data=rats1out normal;
var resid;
histogram;
qqplot/normal(mu=est sigma=est);
run;
%mend;
%doit



/*********************data are splited***********/
%let a=f;
title 'FV';
```

```
%let model=%str(dose|time);
data rats2&a; set rats2;
where route="&r";
run;
proc transreg data=rats1&a details;
model boxcox(&y)=identity(&model);
run;
proc rsreg data=rats2&a;
model &y=dose time/lackfit press;
run;
proc glm data=rats2&a;
model &y=&model;
output out=rats1&a.out p=yhat r=resid;
run;quit;
proc gplot data=rats1&a.out;
plot &y*yhat;
plot resid*dose;
plot resid*time;
plot resid*yhat;
run;
quit;
proc univariate data=rats1&a.out  normal;
var resid;
histogram;
qqplot/normal(mu=est sigma=est);
run;



/*******2-D plot by time with predicted values with labeled experimental points******/

data grid2t;
do time=5,13.05,32.5,51.95,60;
do dose=100 to 1000 by 10;
ypred=exp(2.463982+ 0.007818*dose-0.085868*time+0.000017132*dose*time-
0.000004207*dose*dose+0.000646*time*time);
output;
end;
end;
run;
proc sort data=rats2&a;
by time dose;
run;
data anno2t;
length color1-color5 $8;
set rats2&a;
```

```
by time;
retain i 0 color1 'blue' color2 'green' color3 'yellow' color4 'orange' color5 'red' xsys ysys
'2';
array colors{*} color1-color5;
if first.time then i+1;
function='symbol'; x=dose; y=blood; text='X'; color=colors{i}; style='swiss'; size=1.5;
output;
run;
ods listing close;
ods html file='C:\Documents and Settings\zlu\Desktop\Rats Study\Rats2 study\rats2
results\test.html'
      gpath='C:\Documents and Settings\zlu\Desktop\Rats Study\Rats2 study\rats2
results\';

goptions reset=all cback=black transparency disposal=background ctext=white
ftext=swissb htext=1.5;
goptions device=win target=winprtc;
title height=2 color=white  ' FV';

axis1 color=white
      width=20
            label=(font=swiss height=2)
      value=(font=swiss height=2)
      major=(width=2);
axis2 color=white
      width=20
            label=(a=90 font=swiss height=2)
      value=(font=swiss height=2)
      major=(width=3 height=1)
      order=0 to 400 by 100;
symbol1 c=blue i=spline v=none w=30;
symbol2 c=green i=spline v=none w=30;
symbol3 c=yellow i=spline v=none w=30;
symbol4 c=orange i=spline v=none w=30;
symbol5 c=red i=spline v=none w=30;
proc gplot data=grid2t;
plot ypred*dose=time/anno=anno2t haxis=axis1 vaxis=axis2;
label dose='Dose(mg/m2)'
      time='Time(mins)'
      ypred='Blood(uM)';
run;quit;
ods html close;
ods listing;


/*******2-D plot by dose with predicted values with labeled experimental points*****/
```

```
data grid2t;
do time=5 to 60 by 5;
do dose=100, 232, 550, 868, 1000;
ypred=exp(2.463982+ 0.007818*dose-0.085868*time+0.000017132*dose*time-
0.000004207*dose*dose+0.000646*time*time);
output;
end;
end;
run;
proc sort data=rats2&a;
by dose time;
run;
data anno2t;
length color1-color5 $8;
set rats2&a;
by dose;
retain i 0 color1 'blue' color2 'green' color3 'yellow' color4 'orange' color5 'red' xsys ysys
'2';
array colors{*} color1-color5;
if first.dose then i+1;
function='symbol'; x=time; y=blood; text='X'; color=colors{i}; style='swiss'; size=1.5;
output;
run;
ods listing close;
ods html file='C:\Documents and Settings\zlu\Desktop\Rats Study\Rats2 study\rats2
results\test.html'
      gpath='C:\Documents and Settings\zlu\Desktop\Rats Study\Rats2 study\rats2
results\';

goptions reset=all cback=black transparency disposal=background ctext=white
ftext=swissb htext=1.5;
goptions device=win target=winprtc;
title height=2 color=white  'FV';

axis1 color=white
      width=20
            label=(font=swiss height=2)
      value=(font=swiss height=2)
      major=(width=2);
axis2 color=white
      width=20
            label=(a=90 font=swiss height=2)
      value=(font=swiss height=2)
      major=(width=3 height=1)
      order=0 to 400 by 100;
```

```
symbol1 c=blue i=spline v=none w=30;
symbol2 c=green i=spline v=none w=30;
symbol3 c=yellow i=spline v=none w=30;
symbol4 c=orange i=spline v=none w=30;
symbol5 c=red i=spline v=none w=30;
proc gplot data=grid2t;
plot ypred*time=dose/anno=anno2t haxis=axis1 vaxis=axis2;
label dose='Dose(mg/m2)'
      time='Time(mins)'
      ypred='Blood(uM)';
run;quit;
ods html close;
ods listing;



/*************combine contour plot with spin surface plot************/


goptions reset=all ftext=swiss htext=6  gunit=pct border;
data grid;
do dose=50to 500 by 45;
do time=15 to 60 by 4.5;
ypred=exp(0.5543+ 0.00365*dose-0.031*time-0.000027*dose*time);
output;
end;
end;
run;
%let nlevels=8;
%let colors='yellow vibg cyan green lime gold orange red';
proc means data=grid noprint min max;
var dose time ypred;
output out=range min=dmin tmin ymin
max=dmax tmax ymax;
run;
data _null_;
set range;
call symput('dmin',dmin);
call symput('dmax',dmax);
call symput('tmin',tmin);
call symput('tmax',tmax);
call symput('ymin',ymin);
call symput('ymax',ymax);
call symput('step',(ymax-ymin)/&nlevels);
call symput('floor', int(ymin-4));
call symput('ceil',int(ymax+2));
```

```
run;
proc sort data=grid;
by time dose;
run;
data plane1 surf1;
length function color $8;
retain xsys ysys zsys '2';
set grid;
by time;
x=time; y=dose; z=&floor;
if first.time then function='move';
else do;
function='draw'; size=2;
ncol=min(&nlevels,int(1+(ypred-&ymin)/&step));
color=scan(&colors,ncol);
end;
output plane1;
z=ypred; output surf1;
run;
proc sort data=grid;
by dose time;
run;
data plane2 surf2;
length function color $8;
retain xsys ysys zsys '2';
set grid;
by dose;
x=time; y=dose; z=&floor;
if first.dose then function='move';
else do;
function='draw'; size=2;
ncol=min(&nlevels,int(1+(ypred-&ymin)/&step));
color=scan(&colors,ncol);
end;
output plane2;
z=ypred; output surf2;
run;
data legend;
length function color $8;
retain xsys ysys zsys '2';
do legend=&ymin to (&ymax-&step) by &step;
x=&tmin; y=&dmax; z=legend;
function='poly'; style='solid';
ncol=min(&nlevels,int(1+(legend-&ymin)/&step));
color=scan(&colors,ncol);output;
z=legend+&step;
```

```
function='polycont'; output;
x=&tmin+1; output;
z=legend; output;
end;
run;
proc means data=rats1&a noprint mean nway;
class dose time;
var liver tumor ratio blood;
output out=meanout mean=lmean tmean rmean bmean;
run;

data back;
merge rats1&a meanout;
by dose time;
retain color 'purple' xsys ysys zsys '2';
function='label'; x=time; y=dose; z=ratio; size=1; text='X';  output;
function='move'; x=time; y=dose; z=rmean; size=1; output;
function='draw'; x=time; y=dose; z=&floor; size=2; output;
run;

data annoall;
set  surf1 surf2 plane1 plane2 legend back;
run;
data plotdata;
dose=&dmin; time=&tmin; ypred=&floor; output;
dose=&dmax; time=&tmax; output;
run;

%macro animate;
%local angle;
%do angle=0 %to 360 %by 10;
%if &angle=0 %then %do;
goptions reset=all gsfname=out dev=gifanim gsfmode=replace delay=100 cback=black
transparency disposal=background
       ftext=swissb htext=1.5;
title height=2 color=white  'by portal vein';
filename out 'C:\Documents and Settings\zlu\Desktop\Rats Study\Rats1 study\rats1
results\ratiospin.gif';
%end;
%else %do; goptions gsfmode=append; %end;
%if &angle=360 %then %do; goptions gepilog='3B'x;
%end;
proc g3d data=plotdata;
scatter dose*time=ypred/rotate=&angle shape='point'
xticknum=4 yticknum=4 zticknum=6 zmin=&floor zmax=9.0 ctext=white
annotate=annoall;
```

```
label dose='Dose(mg/m2)'
      time='Time(mins)'
      ypred='Ratio';
run;
%end;
%mend;
%animate

/*************Model selection and confidence interval***************/

PROC IMPORT OUT= WORK.rats2
         DATAFILE= "C:\Documents and Settings\zlu\Desktop\Rats Study\Rats2
study\rats2 data\062206.xls"
         DBMS=EXCEL REPLACE;
    SHEET="Sheet1$";
    GETNAMES=YES;
    MIXED=NO;
    SCANTEXT=YES;
    USEDATE=YES;
    SCANTIME=YES;
RUN;

data rats2trans;
drop liver1 tumor1;
set rats2;
lliver=log10(liver2);
ltumor=log10(tumor2);
lratiolt=log10(ratiolt);
lblood=log10(blood);
lratiolb=log10(ratiolb);
lratiotb=log10(ratiotb);
run;
proc sort data=rats2trans;
by dose time route;
run;
proc means data=rats2trans noprint;
var liver2 tumor2 ratiolt blood ratiolb ratiotb lliver ltumor lratiolt lblood lratiolb lratiotb;
by dose time route;
output out=rats2transstd std=sliver2 stumor2 sratiolt sblood sratiolb sratiotb slliver
sltumor slratiolt slblood slratiolb slratiotb;
run;
data rats2wt;
array stds {*} sliver2 stumor2 sratiolt sblood sratiolb sratiotb slliver sltumor slratiolt
slblood slratiolb slratiotb;
array wts {*} wliver2 wtumor2 wratiolt wblood wratiolb wratiotb wlliver wltumor
wlratiolt wlblood wlratiolb wlratiotb;
```

```
merge rats2trans rats2transstd;
by dose time route;
do i=1 to dim(stds);
wts{i}=1/stds{i};
end;
drop i _type_ _freq_;
run;
proc sort data=rats2wt;
by route dose time;
run;
data rats2reg;
array vars{*} liver2 tumor2 ratiolt blood ratiolb ratiotb lliver ltumor lratiolt lblood
lratiolb lratiotb;
set rats2wt;
by route dose;
rdum=(route='SC');
dose2=(dose-550)*(dose-550);
time2=(time-32.5)*(time-32.5);
td=time*dose;
rdose=rdum*dose;
rtime=rdum*time;
rtd=rdum*td;
rdose2=rdum*dose2;
rtime2=rdum*time2;
output;
if last.dose then do;
do i=1 to dim(vars);
vars{i}=.;
end;
do time= 6 to 59;
time2=(time-32.5)*(time-32.5);
rtime=rdum*time;
rtime2=rdum*time2;
td=time*dose;
rtd=rdum*td;
output;
end;
end;
run;
proc reg data=rats2reg;
model lblood=dose time dose2 time2 td rdum rdose rtime rtd rdose2
rtime2/selection=stepwise sle=0.05 sls=0.05;
weight wlblood;
output out=rats2wtregb p=yhat r=resid lclm=yl uclm=yu;
run; quit;
proc sort data=rats2trans;
```

```
by route dose time;
run;
proc sort data=rats2wtregb;
by route dose time;
run;
data anno1;
length color1-color5 $8;
set rats2trans(where=(blood gt .));
by route dose;
retain i 0 color1 'blue' color2 'green' color3 'yellow' color4 'orange' color5 'red' xsys ysys
'2';
array colors{*} color1-color5;
if first.route then i=0;
if first.dose then i+1;
function='symbol'; x=time; y=blood; text='X'; color=colors{i}; style='swiss'; size=2;
output;
run;
data rats2wtregbo;
set rats2wtregb;
yhat=10**yhat;
yl=10**yl;
yu=10**yu;
run;

data rats2wtregbanno;
set rats2wtregb;
yl=10**yl;
yu=10**yu;
keep dose time route yl yu;
run;
data anno2;
length color1-color5 $8;
set rats2wtregbanno;
by route dose;
retain i 0 color1 'blue' color2 'green' color3 'yellow' color4 'orange' color5 'red' xsys ysys
'2';
array colors{*} color1-color5;
if first.route then i=0;
if first.dose then i+1;
retain j -0.1;
if first.dose then j+0.1;
function='move'; x=time+j; y=yu; color=colors{i}; style='swiss'; size=1.5; output;
function='draw'; x=time+j; y=yl; color=colors{i}; style='swiss'; size=1.5; output;
run;
data annoall;
set anno1 anno2;
```

```
run;
proc sort data=annoall;
by route dose time;
run;

ods listing close;
ods html file='C:\Documents and Settings\zlu\Desktop\Rats Study\Rats2 study\rats2
results\122906\test.html'
        gpath='C:\Documents and Settings\zlu\Desktop\Rats Study\Rats2 study\rats2
results\122906';

goptions reset=all cback=white transparency disposal=background ctext=black
ftext=swissb htext=2;
goptions device=JPEG target=winprtc;


axis1 color=black
      width=30
                label=(font=swiss height=2.5)
      value=(font=swiss height=2.5)
      major=(width=2.5);
axis2 color=black
      width=30
                label=(a=90 font=swiss height=2.5)
      value=(font=swiss height=2.5)
      major=(width=3.5 height=1.5)
      order=0 to 400 by 100;
symbol1 c=blue i=spline v=none w=35;
symbol2 c=green i=spline v=none w=35;
symbol3 c=yellow i=spline v=none w=35;
symbol4 c=orange i=spline v=none w=35;
symbol5 c=red i=spline v=none w=35;
proc gplot data=rats2wtregbo;
plot yhat*time=dose/anno=annoall haxis=axis1 vaxis=axis2;
by route;
label dose='Dose(mg/m2)'
    time='Time(mins)'
    yhat='Blood(uM)';
run;quit;
ods html close;
ods listing;
```

APPENDIX E

Data for chapter 6

Table E.1. Concentrations of amifostine and WR-1065 in plasma/blood of 5 patients and covariates prepared for NONMEM analysis

C PK modeling for Amifostine and active metabolite WR1065 after single IV bolus dose of Amifostine
C No. of subjects= 5, Dose = umols/kg, DV= Plasma concentration of Amifostine and WR1065(uM), Time=mins

CID	Time	OBS	DV	Anum	AMT	Sex	WT	Age	CMT	EVID	MDV
1	0	0	0	1	30.6	0	110.23	44	1	1	1
1	1	187	5.231109	1	0	0	110.23	44	1	0	0
1	1	14.24	2.656055	1	0	0	110.23	44	2	0	0
1	5	85.55	4.449101	1	0	0	110.23	44	1	0	0
1	5	28.49	3.349553	1	0	0	110.23	44	2	0	0
1	15	12.1	2.493205	1	0	0	110.23	44	1	0	0
1	15	13.43	2.597491	1	0	0	110.23	44	2	0	0
1	30	1.03	0.029559	1	0	0	110.23	44	1	0	0
1	30	3.25	1.178655	1	0	0	110.23	44	2	0	0
1	45	1.19	0.173953	1	0	0	110.23	44	2	0	0
1	60	0.83	-0.18633	1	0	0	110.23	44	2	0	0
1	120	0.4	-0.91629	1	0	0	110.23	44	2	0	0
1	180	0.35	-1.04982	1	0	0	110.23	44	2	0	0
1	240	0.13	-2.04022	1	0	0	110.23	44	2	0	0
2	0	0	0	1	45.9	0	55.4	48	1	1	1
2	1	476	6.165418	1	0	0	55.4	48	1	0	0
2	1	40.41	3.699077	1	0	0	55.4	48	2	0	0
2	5	41.5	3.725693	1	0	0	55.4	48	1	0	0
2	5	23.87	3.172622	1	0	0	55.4	48	2	0	0
2	15	4.46	1.495149	1	0	0	55.4	48	1	0	0
2	15	12.82	2.551006	1	0	0	55.4	48	2	0	0

2	30	2.37	0.86289	1	0	0	55.4	48	2	0	0
2	45	1.85	0.615186	1	0	0	55.4	48	2	0	0
2	60	1.32	0.277632	1	0	0	55.4	48	2	0	0
2	120	0.51	-0.67334	1	0	0	55.4	48	2	0	0
2	180	0.27	-1.30933	1	0	0	55.4	48	2	0	0
2	240	0.25	-1.38629	1	0	0	55.4	48	2	0	0
2	300	0.16	-1.83258	1	0	0	55.4	48	2	0	0
2	360	0.15	-1.89712	1	0	0	55.4	48	2	0	0
3	0	0	0	1	32.8	1	110	54	1	1	1
3	1	167	5.117994	1	0	1	110	54	1	0	0
3	1	2.173	0.776109	1	0	1	110	54	2	0	0
3	3	126.17	4.83763	1	0	1	110	54	1	0	0
3	3	16.176	2.783529	1	0	1	110	54	2	0	0
3	5	44.12	3.786913	1	0	1	110	54	1	0	0
3	5	14.357	2.664238	1	0	1	110	54	2	0	0
3	15	6.56	1.880991	1	0	1	110	54	1	0	0
3	15	6.554	1.880076	1	0	1	110	54	2	0	0
3	30	1.734	0.550431	1	0	1	110	54	1	0	0
3	30	2.436	0.890357	1	0	1	110	54	2	0	0
3	45	1.222	0.200489	1	0	1	110	54	2	0	0
3	60	0.7068	-0.34701	1	0	1	110	54	2	0	0
3	120	0.205	-1.58475	1	0	1	110	54	2	0	0
3	240	0.1417	-1.95404	1	0	1	110	54	2	0	0
3	360	0.061	-2.79688	1	0	1	110	54	2	0	0
4	0	0	0	1	36	0	85	53	1	1	1
4	1	325.6	5.78567	1	0	0	85	53	1	0	0
4	1	4.675	1.542229	1	0	0	85	53	2	0	0
4	3	169.43	5.13244	1	0	0	85	53	1	0	0
4	3	11.69	2.458734	1	0	0	85	53	2	0	0
4	5	81.93	4.405865	1	0	0	85	53	1	0	0
4	5	11.455	2.438426	1	0	0	85	53	2	0	0
4	15	3.34	1.205971	1	0	0	85	53	1	0	0
4	15	5.45	1.695616	1	0	0	85	53	2	0	0

4	30	0.994	-0.00602	1	0	0	85	53	1	0	0
4	30	1.97	0.678034	1	0	0	85	53	2	0	0
4	45	0.849	-0.1637	1	0	0	85	53	2	0	0
4	60	0.56	-0.57982	1	0	0	85	53	2	0	0
4	120	0.237	-1.4397	1	0	0	85	53	2	0	0
4	240	0.121	-2.11196	1	0	0	85	53	2	0	0
4	360	0.105	-2.25379	1	0	0	85	53	2	0	0
5	0	0	0	1	42.3	1	70	69	1	1	1
5	1	342.1	5.835103	1	0	1	70	69	1	0	0
5	1	10.7	2.370244	1	0	1	70	69	2	0	0
5	3	141.4	4.951593	1	0	1	70	69	1	0	0
5	3	35.25	3.562466	1	0	1	70	69	2	0	0
5	5	58.21	4.064057	1	0	1	70	69	1	0	0
5	5	34.67	3.545875	1	0	1	70	69	2	0	0
5	15	5	1.609438	1	0	1	70	69	1	0	0
5	15	13.78	2.623218	1	0	1	70	69	2	0	0
5	30	0.272	-1.30195	1	0	1	70	69	1	0	0
5	30	4.67	1.541159	1	0	1	70	69	2	0	0
5	45	2.255	0.81315	1	0	1	70	69	2	0	0
5	60	1.267	0.236652	1	0	1	70	69	2	0	0
5	120	0.59	-0.52763	1	0	1	70	69	2	0	0
5	240	0.174	-1.7487	1	0	1	70	69	2	0	0
5	360	0.102	-2.28278	1	0	1	70	69	2	0	0

APPENDIX F

NONMEM codes for chapter 6

```
$PROBLEM Parent drug & active metabolite    ;Units: Time=mins,
Concentration=uM(umols/L), Amount=umols/kg
                                ;Age=yrs, Weight=kg
                                ;Sex=1(is male) or 0(is female)
                                ;Anum=1(is EC) or 2(is FL)
$DATA AW2LN.CSV IGNORE=C
$INPUT ID TIME OBS DV ANUM AMT SEX WT AGE BSA PT PTT INR CMT
EVID MDV

$SUBROUTINE ADVAN6 TRANS1 TOL=5
$MODEL
NCOMP=3
COMP=(PARENT)
COMP=(METAB1)
COMP=(METAB2)

$PK
CL1=THETA(1)*EXP(ETA(1))
TVV1=THETA(2)*(WT/70)
V1=TVV1*EXP(ETA(2))
CLM=THETA(3)*EXP(ETA(3))
Q=THETA(4)*EXP(ETA(4))
V2=THETA(5)*EXP(ETA(5))
V3=THETA(6)*EXP(ETA(6))
S1=V1
S2=V2
K12=CL1/V1
K20=CLM/V2


$DES
C1=A(1)/V1
C2=A(2)/V2
C3=A(3)/V3
DADT(1)=-CL1*C1
DADT(2)=CL1*C1+Q/V3*A(3)+ Q*(C3-C2)-CLM*C2
DADT(3)=Q*(C2-C3)

$ERROR
IPRED=LOG(F)
W1=THETA(7)
```

```
W2=THETA(8)
P1=0
IF(CMT.EQ.1)P1=1
P2=0
IF(CMT.EQ.2)P2=1
Y1=LOG(F)+W1*ERR(1)+ERR(2)
Y2=LOG(F)+W2*ERR(3)+ERR(4)
Y=P1*Y1+P2*Y2
IRES=DV-IPRED
IWRES=IRES/(P1*W1+P2*W2)

$THETA
(0,0.04,1000000);CL1
(0,0.25,1000000) ;V1
(0,0.2,1000000) ;CLM
(0,0.03,1000000) ;Q
(0,1,1000000) ;V2
(0,2.5,1000000) ;V3
(0,0.2)
(0,0.2)

$OMEGA
0 FIX ;assuming 50% error
0 FIX
0.25
0 FIX
0 FIX
0 FIX

$SIGMA
1 FIX
0 FIX
1 FIX
0 FIX


$ESTIMATION METHOD=1 INTERACTION MAXEVAL=9999 PRINT=5

$COVARIANCE

$TABLE ID TIME OBS AMT SEX WT AGE BSA PT PTT INR CMT IPRED IRES
IWRES ETA1 ETA2 ETA3 ETA4 ETA5 ETA6
NOPRINT ONEHEADER FILE=OUTAMIWR.TXT
```

APPENDIX G

S-plus codes for chapter 6

```
# INPUT DATA
amiwrec=read.table('C:\\Documents and Settings\\zlu\\Desktop\\Human
    study\\Lu\\outamiwr.txt', skip=1, header=T)
amiwrecm=amiwrec[amiwrec$TIME>0,]
summary(amiwrecm)

# DISTRIBUTION OF UNTRANSFORMED AND TRANSFORMED
    OBSERVATIONS
graphsheet()
par(mfrow=c(2,2),mar=c(5,5,4,4))
hist(amiwrecm$OBS, prob=T, ylab='Probability', xlab='Untransformed Observation')
lines(density(amiwrecm$OBS),col=8, lwd=3,lty=3)
qqnorm(amiwrecm$OBS, pch=16, col=2,ylab='Untransformed Observation' )
qqline(amiwrecm$OBS, lwd=3, col=5)

hist(amiwrecm$DV, prob=T, ylab='Probability', xlab='Transformed Observation')
lines(density(amiwrecm$DV),col=8, lwd=3,lty=3)
qqnorm(amiwrecm$DV, pch=16, col=2,ylab='Transformed Observation' )
qqline(amiwrecm$DV, lwd=3, col=5)


# DISTRIBUTION OF RESIDUALS
graphsheet()
par(mfrow=c(2,2), mar=c(5,5,3,3))
hist(amiwrecm$IWRE,prob=T, ylab='Probability', xlab='IWRE')
lines(density(amiwrecm$IWRE),col=8, lwd=3,lty=3)
qqnorm(amiwrecm$IWRE, pch=16, col=2,ylab='IWRE' )
qqline(amiwrecm$IWRE, lwd=3, col=5)

hist(amiwrecm$WRES,prob=T,ylab='Probability',xlab='WRES', ylim=c(0,0.4),xlim=c(-
    2,5))
lines(density(amiwrecm$WRES),col=8, lwd=3,lty=3)
qqnorm(amiwrecm$WRES, pch=16, col=2,ylab='WRES')
qqline(amiwrecm$WRES, lwd=3, col=5)


# RESIDUAL PLOTS
graphsheet()
par(mfrow=c(2,2),mar=c(5,5,4,4))
plot(amiwrecm$IPRE, amiwrecm$IWRE, pch=16, col=2, xlab='IPRE', ylab='IWRES',
    xlim=c(-1.5,3), ylim=c(-3.5,3.5), cex=1.2)
```

```
abline(h=0,lwd=3, col=5)
abline(h=c(-2,2), lwd=3, col=5, lty=4)
lines(lowess(amiwrecm$IPRE, amiwrecm$IWRE),lwd=2, col=3)
plot(amiwrecm$TIME, amiwrecm$IWRE, pch=16, col=2, xlab='TIME', ylab='IWRES',
     xlim=c(0,400), ylim=c(-3.5,3.5), cex=1.2)
abline(h=0,lwd=3, col=5)
#abline(h=c(-2.5,2.5), lwd=3, col=5, lty=4)
lines(lowess(amiwrecm$TIME, amiwrecm$IWRE),lwd=2, col=3)
plot(amiwrecm$PRED, amiwrecm$WRES, pch=16, col=2, xlab='PRED', ylab='WRES',
     xlim=c(-1.5,3), ylim=c(-4,4), cex=1.2)
abline(h=0,lwd=3, col=5)
abline(h=c(-2,2), lwd=3, col=5, lty=4)
lines(lowess(amiwrecm$PRED, amiwrecm$WRES),lwd=2, col=3)
plot(amiwrecm$TIME, amiwrecm$WRES, pch=16, col=2, xlab='TIME', ylab='WRES',
     xlim=c(0,400), ylim=c(-4,4), cex=1.2)
abline(h=0,lwd=3, col=5)
#abline(h=c(-2.5,2.5), lwd=3, col=5, lty=4)
lines(lowess(amiwrecm$TIME, amiwrecm$WRES),lwd=2, col=3)

# ETA PLOTS (1)
graphsheet()
par(mfrow=c(6,3), mar=c(8,8,4,4))
plot(amiwrecm$WT, amiwrecm$ETA1, xlab='Weight(kg)',ylab='ETACL1', col=2,
     pch=16, cex=1.0)
lines(lowess(amiwrecm$WT, amiwrecm$ETA1), col=5, lwd=3)
plot(amiwrecm$AGE, amiwrecm$ETA1, xlab='Age(yrs)',ylab='ETACL1', col=2, pch=16,
     cex=1.0)
lines(lowess(amiwrecm$AGE, amiwrecm$ETA1), col=5, lwd=3)
boxplot(split(amiwrecm$ETA1,amiwrecm$SEX), names=c('Female','Male'),
     ylab='ETACL1', cex=1.0)

plot(amiwrecm$WT, amiwrecm$ETA2, xlab='Weight(kg)',ylab='ETAV1', col=2, pch=16,
     cex=1.0)
lines(lowess(amiwrecm$WT, amiwrecm$ETA2), col=5, lwd=3)
plot(amiwrecm$AGE, amiwrecm$ETA2, xlab='Age(yrs)',ylab='ETAV1', col=2, pch=16,
     cex=1.0)
lines(lowess(amiwrecm$AGE, amiwrecm$ETA2), col=5, lwd=3)
boxplot(split(amiwrecm$ETA2,amiwrecm$SEX), names=c('Female','Male'),
     ylab='ETAV1', cex=1.0)

plot(amiwrecm$WT, amiwrecm$ETA3, xlab='Weight(kg)',ylab='ETACLM', col=2,
     pch=16, cex=1.0)
lines(lowess(amiwrecm$WT, amiwrecm$ETA3), col=5, lwd=3)
plot(amiwrecm$AGE, amiwrecm$ETA3, xlab='Age(yrs)',ylab='ETACLM', col=2,
     pch=16, cex=1.0)
lines(lowess(amiwrecm$AGE, amiwrecm$ETA3), col=5, lwd=3)
```

```
boxplot(split(amiwrecm$ETA3,amiwrecm$SEX), names=c('Female','Male'),
    ylab='ETACLM', cex=1.0)

plot(amiwrecm$WT, amiwrecm$ETA4, xlab='Weight(kg)',ylab='ETAQ', col=2, pch=16,
    cex=1.0)
lines(lowess(amiwrecm$WT, amiwrecm$ETA4), col=5, lwd=3)
plot(amiwrecm$AGE, amiwrecm$ETA4, xlab='Age(yrs)',ylab='ETAQ', col=2, pch=16,
    cex=1.0)
lines(lowess(amiwrecm$AGE, amiwrecm$ETA4), col=5, lwd=3)
boxplot(split(amiwrecm$ETA4,amiwrecm$SEX), names=c('Female','Male'),
    ylab='ETAQ', cex=1.0)

plot(amiwrecm$WT, amiwrecm$ETA5, xlab='Weight(kg)',ylab='ETAV2', col=2, pch=16,
    cex=1.0)
lines(lowess(amiwrecm$WT, amiwrecm$ETA5), col=5, lwd=3)
plot(amiwrecm$AGE, amiwrecm$ETA5, xlab='Age(yrs)',ylab='ETAV2', col=2, pch=16,
    cex=1.0)
lines(lowess(amiwrecm$AGE, amiwrecm$ETA5), col=5, lwd=3)
boxplot(split(amiwrecm$ETA5,amiwrecm$SEX), names=c('Female','Male'),
    ylab='ETAV2', cex=1.0)

plot(amiwrecm$WT, amiwrecm$ETA6, xlab='Weight(kg)',ylab='ETAV3', col=2, pch=16,
    cex=1.0)
lines(lowess(amiwrecm$WT, amiwrecm$ETA6), col=5, lwd=3)
plot(amiwrecm$AGE, amiwrecm$ETA6, xlab='Age(yrs)',ylab='ETAV3', col=2, pch=16,
    cex=1.0)
lines(lowess(amiwrecm$AGE, amiwrecm$ETA6), col=5, lwd=3)
boxplot(split(amiwrecm$ETA6,amiwrecm$SEX), names=c('Female','Male'),
    ylab='ETAV3', cex=1.0)

# ETA PLOTS (2)
graphsheet()
par(mfrow=c(6,3), mar=c(8,8,4,4))
plot(amiwrecm$PT, amiwrecm$ETA1, xlab='PT',ylab='ETACL1', col=2, pch=16,
    cex=1.0)
lines(lowess(amiwrecm$PT, amiwrecm$ETA1), col=5, lwd=3)
plot(amiwrecm$PTT, amiwrecm$ETA1, xlab='PTT',ylab='ETACL1', col=2, pch=16,
    cex=1.0)
lines(lowess(amiwrecm$PTT, amiwrecm$ETA1), col=5, lwd=3)
plot(amiwrecm$INR, amiwrecm$ETA1, xlab='INR',ylab='ETACL1', col=2, pch=16,
    cex=1.0)
lines(lowess(amiwrecm$INR, amiwrecm$ETA1), col=5, lwd=3)

plot(amiwrecm$PT, amiwrecm$ETA2, xlab='PT',ylab='ETAV1', col=2, pch=16, cex=1.0)
lines(lowess(amiwrecm$PT, amiwrecm$ETA2), col=5, lwd=3)
```

```
plot(amiwrecm$PTT, amiwrecm$ETA2, xlab='PTT',ylab='ETAV1', col=2, pch=16,
    cex=1.0)
lines(lowess(amiwrecm$PTT, amiwrecm$ETA2), col=5, lwd=3)
plot(amiwrecm$INR, amiwrecm$ETA2, xlab='INR',ylab='ETAV1', col=2, pch=16,
    cex=1.0)
lines(lowess(amiwrecm$INR, amiwrecm$ETA2), col=5, lwd=3)

plot(amiwrecm$PT, amiwrecm$ETA3, xlab='PT',ylab='ETACLM', col=2, pch=16,
    cex=1.0)
lines(lowess(amiwrecm$PT, amiwrecm$ETA3), col=5, lwd=3)
plot(amiwrecm$PTT, amiwrecm$ETA3, xlab='PTT',ylab='ETACLM', col=2, pch=16,
    cex=1.0)
lines(lowess(amiwrecm$PTT, amiwrecm$ETA3), col=5, lwd=3)
plot(amiwrecm$INR, amiwrecm$ETA3, xlab='INR',ylab='ETACLM', col=2, pch=16,
    cex=1.0)
lines(lowess(amiwrecm$INR, amiwrecm$ETA3), col=5, lwd=3)

plot(amiwrecm$PT, amiwrecm$ETA4, xlab='PT',ylab='ETAQ', col=2, pch=16, cex=1.0)
lines(lowess(amiwrecm$PT, amiwrecm$ETA4), col=5, lwd=3)
plot(amiwrecm$PTT, amiwrecm$ETA4, xlab='PTT',ylab='ETAQ', col=2, pch=16,
    cex=1.0)
lines(lowess(amiwrecm$PTT, amiwrecm$ETA4), col=5, lwd=3)
plot(amiwrecm$INR, amiwrecm$ETA4, xlab='INR',ylab='ETAQ', col=2, pch=16,
    cex=1.0)
lines(lowess(amiwrecm$INR, amiwrecm$ETA4), col=5, lwd=3)

plot(amiwrecm$PT, amiwrecm$ETA5, xlab='PT',ylab='ETAV2', col=2, pch=16, cex=1.0)
lines(lowess(amiwrecm$PT, amiwrecm$ETA5), col=5, lwd=3)
plot(amiwrecm$PTT, amiwrecm$ETA5, xlab='PTT',ylab='ETAV2', col=2, pch=16,
    cex=1.0)
lines(lowess(amiwrecm$PTT, amiwrecm$ETA5), col=5, lwd=3)
plot(amiwrecm$INR, amiwrecm$ETA5, xlab='INR',ylab='ETAV2', col=2, pch=16,
    cex=1.0)
lines(lowess(amiwrecm$INR, amiwrecm$ETA5), col=5, lwd=3)

plot(amiwrecm$PT, amiwrecm$ETA6, xlab='PT',ylab='ETAV3', col=2, pch=16, cex=1.0)
lines(lowess(amiwrecm$PT, amiwrecm$ETA6), col=5, lwd=3)
plot(amiwrecm$PTT, amiwrecm$ETA6, xlab='PTT',ylab='ETAV3', col=2, pch=16,
    cex=1.0)
lines(lowess(amiwrecm$PTT, amiwrecm$ETA6), col=5, lwd=3)
plot(amiwrecm$INR, amiwrecm$ETA6, xlab='INR',ylab='ETAV3', col=2, pch=16,
    cex=1.0)
lines(lowess(amiwrecm$INR, amiwrecm$ETA6), col=5, lwd=3)

# ETA PLOTS (3)
graphsheet()
```

```
par(mfrow=c(3,4), mar=c(8,8,4,4))
plot(amiwrecm$WT, amiwrecm$ETA1, xlab='Weight(kg)',ylab='ETACL1', col=2,
    pch=16, cex=1.0)
lines(lowess(amiwrecm$WT, amiwrecm$ETA1), col=5, lwd=3)
plot(amiwrecm$BSA, amiwrecm$ETA1, xlab='BSA',ylab='ETACL1', col=2, pch=16,
    cex=1.0)
lines(lowess(amiwrecm$BSA, amiwrecm$ETA1), col=5, lwd=3)


plot(amiwrecm$WT, amiwrecm$ETA2, xlab='Weight(kg)',ylab='ETAV1', col=2, pch=16,
    cex=1.0)
lines(lowess(amiwrecm$WT, amiwrecm$ETA2), col=5, lwd=3)
plot(amiwrecm$BSA, amiwrecm$ETA2, xlab='BSA',ylab='ETAV1', col=2, pch=16,
    cex=1.0)
lines(lowess(amiwrecm$BSA, amiwrecm$ETA2), col=5, lwd=3)


plot(amiwrecm$WT, amiwrecm$ETA3, xlab='Weight(kg)',ylab='ETACLM', col=2,
    pch=16, cex=1.0)
lines(lowess(amiwrecm$WT, amiwrecm$ETA3), col=5, lwd=3)
plot(amiwrecm$BSA, amiwrecm$ETA3, xlab='BSA',ylab='ETACLM', col=2, pch=16,
    cex=1.0)
lines(lowess(amiwrecm$BSA, amiwrecm$ETA3), col=5, lwd=3)


plot(amiwrecm$WT, amiwrecm$ETA4, xlab='Weight(kg)',ylab='ETAQ', col=2, pch=16,
    cex=1.0)
lines(lowess(amiwrecm$WT, amiwrecm$ETA4), col=5, lwd=3)
plot(amiwrecm$BSA, amiwrecm$ETA4, xlab='BSA',ylab='ETAQ', col=2, pch=16,
    cex=1.0)
lines(lowess(amiwrecm$BSA, amiwrecm$ETA4), col=5, lwd=3)


plot(amiwrecm$WT, amiwrecm$ETA5, xlab='Weight(kg)',ylab='ETAV2', col=2, pch=16,
    cex=1.0)
lines(lowess(amiwrecm$WT, amiwrecm$ETA5), col=5, lwd=3)
plot(amiwrecm$BSA, amiwrecm$ETA5, xlab='BSA',ylab='ETAV2', col=2, pch=16,
    cex=1.0)
lines(lowess(amiwrecm$BSA, amiwrecm$ETA5), col=5, lwd=3)

plot(amiwrecm$WT, amiwrecm$ETA6, xlab='Weight(kg)',ylab='ETAV3', col=2, pch=16,
    cex=1.0)
lines(lowess(amiwrecm$WT, amiwrecm$ETA6), col=5, lwd=3)
plot(amiwrecm$BSA, amiwrecm$ETA6, xlab='BSA',ylab='ETAV3', col=2, pch=16,
    cex=1.0)
lines(lowess(amiwrecm$BSA, amiwrecm$ETA6), col=5, lwd=3)
```

```
# OBS VS PRED
graphsheet()
par(mar=c(5,5,4,4), cex=1.2)
plot(amiwrecm$CONC, amiwrecm$IPRE, xlab='',ylab='', xlim=c(0,500),ylim=c(0,500),
     col=2, pch=16, cex=1.2)
par(new=T, xaxs='d')
plot(amiwrecm$CONC, amiwrecm$PRED, xlab='',ylab='', xlim=c(0,500),ylim=c(0,500),
     col=3, pch=17, cex=1.2)
abline(0,1,lwd=3,col=5)
title(main='Observed vs Predicted concentration - PK', xlab='Observed
     concentration(uM)', ylab='Predicted concentration(uM)', cex=1.2)
key(text=c('Population predictions(PRED)','Individual predictions(IPRED)'),
     points=list(pch=list(17,16)), corner=c(0,1),cex=1.1)


# DV, PRED, IPRED ON LOG SCALE
graphsheet()
par(mfrow=c(2,3),mar=c(5,5,4,4))
temp.col=0
for (i in unique(amiwrecm$ID)){
j=amiwrecm$ID==i
temp.col=temp.col+1
plot(amiwrecm$TIME[j&amiwrecm$CMT==2],
     amiwrecm$CONC[j&amiwrecm$CMT==2], xlab='Time(mins)',ylab='Blood
     concentration(uM)',col=temp.col,pch=temp.col,cex=1.2,xlim=c(0,400),ylim=c(0.01,1
     00),log='y', type='p')
lines(amiwrecm$TIME[j&amiwrecm$CMT==2],amiwrecm$PRED[j&amiwrecm$CMT=
     =2], lty=1, lwd=5, col=temp.col, type='l',cex=1.2)
lines(amiwrecm$TIME[j&amiwrecm$CMT==2],amiwrecm$IPRE[j&amiwrecm$CMT=
     =2], lty=4, lwd=5, col=temp.col, type='l',cex=1.2)
title(paste('ID #',i,sep=''))
key(text=list(c('DV','PRED','IPRED'), col=temp.col), lines=list(pch=temp.col,
     col=temp.col, lty=c(4,1), type=c('p','l','l')), cex=0.8, corner=c(1,1))
}

graphsheet()
par(mfrow=c(2,3),mar=c(5,5,4,4))
temp.col=0
for (i in unique(amiwrecm$ID)){
j=amiwrecm$ID==i
temp.col=temp.col+1
plot(amiwrecm$TIME[j&amiwrecm$CMT==1],
     amiwrecm$CONC[j&amiwrecm$CMT==1], xlab='Time(mins)',ylab='Blood
```

```
    concentration(uM)',col=temp.col,pch=temp.col,cex=1.2,xlim=c(0,35),ylim=c(0.01,10
    00),log='y', type='p')
lines(amiwrecm$TIME[j&amiwrecm$CMT==1],amiwrecm$PRED[j&amiwrecm$CMT=
    =1], lty=1, lwd=5, col=temp.col, type='l',cex=1.2)
lines(amiwrecm$TIME[j&amiwrecm$CMT==1],amiwrecm$IPRE[j&amiwrecm$CMT=
    =1], lty=4, lwd=5, col=temp.col, type='l',cex=1.2)
title(paste('ID #',i,sep=''))
key(text=list(c('DV','PRED','IPRED'), col=temp.col), lines=list(pch=temp.col,
    col=temp.col, lty=c(4,1), type=c('p','l','l')), cex=0.8, corner=c(1,1))
}


#Bootstrapping
tab=read.table('C:\\Documents and Settings\\zlu\\Desktop\\Human
    study\\Lu\\aw2ln.csv',skip=2, sep=',', header=T)
n.sub=length(unique(tab$CID))
n.rep=100
n.thetas=8
boot.results=matrix(nrow=n.rep, ncol=n.thetas)

for (i in 1:n.rep){
    print(i)
    temp.id=sample(unique(tab$CID), replace=T)
    temp.data=NULL
    while(length(temp.id)>0){
        temp.data=rbind(temp.data,tab[tab$CID%in%temp.id,])
        temp.id=temp.id[duplicated(temp.id)]
    }
    #temp.data=sort.col(temp.data,"@ALL", c('CID','TIME'))
    exportData(temp.data,'C:\\Documents and Settings\\zlu\\Desktop\\Human
    study\\Lu\\myNonmemdatasetBoot.csv', delimiter=',', quote=F)
    dos('nmfe6 amiwr.ctl amiwr.lst')
    junk=scan('amiwr.lst')
    junk.pos=grep('FIXED',junk)

    if (length(junk.pos)==0) next
        #junk[junk.pos:(junk.pos+100)]
        thetas=as.numeric(junk[(junk.pos[2]+20):(junk.pos[2]+27)])

        boot.results[1,]=thetas

    }


# ETA VS VARIOUS COVARIATES
graphsheet()
```

```
par(mfrow=c(2,3), mar=c(5,5,4,4))
plot(pk001m$WT, pk001m$ETA1, xlab='Weight(kg)',ylab='Estimated random effects on
    Clearance', col=2, pch=16, cex=1.0)
lines(lowess(pk001m$WT, pk001m$ETA1), col=5, lwd=3)
plot(pk001m$AGE, pk001m$ETA1, xlab='Age(yrs)',ylab='Estimated random effects on
    Clearance', col=2, pch=16, cex=1.0)
lines(lowess(pk001m$AGE, pk001m$ETA1), col=5, lwd=3)
boxplot(split(pk001m$ETA1,pk001m$SEX), names=c('Female','Male'), ylab='Estimated
    random effects on Clearance', cex=1.0)

# WRES AND IWRES VS TIME
graphsheet()
par(mfrow=c(2,2),mar=c(5,5,4,4))
plot(wrlum$TIME, wrlum$IWRE, pch=16, col=2, xlab='TIME(mins)', ylab='IWRES',
    xlim=c(0,400), ylim=c(-2.5,2.5), cex=1.2)
abline(h=0, lwd=3,col=5)
lines(lowess(wrlum$TIME,wrlum$IWRE),lwd=3,col=3)
plot(wrlum$TIME, abs(wrlum$IWRE), pch=16, col=2, xlab='TIME(mins)',
    ylab='|IWRES|', xlim=c(0,400), ylim=c(0,2.5), cex=1.2)
lines(lowess(wrlum$TIME,abs(wrlum$IWRE)),lwd=3,col=3)

# PARENT DRUG AND METABOLITE TOGETHER IN LOG SCALE
graphsheet()
par(mfrow=c(2,3),mar=c(5,5,4,4))
for (i in unique(aw2m$CID)){
j=aw2m$CID==i
plot(aw2m$Time[j],aw2m$DV[j],type='n',xlim=c(0,400),ylim=c(0.01,1000),xlab='Time(
    mins)',ylab='Blood concentration(uM)',log='y',cex=1.2)
lines(aw2m$Time[j & aw2m$CMT==2], aw2m$DV[j & aw2m$CMT==2],pch=2,
    col=8,type='o',lty=1,lwd=3,cex=1.2)
lines(aw2m$Time[j & aw2m$CMT==1], aw2m$DV[j & aw2m$CMT==1],pch=1,
    col=2,type='o',lty=1,lwd=3,cex=1.2)
title(paste('ID #',i,sep=''))
key(text=list(c('Amifostine','WR1065')), lines=list(pch=1:2, col=c(2,8), type=rep('o',2)),
    cex=0.7, corner=c(1,1))
}
plot(aw2m$Time,aw2m$DV,type='n',xlim=c(0,400),ylim=c(0.01,1000),xlab='Time(mins
    )',ylab='Blood concentration(uM)',log='y',cex=1.2)
temp.col=0
for (i in unique(aw2m$CID)){
j=aw2m$CID==i
temp.col=temp.col+1
lines(aw2m$Time[j & aw2m$CMT==2], aw2m$DV[j & aw2m$CMT==2],pch=temp.col,
    col=temp.col,type='o',lty=1,lwd=3,cex=1.2)
lines(aw2m$Time[j & aw2m$CMT==1], aw2m$DV[j & aw2m$CMT==1],pch=temp.col,
    col=temp.col+5,type='o',lty=1,lwd=3,cex=1.2)
```

```
key(text=list(c('Amifostine',",",",",",'WR1065',",",",",")), lines=list(pch=1:5,
    col=c(6:10,1:5),type=rep('o',10)), cex=0.5, corner=c(1,1))
title('ID #1~5')
}

# LOG SCALE OF CONCENTRATION VS TIME PROFILES OF WR1065 -
    INDIVIDUALS AND ALL PATIENTS
graphsheet()
par(mfrow=c(2,3),mar=c(5,5,4,4))
temp.col=0
for (i in unique(wrflm$ID)){
j=wrflm$ID==i
temp.col=temp.col+1
plot(wrflm$Time[j], wrflm$DV[j], xlab='Time(mins)',ylab='Blood concentration(uM)',
    type='o',col=temp.col,pch=temp.col,lwd=3,lty=1,cex=1.2,xlim=c(0,400),ylim=c(0.01,
    100),log='y')
title(paste('ID #',i,sep=''))
}
plot(wrflm$Time,wrflm$DV, type='n', xlim=c(0,400), ylim=c(0.01,100), log='y',
    xlab='Time(mins)', ylab='Blood concentration(uM)',cex=1.2)
temp.col=0
for (i in unique(wrflm$ID)){
j=wrflm$ID==i
temp.col=temp.col+1
points(wrflm$Time[j], wrflm$DV[j],
    type='o',col=temp.col,pch=temp.col,lwd=3,lty=1,cex=1.2)
}
export.graph(FileName='C:\\Documents and Settings\\zheng lu\\Desktop\\Human
    study\\Lu\\wr.gif', Name='GSD2', ExportType='GIF')
export.graph(FileName='C:\\Documents and Settings\\zheng lu\\Desktop\\Human
    study\\Lu\\wr.jpg', Name='GSD2', ExportType='JPG')

# DV,PRED,IPRED ON ORIGINAL SCALE
graphsheet()
par(mar=c(5,5,4,4))
xyplot(CONC~TIME|ID, data=pk006, xlim=c(0,400), ylim=c(0,45), xlab='', ylab='',
    cex=1.2, pch=16, col=2)
title(main='PK plots', xlab='Time(mins)',ylab='Concentration(uM)',cex=1.1)
par(new=T, xaxs='d')
xyplot(PRED~TIME|ID, data=pk006, xlim=c(0,400), ylim=c(0,45), xlab='', ylab='',
    cex=1.2, lwd=5,lty=1,type='l', col=3)
par(new=T, xaxs='d')
xyplot(IPRE~TIME|ID, data=pk006, xlim=c(0,400), ylim=c(0,45), xlab='', ylab='',
    cex=1.2, lwd=5,lty=4,type='l', col=5)
export.graph(FileName='C:\\Documents and Settings\\zheng lu\\Desktop\\plot1.jpg',
    Name='GSD2', ExportType='JPG')
```